Schweizerische Eidgenossenschaft
Confédération suisse
Confederazione Svizzera
Confederaziun svizra

Federal Department of the Environment, Transport,
Energy and Communications DETEC
Swiss Federal Office of Energy SFOE

Federal Department of Defence,
Civil Protection and Sport DDPS
Swiss Federal Office of Topography swisstopo

UNCONGAS

Evaluation of unconventional resource potential in the Swiss Plateau:
an integrated subsurface study

Andrea Moscariello, Damien Do Couto, Silvia Omodeo Salé

2023

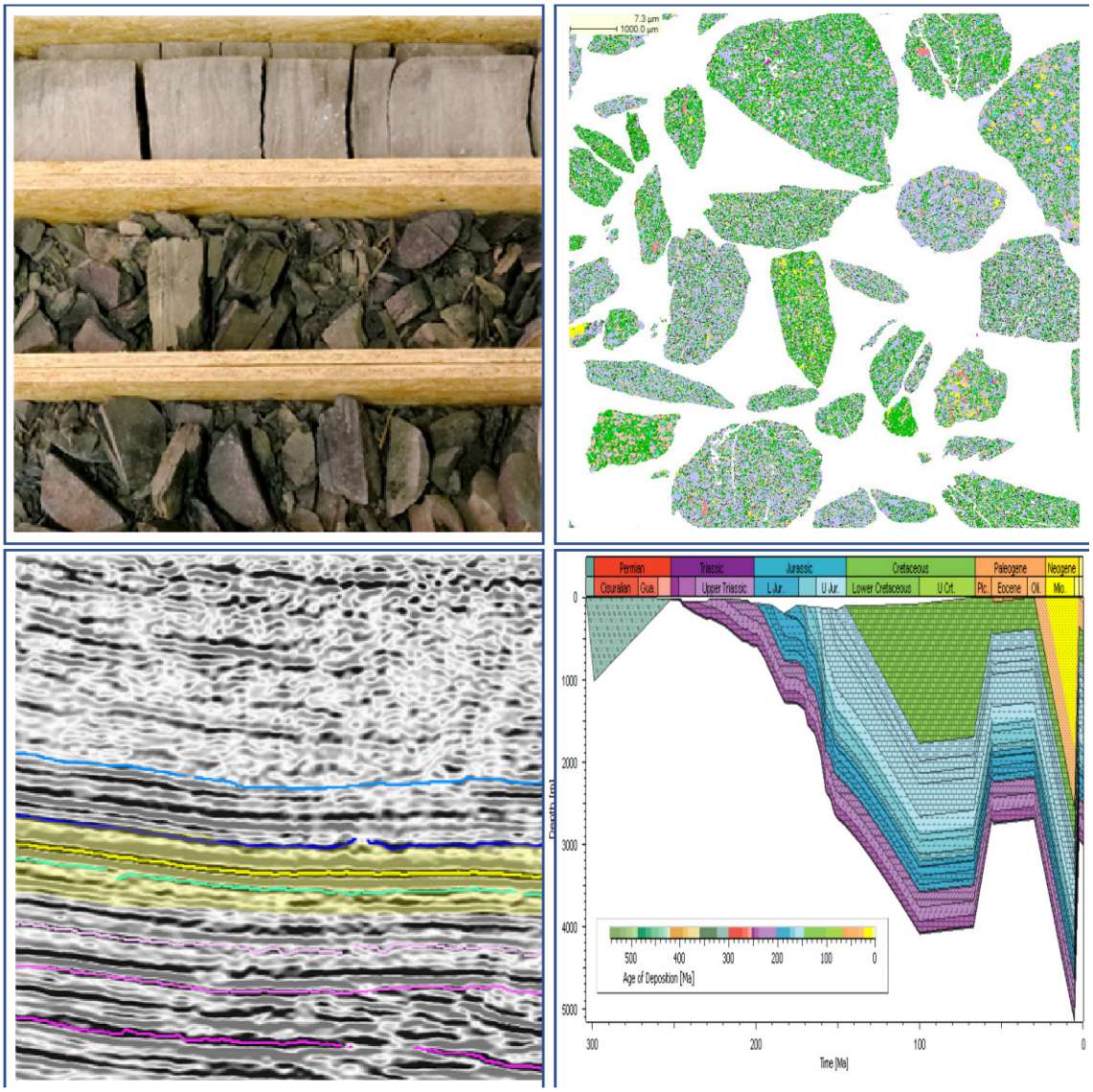

Clients:
Swiss Federal Office of Energy
Geothermal Energy research programme
CH-3003 Bern
www.ofen.admin.ch

Swiss Federal Office of Topography swisstopo
Seftigenstrasse 264
CH-3084 Wabern
www.swisstopo.admin.ch

Contractor:
Department of Earth Sciences, University of Geneva, Geneva
13 Rue des Maraichers, CH-1205 Geneva
http://www.unige.ch/sciences/terre/en/

Authors:
Prof. Dr. Andrea Moscariello, Dr. Damien Do Couto, Dr. Silvia Omodeo Salé
Geo-Energy / Reservoir Geology and Basin Analysis Group
Department of Earth Sciences, University of Geneva, Geneva
andrea.moscariello@unige.ch

Head of domain SFOE: Gunter Siddiqi, gunter.siddiqi@bfe.admin.ch
Head of programme SFOE: Rudolf Minder, rudolf.minder@bluewin.ch
Contract number SFOE: SI/5001098-01

The report was submitted on 31st December 2017

Swiss Federal Office of Energy SFOE
Mühlestrasse 4, 3063 Ittigen, Mailing address: 3003 Bern
Tél. +41 58 462 56 11 · fax +41 58 463 25 00 · contact@bfe.admin.ch · www.ofen.admin.ch

Summary

Possible hydrocarbon occurrences have a major impact on the prospecting and development of geothermal reservoirs as well as potential uses of the deep subsurface as sites for energy and CO_2-storage. The deep subsurface of the Swiss Plateau from Lake Geneva to Lake Constance comprises a heterogeneous sedimentary succession, which documents a complex paleogeographic, climatic and tectonic history dating back around 300 million years. During this period, organic-rich formations accumulated from which hydrocarbons were generated, as revealed by several surface occurrences visible today (Roulavaz, Eclepens and others). The available data from deep reflection seismic and sparse well data, acquired mostly between the 1960s and 1980s for hydrocarbon prospection, indicate the presence of a series of tight reservoirs and source-rock intervals, at least within the main study area of the Lake Geneva basin. The series may serve as unconventional reservoirs for both oil and gas accumulations. This study evaluates the petroleum play elements of the Swiss Plateau and thus provides an independent and unbiased view on the occurrence of subsurface hydrocarbon resources within the study area, which is extrapolated to the entire Swiss Plateau.

Zusammenfassung

Mögliche Kohlenwasserstoffvorkommen haben grossen Einfluss auf das Aufsuchen und Erschliessen von Geothermie-Reservoiren sowie möglicher Nutzungen des tiefen Untergrunds als Energie-, oder CO2-Speicher. Der tiefe Untergrund des schweizerischen Molassebeckens zwischen dem Boden- und Genfersee besteht aus einer heterogenen sedimentären Schichtenfolge, welche eine komplexe paläo-geographische, klimatische und tektonische Geschichte hat, die mindestens 300 Millionen Jahre umfasst. Während dieser Periode haben sich Organika-reiche Sedimente abgelagert, was sich in den daraus gebildeten Kohlenwasserstoffen heute manifestiert (Roulavaz, Eclépens und andere). Die hauptsächlich zwischen den 1960er und 1980er Jahren im Rahmen von Kohlenwasserstoffprospektion gewonnenen Daten aus Reflexionsseismik sowie den wenigen Tiefbohrungen zeigen an, dass es zumindest im Hauptuntersuchungsgebiet des Genferseebeckens eine Serie von dichten Reservoiren und Muttergestein gibt, die als mögliche unkonventionelle Erdgas- und Erdölreservoire fungieren könnten. Diese Studie zielt darauf ab, Elemente systematischer Kohlenwasserstoffvorkommen (sogenannte «plays») des schweizerischen Molassebeckens zu bestimmen, darauf abstützend, eine erste unabhängige und unvoreingenommene Abschätzung der Kohlenwasserstoffvorkommen des Untersuchungsgebiets vorzunehmen und diese grob für das gesamte Mittelland zu extrapolieren.

Résumé

Les éventuelles occurrences d'hydrocarbures ont une influence majeure sur la prospection et la mise en valeur de réservoirs géothermiques, ainsi que sur les utilisations possibles des profondeurs souterraines comme stockage d'énergie ou de CO_2. Le sous-sol profond du Plateau suisse du lac Léman au lac de Constance est constitué par une succession sédimentaire hétérogène qui témoigne d'une paléogéographie et une histoire climatique et tectonique complexe durée environ 300 millions d'années. Pendant cette période, des formations riches en matière organique ont été accumulées qui ont généré des hydrocarbures comme indiqué par plusieurs manifestations de surface visibles aujourd'hui (Roulavaz, Eclépens, etc.). Au moins dans le bassin Lémanique, périmètre principale de cette étude, les quelques puits et les données sismiques acquis principalement entre les années 1960 et 1980 pour la prospection d'hydrocarbures, indiquent la présence d'une série de réservoirs à basse perméabilité et des intervalles de 'schistes' qui pourraient constituer des possible réservoirs non-conventionnels de pétrole et de gaz. Cette étude vise à évaluer les éléments du système pétrolier du plateau suisse, ainsi fournir une vue indépendante et impartiale sur la présence des ressources en hydrocarbures du sous-sol de la région étudié et extrapoler celle-ci au Plateau suisse entier.

Table of contents

Figures

Tables

Annexes

1. Introduction

1.1. Project context

A number of geothermal wells drilled in recent years in Switzerland have encountered natural gas, either of biogenic or thermogenic origin. Examples include wells drilled to install ground-source heat pumps in the Pre-alps (Spiez, BE) and in the Swiss Molasse Basin (Oftringen, AG). Another example is the one drilled in 2013 in St. Gallen (SG), which traverses large portions of the stratigraphic records of the Swiss Molasse Basin. This leads to the conclusion that natural gas associated with or encountered during geothermal resource exploration and development is a hazard that needs to be managed (Wyss 2002). There is a non-zero risk that this hazard may con-tribute to a top Health, Safety and Environment" event such as loss of containment, explosions or fires. A technical note from SUVA, the Swiss National Accident Insurance Agency acting in a regulatory capacity, defines hazard levels that depends on, among other things, the regional geology and in particular its hydrocarbon characteristics. When drilling for geothermal resources, it should be good practice to expect the occurrence of hydrocarbons, HS and H_2S which consequently has implication on managing health, safety and environmental aspects. In the case of possible or likely natural gas occurrences, for example, SUVA requires an expert (geo-logical) assessment on the occurrence and the rates and modes of degassing. While hazards in connection with natural gas occurrences arguably may have more severe consequences, those associated with oil should not be neglected.

Safety issues are thus intimately connected to a fundamental question about hydrocarbon occurrences. The 2013 geothermal well SG-1 of the « St. Galler Stadtwerke » (the city's utility company) is a case in point, when the well encountered a natural gas reservoir of unknown but probably limited quantity. This event re-emphasizes the fundamental question of the link between geo-thermal reservoirs and hydrocarbon occurrences. Is it possible that – similar to the case in The Netherlands – hot aquifer geothermal resources in sedimentary basins often contain associated natural gas or even oil? Such considerations have to be addressed to identify hazards and risks during the entire life-cycle of geothermal projects, from prospecting, exploration and development to the abandonment of wells. Based on the knowledge of the likelihood of hydrocarbon occurrences in conjunction with geothermal reservoirs, project developers are well advised to de-rive strategies and measures to deal with such risks.

In the past few years, several projects aimed at assessing the deep geothermal potential and the feasibility for CO_2 capture and storage (CCS) have originated in Europe and more specifically in Switzerland, where the future supply of energy is challenging the scientific community. In parallel, with the advent of large-scale development of unconventional hydrocarbon resources, the industry has gained an interest in exploring such resources in Switzerland. They often speculated on the huge resource potential and the possibility of commercially exploita-ble reserves and thus generated considerable attention from potential investors, cantons and the public – not in the least from the media.

Today hydrocarbons still play an important role in the Swiss energy mix. In 2021, for instance, without consid-ering the fuel consumption that dominates energy supply for transportation, crude oil represents 36.3% of the energy end use whereas gas constitutes 12.8%*. In the future, the role of gas may increase in view of the federal energy strategy, which foresees the installation of gas-fired power stations to respond to the energy (electricity) demand after 2032.

In this context, it has to be considered that the global energy industry is highly competitive, achieving impressive cost reductions in even highly mature markets. Therefore, foreign hydrocarbons supplied to Switzerland will remain the preferred source, unless severe and long-term supply disruptions occur (economical conflicts, terri-torial wars, etc.). Although there is probably only limited scope for developing such resources domestically under

* https://www.eda.admin.ch/aboutswitzerland/en/home/wirtschaft/energie/energie---fakten-und-zahlen.html

current legal circumstances, no independent evaluation by federal or cantonal offices of Switzerland's unconventional hydrocarbon resource potential exists to date. Considering the dominant role that hydrocarbons play today, the intensely debated Swiss energy mix for the future and the questions regarding the security of supply, it is most timely now for Switzerland to have an independent assessment of its indigenous hydrocarbon resources.

The above-mentioned situation emphasizes the need to gain knowledge about the subsurface geology of Switzerland and to assess the potential energetic resources (both fossil and renewable). On this basis, the Swiss Federal Office of Energy (SFOE) and the Federal Office of Topography (swisstopo) have decided to sponsor the joint UNCONGAS project aiming to assess the unconventional resources beneath the Swiss Plateau, a planned geomorphological region included between the Alpine Chain and the Jura Mountain Chains (Figure 1).

The Swiss Plateau forms part of the Swiss Foreland Basin, which comprises a heterogeneous sedimentary succession, documenting a complex paleogeographic, climatic and tectonic history spanning an age of around 300 million years, from the Paleozoic to the present. During this period, a thick series of sedimentary rocks (up to 5000 m thick) composed of carbonates, siliciclastics and evaporites accumulated. Some of these sedimentary formations contain organic-rich layers that are sources of hydrocarbons (oil and gas), as revealed by several surface occurrences visible today (LEU 2012). These occurrences show that a petroleum system *sensu lato* is actually active beneath the Swiss Foreland Basin (Figure 1; AJUABA et al. 2023; DO COUTO et al. 2021; MOSCARIELLO 2019; OMODEO SALÉ et. Al. 2020, 2021). In addition, available data (2D seismic and well data) indicate the presence of tight reservoirs and potential source rocks, which may be investigated as possible unconventional reservoirs of both oil and gas accumulations.

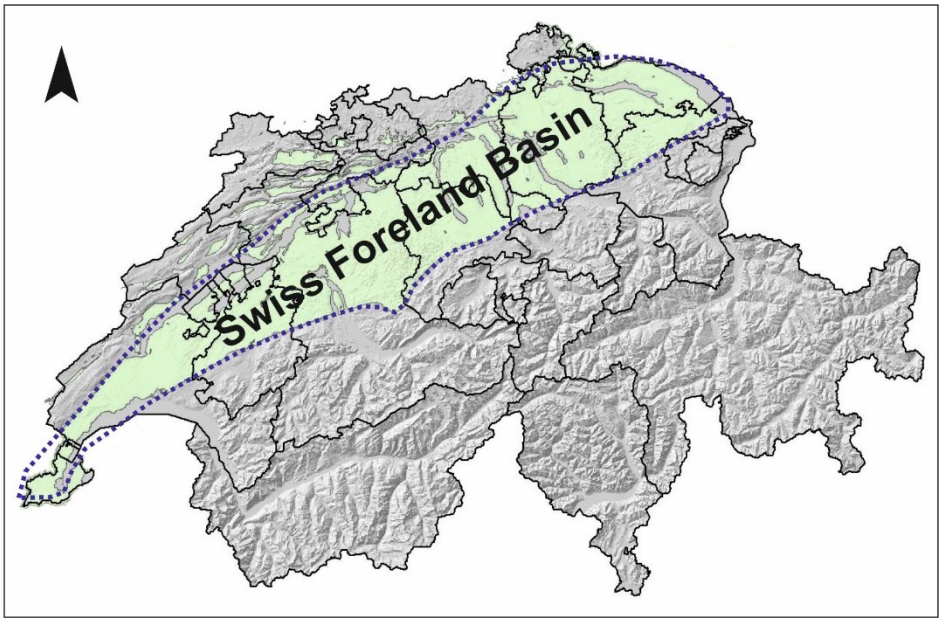

Figure 1: Location of the Swiss Foreland Basin, forming the Swiss Plateau geomorphological area.

The goal of the UNCONGAS project is to evaluate the unconventional petroleum plays of the western Swiss Plateau using relevant accessible data and to provide an independent and unbiased view on the occurrence of subsurface hydrocarbon resources within this region. The strategy is to enhance the pool of existing data and knowledge, filling knowledge gaps by targeting specific study areas in order to get a regional understanding of the unconventional resources.

1.2. Definition of unconventional petroleum geology

The term "unconventional petroleum system" refers to non-conventional oil and gas accumulations generally hosted in low- to very low-permeability rock formations (< 0.1 mD), which can be rather widespread and continuous and which have no obvious trap and caprock nor uniform contacts between gas and oil or oil and water (ZOU 2017; Figure 2). There is actually no clear classification scheme for unconventional accumulations, compared to the conventional accumulation classified on the basis of traps. Unconventional gas accumulations include shale gas, tight-sandstone gas, coal-bed methane (CBM), biogenic gas and natural gas hydrates. Oil and gas accumulation in unconventional reservoirs (volcanic or metamorphic rocks, fracture-cavity carbonate rocks) may also be included in unconventional petroleum resources.

Based on past exploration, ZOU (2017) proposed a method to differentiate the types of unconventional hydrocarbon accumulations according to the reservoir continuity, the migration mechanism and the accumulation pattern. In Figure 2 a classification of unconventional vs. conventional petroleum accumulations is proposed.

To explore the hydrocarbon potential of an area, a series of relevant steps needs to be followed. The first step is to constrain the geological model, determining the geometries of the stratigraphic unit that form the basin infill, their lithological properties and the main structural elements of the area. These elements represent the key parameters controlling the burial depth of the rocks and the main fluid migration paths, which are necessary for the understanding of the generation and migration of hydrocarbons. For the Swiss Plateau, well and seismic data are most commonly used.

Once the geological model is defined, a second step is to identify the source rocks and the reservoirs of the petroleum system. In order to determine the amount and type (oil and/or gas) of hydrocarbons that could be generated in the basin, the potential source rocks are characterized by means of a detailed geochemical screening. Reservoir properties are also defined, so that the geological units with potential hydrocarbon accumulation can be determined. To estimate the volume of hydrocarbons that could be stored, structural and stratigraphical traps are distinguished, mostly by interpreting seismic data.

1.3. Study plan

Launching the UNCONGAS project was possible thanks to the access to a vast data set provided by swisstopo with the authorisation of the National Cooperative for the Disposal of Radioactive Waste (NAGRA) and the «Aktiengesellschaft für Schweizerisches Erdöl (SEAG)» data providers. The agreements between the University of Geneva (UNIGE) and the data providers NAGRA and SEAG were concluded by end of August 2015. Thereafter, all the available digital seismic lines and well data were delivered to swisstopo. These data were integrated in a common exploration project involving the KingdomSuite© and Petrel© (Schlumberger) software suites, including correlation and analysis.

The study was subdivided into four parts, and the following results are described separately in this report:

- **Part 1 (2015-2016)** was dedicated to establishing a solid understanding of a pilot area in the southwestern Swiss Plateau (Canton of Geneva and neighboring France), where most of the data were readily available. In this phase, seven wells (in alphabetic order: Chaleyriat-1, Chatillon-1, Chapéry-1, Charmont-1, Faucigny-1, Humilly-2 and La Chandelière-1D) were inspected, logged and sampled to analyse the potential source-rock and reservoir formations, including the Toarcian shales and the Permo-Carboniferous coal. Then, a comprehensive series of analyses including detailed petrography, inorganic and organic geochemistry were made. A major portion of this period was also dedicated to reaching the agreements with the data providers (swisstopo, NAGRA and SEAG).
- **Part 2 (2016-2017)** was aimed at assessing the potential for subsurface unconventional hydrocarbon resources in the Swiss Plateau region, focusing on the western Swiss Plateau. The particular target was to investigate the geochemistry and the thermal maturity of two important source rocks, the Toarcian Posidonia shale and the Permo-Carboniferous carbonaceous unit. More precisely, the second part of the UNCONGAS project was subdivided into tasks that included (1) seismic interpretation of deep intervals and well-log correlation, (2) detailed geochemical analysis of the source rocks by measuring their vitrinite reflectance, (3) organic geochemistry of biomarkers within the source rocks and the superficial oil and gas seeps.

- **Part 3 (2017)** was devoted to 1D and 3D Basin and Petroleum System Modelling (BPSM) of the pilot area located in the south-western part of the Swiss Plateau (Canton of Geneva).
- **Part 4 (2017)** summarized the calculation methods for estimating the unconventional hydrocarbon resources of the entire Swiss Plateau, using the workflows applied to the south-western part of the Swiss Plateau (Canton of Geneva) and the acquired knowledge. To this end the results of Parts 1 and 2 where extrapolated with the help of data from the GeoMol project of swisstopo. The two main source rocks, the continental Permo-Carboniferous coal-bearing units and the marine Toarcian (Lower Jurassic) black shales, were involved in this work.
-

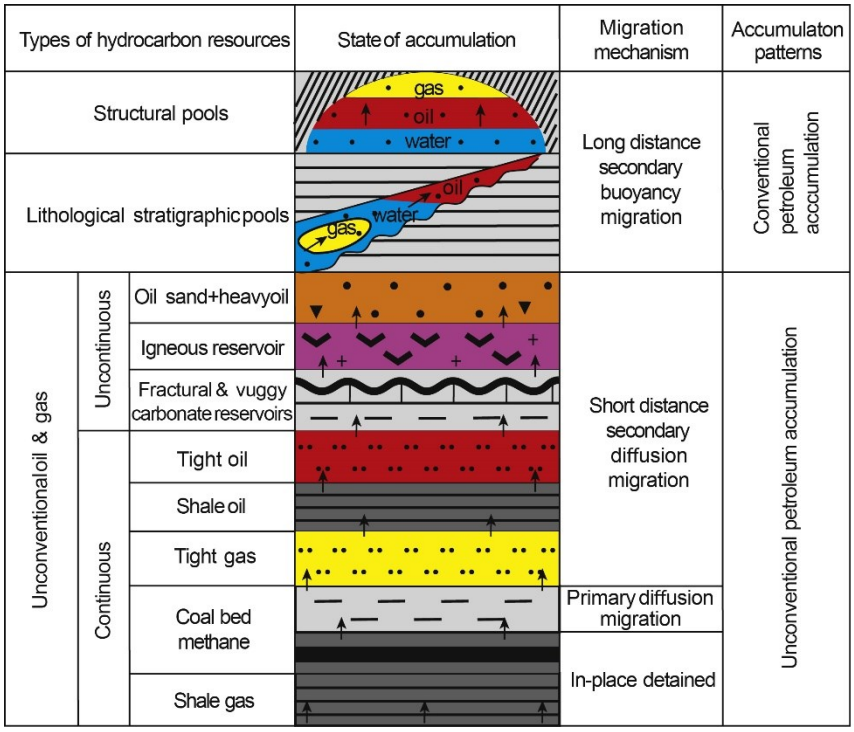

Figure 2: Hydrocarbon resource types and accumulation patterns (ZOU 2017)

1.4. Methodology

In order to characterize the various petroleum plays that have been described in the past and to constrain the unconventional petroleum resources, the UNCONGAS project aimed at distinguishing the different elements comprising the unconventional petroleum system (source rock, reservoir and seal). Hence, UNCONGAS is a multidisciplinary project that investigated the following characteristics:

- spatial distribution and thickness of the potential source rocks and reservoirs
- petrography of potential source rocks, in particular that of the Toarcian (Posidonia) shales, and petrography and spatial variability of the reservoirs
- inorganic geochemistry (major and trace elements) of the source rocks and reservoirs
- organic geochemistry and maturation of the source rocks.

1.4.1. Interpretation of the subsurface geology

A large set of 2D seismic data provided by NAGRA and SEAG via swisstopo (Figure 3), combined with data from several wells, was used to define the spatial distribution and thickness of the potential source rocks and reservoirs. The interpretation of the seismic lines is still ongoing and is thus not detailed in this report.

The agreements with our partners swisstopo, NAGRA and SEAG provided UNIGE with access to the seismic lines and interpretations used within the scope of the GeoMol project. Access to the majority of the data is

restricted. Because of the current situation in Switzerland regarding data access and management, each canton manages its own subsurface data, resulting in a non-harmonised dataset. The datum (level of reference) used in acquiring and processing the seismic lines is also not consistent. Therefore, in this project many seismic lines throughout the Swiss Plateau require vertical shifts to enable correlation within the area of study (Figure 4). This process of manual shifting is ongoing, beginning at the French-Geneva border area and progressing eastward.

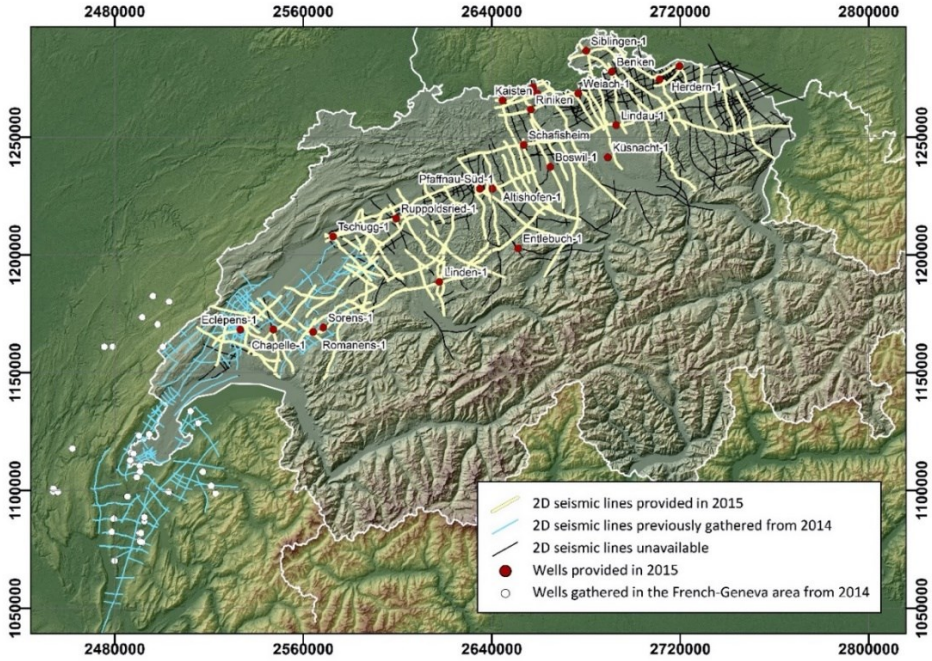

Figure 3: Location map of the 2D seismic lines received in 2015 and the seismic lines gathered over many years at the University of Geneva. Red dots are the wells received in 2015 and provided by swisstopo.

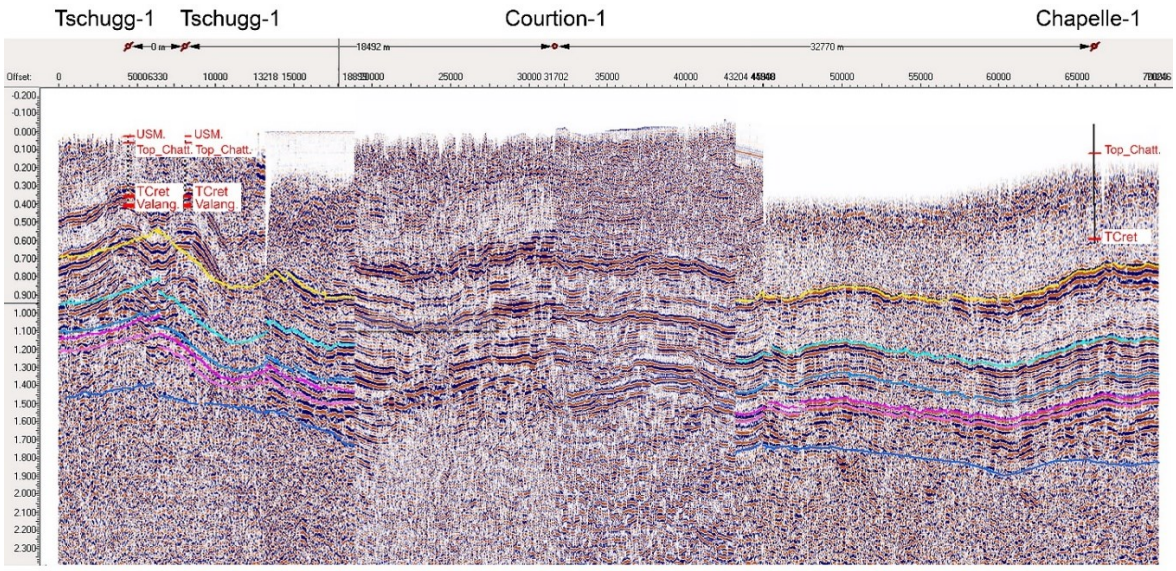

Figure 4: Screen capture showing the current state of the seismic line mismatch: arbitrary lines located between the Tschugg-1 and Chapelle-1 wells. In this case, time-demanding manual vertical shifts need to be applied line by line before starting the actual seismic interpretation.

1.4.2. Analytical workflow

The workflow used to perform all the analyses of the unconventional petroleum systems of the Swiss Plateau can be summarized as follows (Figure 5):

- A petrographic analysis is performed using the QEMSCAN high-resolution and automated petrographic solution, which also help to analyse the 2D porosity of each sample and identify the clay fraction.
- The QEMSCAN analysis is coupled with X-ray diffraction to identify more specifically the small clay fraction that cannot be recognized by QEMSCAN analysis because of its small size or complex chemistry.
- In parallel, a complete geochemical analysis is carried out on each sample, measuring both major and trace elements by the ICP-MS method (Inductively Coupled Plasma Mass Spectrometry), which helps to correlate the rock chemistry with its petrography and to identify possible chemostratigraphic trends in the wells.
- The rock's organic geochemistry is analysed in two to three steps, from the classical Rock-Eval pyrolysis (to characterize the amount and actual state of the remnant organic matter enclosed in the rock) to the vitrinite reflectance analysis (to investigate the thermal maturity of the organic matter) and, when possible, to the biomarker analysis (to determine the origin and migration of currently existing petroleum deposits).
-

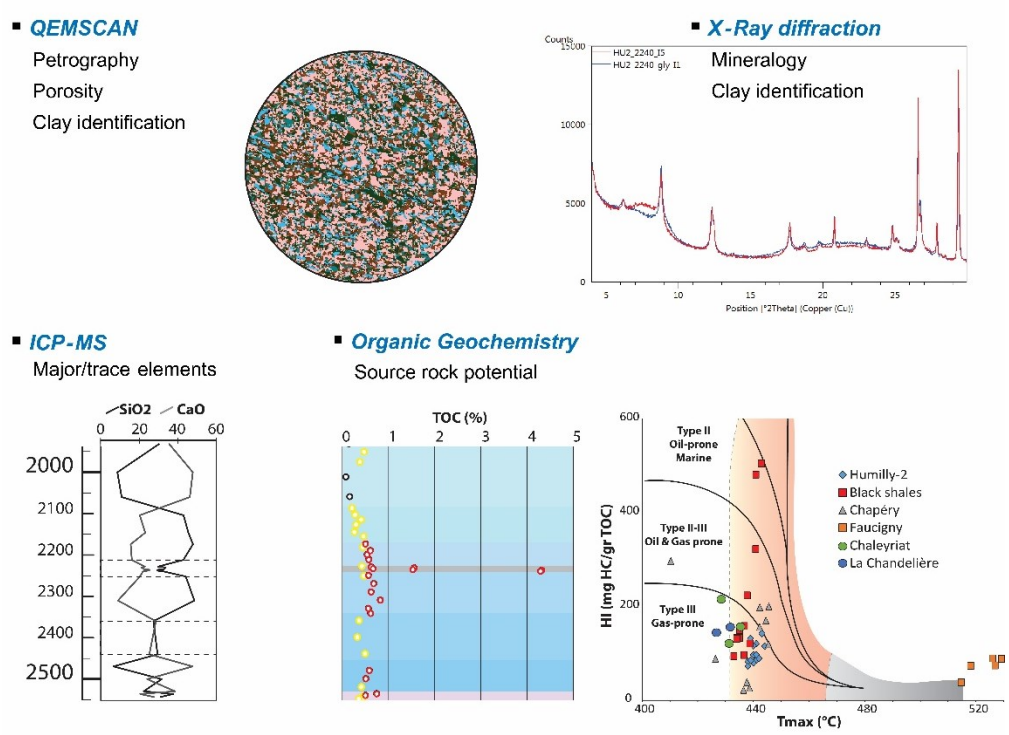

Figure 5: Depiction of the analytical workflow in the UNCONGAS project. See the text for details.

1.4.3. Modelling

Modelling (BPSM) is an excellent tool for reconstructing the thermal history of a basin and simulating the formation of oil and gas accumulations in the basin. It permits to take into account of a large number of geological variables (e.g. lithology, thickness, geometry, heat flow, compaction factor, fluid circulation, faulting, type of organic matter etc.), and to quantify their effect on the thermal maturation of the organic matter and the hydrocarbon generation, migration and accumulation. In this work the Geneva Basin area was modelled, integrating geological and geochemical information.

2. UNCONGAS Part 1 (2015–2016) Preliminary prospection

2.1. Geological settings and data

The south-western Molasse Basin (our first study site), also defined as the Geneva Basin, forms an asymmetric foreland basin characterized by an erosional north-western border along the Jura Mountains and a thrusted south-easters border hidden beneath the Alpine nappes (Figure 6). The Geneva Basin is bounded by (1) the Jura Mountains toward the NW, forming an arcuate fold-and-thrust belt and (2) the Alpine units toward the SE, forming a nappe stack (Figure 6).

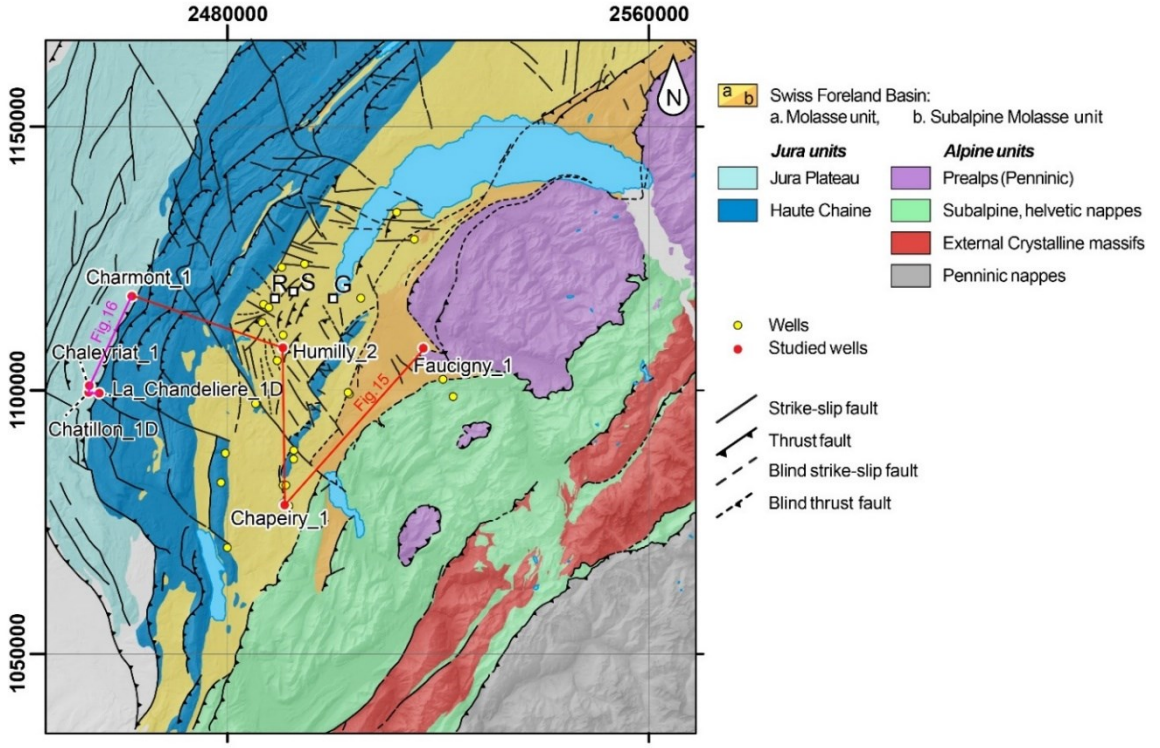

Figure 6: Geological map of the study area showing the location of the wells used for the source-rock analysis.

The Geneva Basin consists of a thick Mesozoic and Cenozoic sedimentary cover (3000-5000 m thick), which overlies the Variscan crystalline basement gently dipping S-SE (1°-3°). The oldest units do not outcrop in the basin but are described in the literature through the information from several wells (CHAROLLAIS et al. 2007, GORIN et al. 1993, SIGNER & GORIN 1995, SOMMARUGA et al. 2012). Above the crystalline basement, the stratigraphic succession extends from the Late Carboniferous to the Quaternary (Figure 6) and can be summarized as follows:

- Late Carboniferous and Permian siliciclastic sediments, containing coals beds, were deposited in southwest-northeast-oriented grabens and constitute relatively small confined basins.
- The Triassic period is marked by the deposition of shallow marine sediments in an epicontinental sea environment. The Lower Triassic (Buntsandstein) is characterized by the deposition of sandstone. It is overlain by Middle Triassic carbonates and dolomites (Muschelkalk) as well as a thick sequence of evaporites (Keuper).
- The deposition of marls and shales during the Lower Jurassic (Lias) evolved into limestones and carbonaceous shales from the Middle to Upper Jurassic (Dogger and Malm).

- The Lower Cretaceous is marked by carbonate platform deposits with bioclastic limestone, whereas the Upper Cretaceous record is missing. A major subaerial erosional surface affecting the top of the Lower Cretaceous is associated with the development of karst, which was filled by oxidized continental deposits attributed to the Late Eocene. Thus the unconformity ranges between the Lower Cretaceous and the Eocene.
- Eocene to Late Miocene siliciclastic deposits of marine and continental origin form the Molasse wedge above the Mesozoic series. The Subalpine Molasse, involved in a series of imbricated thrust sheets, is composed of clastic sandstone and marls of either a marine or a continental freshwater depositional environment, while the rest of the Molasse units (located in the Swiss Foreland Basin) comprises mostly clastic sediments of continental origin.

2.1.1. Petroleum system elements

A common exploration approach in the identification of a petroleum system is to define the Petroleum System Elements (PSE) such as the source rocks, reservoirs, seal and the overburden rocks (MAGOON & DOW 1994). According to the literature and well data, only two major source rocks are defined in the stratigraphic succession of the Swiss Plateau (Figure 6): the Permo-Carboniferous coals and the Lower Jurassic shales (known as the Posidonia or Toarcian shales). In contrast, a wide range of potential reservoirs has been recognized from the Permo-Carboniferous / Lower Triassic sandstones to the Middle and Upper Jurassic carbonates, as well as in the Lower Cretaceous carbonates and the Molasse sandstones. These reservoirs are characterized by a broad spectrum of lithologies and degree of compaction. Consequently, their respective porosity and permeability, which are insufficiently described in the literature, may vary greatly. One of the most significant sealing formations in the western Molasse Basin is the thick dolomitic and evaporitic succession of the Trias (Muschelkalk and Keuper). The Lower Jurassic deposits are mostly shales ad thus may also act as a regional seal.

Consequently, many petroleum plays have been envisaged in the past, such as (1) gas accumulation in the Permo-Carboniferous sandstones, (2) coal-bed methane in the Permo-Carboniferous, given the numerous coal intercalations and (3) oil and/or gas accumulation in the Mesozoic and Cretaceous carbonates as well as (4) the Cenozoic sandstones comprising the Molasse.

2.1.2. Sample collection

Among the seven sampled wells, the Humilly-2 well, located near the French border (Figure 6) and spanning the complete stratigraphic succession from the Permo-Carboniferous to the Molasse, was sampled at regular and high-resolution intervals throughout the succession. The other six wells (Chaleyriat-1, Chatillon-1D, Chapéry-1, Charmont-1, Faucigny-1, and La Chandelière-1D) were sampled at only two specific stratigraphic levels: the Permo-Carboniferous coals (if retrieved from the wells) and the Lower Jurassic shales. It should be noted that during the on-site well description and sampling, the most favourable lithologies had already been taken from cores or cuttings and were thus not available for this study.

Table 1: *Summary samples collected from each well and of the repartition of the analyses performed on samples from specified wells.*

Well	Total number of samples	Plugs and fragments	Cuttings	QEMSCAN	ICP-MS	Rock-Eval pyrolysis	Vitrinite reflectance
Chaleyriat-1	10	5	5	5	5	5	0
Chatillon-1D	8	6	2	2	1	1	1
Chapéry-1	24	9	15	6	14	11	4
Charmont-1	9	1	8	2	4	8	3
Faucigny-1	28	20	8	6	7	7	2
Humilly-2	186	47	139	85	68	142	4
La Chandelière-1D	10	6	4	4	4	4	0

A total of 186 samples were taken along the entire length of the Humilly-2 well and at a particularly higher sampling rate within the Toarcian layers. From the other six wells, a total of 89 samples were collected (see Table 1, Table 2 and Table 3).

Table 2: *Depth and type of samples taken from the Humilly-2 well with the corresponding age according to the final well report (S.N.P.A., 1969). Thick intervals denote double or triple samples separated by their macroscopic lithofacies. In the Toarcian stratigraphic interval, the Posidonia Shales are marked in bold and by (*). Cut: cuttings; Plug: core plug; Frag: fragment.*

Humilly-2		
Depth	**Age**	**Type**
70	Oligocène	Cutting
103		Cutting
140		Cutting
170		Cutting
190		Cutting
230		Cutting
260		Cutting
280		Cutting
310		Cutting
340		Cutting
360		Cutting
380		Cutting
410		Cutting
430	Eocene	Cutting
432		Cutting
458	Barremian	Cutting
470		Cutting
490		Cutting
513		Cutting
538		Cutting
550		Cutting
562	Hauterivian	Cutting
582		Cutting
602		Cutting
622		Cutting
642		Cutting
658		Cutting

Depth	**Age**	**Type**
682	Valang.	Cutting
702		Cutting
722	Berriasian	Cutting
750		Cutting
774		Cutting
782		Cutting
790		Cutting
800		Cutting
808		Cutting
812		Cutting
816	Tithonian	Cutting
824		Cutting
832		Cutting
840		Cutting
848		
856		Cutting
868		Cutting
876		Cutting
884		Cutting
892		Cutting
904		Cutting
940		Cutting
958		Cutting
978		Cutting
994		Cutting

Depth	**Age**	**Type**
1015.5	Kimmeridgian	Plug
1020.5		Plug
1024		Cutting
1052		Cutting
1108		Cutting
1122		Cutting
1144		Cutting
1176		Cutting
1206		Cutting
1230		Cutting
1300	Oxfordian	Cutting
1350		Cutting
1402		Cutting
1450		Cutting
1504		Cutting
1550		Cutting
1574		Cutting
1604		Cutting
1652		Cutting
1700		Cutting
1742		Cutting
1808		Cutting
1846		Cutting
1852.4		Plug
1853.2		Frag
1854.6		Plug

Depth	**Age**	**Type**
1857.3	Bathonian	Plug
1860.8		Plug
1864		Cutting
1900		Cutting
1912		Cutting
1932		Cutting
1952	Bajocian	Cutting
1976		Cutting
1997.3		Plug
2000.1		Frag
2001.2		Plug
2003.5		Plug
2012		Cutting
2060		Cutting
2088	Aalenian	Cutting
2104		Cutting
2116		Cutting
2128		Cutting
2146		Cutting
2156		Cutting
2174	Toarcian	Cutting
2182		Cutting
2190		Cutting
2200		Cutting
2212		Cutting
2228		Cutting
2230		Cutting
2232*		Cutting
2234*		Cutting
2236*		Cutting
2238*		Cutting
2240*		Cutting

Depth	**Age**	**Type**
2250	Pliensbachian	Cutting
2252		Cutting
2270		Cutting
2290		Cutting
2310		Cutting
2330		Cutting
2342		Cutting
2360	Sinemurian	Cutting
2400		Cutting
2440		Cutting
2469.3		Plug
2480		Cutting
2500		Cutting
2520		Cutting
2529.1		Plug
2529.3		Plug
2532	Rhetian	Frag-ment
2536		Cutting
2540		Cutting
2543		Cutting
2546	Keuper	Cutting
2549		Cutting
2580		Cutting
2610		Cutting
2640		Cutting
2670		Cutting
2710		Cutting
2726		Cutting
2742		Cutting
2752		Cutting
2782		Cutting
2812		Cutting
2842		Cutting
2862		Cutting
2884		Cutting

Depth	**Age**	**Type**
2900	Muschelkalk	Cutting
2904.7		Frag
2905.5		Frag
2907		Plug
2907.4		Plug
2908		Plug
2910		Plug
2916.6		Plug
2917.2		Frag
2922.5		Plug
2925.1		Fragment
2927.8		Plug
2929.1		Fragment
2930.3		Plug
2942		Cutting
2951.4		Plug
2958.5		Plug
2966.1		Plug
2966.2		Plug
2980		Cutting
2990		Cutting
3020		Cutting
3027		Cutting
3028.3	Buntsandstein	Plug
3034.5		Frag
3035		Plug
3037.4		Plug
3037.5		Frag
3038		Plug
3038.5		Plug
3039.3	Carbo-nifer	Plug
3039.8		Plug
3049		Cutting

Table 3: *Depth of samples collected from the Chaleyriat-1, Chatillon-1, Chapéry-1, Charmont-1, Faucigny-1, and La Chandelière-1D wells with their corresponding ages according to the final well reports (ESSO REP, 1970a, 1970b, 1989, 1990, 1992a, 1992b).*

Chapéry-1		
Depth	**Age**	**Type**
3600.2	**Dogger**	Plug
3605.6	**Upper Lias**	Plug
3624.0		Cut
3642.0		Cutting
3669.0		Cutting
3670.0		Cutting
3677.0		Cutting
3695.7	**Lower Lias**	Plug
3702.3		Plug
3707.4		Cutting
3719.4		Cutting
3719.8		Cutting
3720.8		Cutting
3720.9		Cutting
3722.7		Cutting
3728.8		Cutting
3948.5	**Muschelkalk**	Plug
3950.9		Fragment
3952.6	**Buntsandstein**	Plug
3953		Plug
4000.5	**Permo-Carbonifer-ous**	Plug
4084.0		Cutting
4114.0		Cutting
4136.0		Cutting

La Chandelière-1		
Depth	**Age**	**Type**
1130.0	**Lias**	Cutting
1150.0		Cutting
1553.2	**Buntsandstein**	Fragment
1556.1		Plug
1557.5		Plug
1558.5		Plug
1561.6	**Permo-Carbonifer-ous**	Plug
1562.1		Fragment
1565.2		Plug
1565.6		Plug

Chaleyriat		
Depth	Age	Type
480	**Lias**	Cutting
510		Cutting
560		Cutting
1251	**Muschelkalk**	Fragment
1252.4		Plug
1266.4		Plug
1320.1	**Buntsandstein**	Plug
1326.5		Plug
1332.5		Plug
1365.0	**Permo-Carbonifer-ous**	Cutting

Charmont-1		
Depth	**Age**	**Type**
1748.6	**Buntsandstein**	Fragment
1753.9		Plug
1798.0	**Permo-Carbonifer-ous**	Sidecore
1825.0		Sidecore
1892.0		Sidecore
1894.0		Sidecore
1920.0		Sidecore
2023.0		Sidecore
2108.5		Sidecore

Chatillon		
Depth	Age	Type
1548.0	**Buntsandstein**	Plug
1554.3		Plug
1570.5	**Permo-Carbonifer-ous**	Plug
1575.6		Plug
1578.5		Fragment
1583.7		Fragment
1589.6		Plug
1592.6		Plug

Faucigny-1		
Depth	**Age**	**Type**
3038.8	**Kimmeridgian**	Plug
3039.4		Plug
3040.6		Plug
3041.5		Plug
3042.4		Plug
3043.1		Plug
3642.8	**Oxfordian**	Plug
3649.1		Plug
3897.5	**Dogger**	Plug
3900.6		Plug
4001.0		Cutting
4007.0	**Lias**	Cutting
4015.0		Cutting
4020.0		Cutting
4026.0		Cutting
4027.0		Cutting
4035.0		Cutting
4464.2	**Muschelkalk**	Plug
4466.0		Plug
4469.0		Plug
4470.5		Plug
4577.2	**Buntsandstein**	Plug
4588.9	**Permo-Carbonifer-ous**	Plug
4592.8		Plug
4593.4		Plug
4715.9		Fragment
4806.1		Plug
4948.0		Plug

2.2. Results and interpretation

2.2.1. Inorganic petrography and geochemistry

a) Petrography of the Toarcian shale from the Humilly-2 well

Sample analysis involved 110 QEMSCAN measurements, an integrated and automated mineralogical and petrographic technique providing quantitative characterization of minerals and rocks (GOTTLIEB et al. 2000; PIRRIE et al. 2004). In the following, the results of the Lower Jurassic shale petrography are described.

The Posidonia shales of Toarcian age (Lower Jurassic) are considered as a potential seal for underground storage of CO_2 (CHEVALIER et al. 2010) in the Molasse Basin. They have also been considered as potential source rocks, given their high content in organic matter (LEU & GAUTSCHI 2014).

In the Humilly-2 well, 71 m of Toarcian shales (between 2169 and 2240 m MD) containing 8 m of bituminous black shales (2232-2240 m MD) were encountered. Eight samples of cuttings, of which six are from the black shale succession, were analysed with the QEMSCAN (Figure 7). From a macroscopic point of view, the sample material appears homogeneous. However, the QEMSCAN analysis revealed various cutting fragments that correspond to distinct lithofacies (Figure 7). The cuttings mostly comprise calcitic fragments (light purple) and clay fragments (green).

The highlights of this analytical work are as follows:

- The results of QEMSCAN analysis (Figure 7) were integrated with X-ray diffraction (XRD) analysis (see for instance Figure 8) on clays. The XRD measurements were carried out on the black-shale interval (2232-2240 m) with the smallest particle size.
- At 2228 and 2236 m, two other types of fragments can be recognized: one mostly comprising fluoro-apatite (and confirmed by XRD measurement) and the other made of pyrite. The pyrite embedded within the shaley fragments shows a framboid morphology (SEM images; Figure 9).
- The complete analysis of the Toarcian shales from the Humilly-2 well allows us to build a modal mineralogy chart (Figure 10). This chart shows mineral percentage calculated from the false colour image of the QEMSCAN measurements. Therefore, each line represents the areal percentage of each mineral phase recognized by the QEMSCAN within one sample of drill cutting.

The black shales from the Humilly-2 well (indicated by the red rectangle in Figure 10) are mostly composed of clays, calcite, silty quartz, pyrite and fluoro-apatite. Most of the clay fraction comprises illite, kaolinite, chlorite, illite-smectite and hydroxy-interlayered minerals (HIM; Figure 10). The calcitic component of the section displayed in Figure 10 shows a decreasing trend from the Sinemurian towards the base of the Toarcian, followed by a slight increase upward within the Toarcian that continues to the Aalenian. Such a trend is in accordance with the macroscopic observations (see stratigraphic log in Figure 10). However, the change from shales to carbonates does not appear as abrupt as in the description of the borehole (S.N.P.A., 1969). This difference is most probably due to the fact that drill cuttings are partially mixed and contaminated by overlying layers as they are brought to the surface by circulating drilling fluids.

The next step consisted of establishing a list of lithofacies characteristics of one interval (such as the clay or the calcitic fragments) and investigating their distribution as a function of depth.

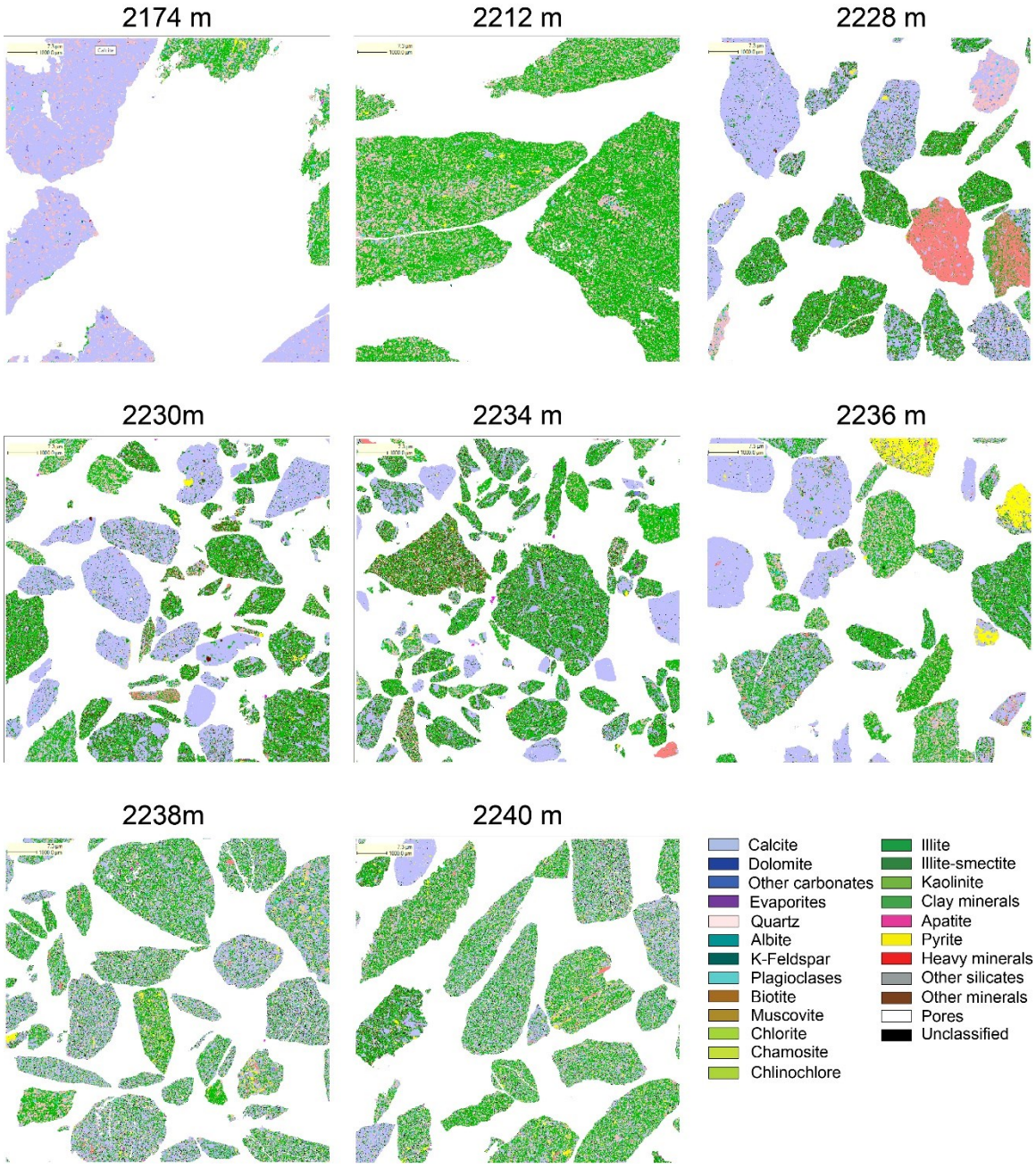

Figure 7: QEMSCAN images of the Humilly-2 well Toarcian cuttings showing minerals and textures in false colours. Samples 2234, 2236, 2238 and 2240 are within the black shales interval. The legend is shown in the lower right corner.

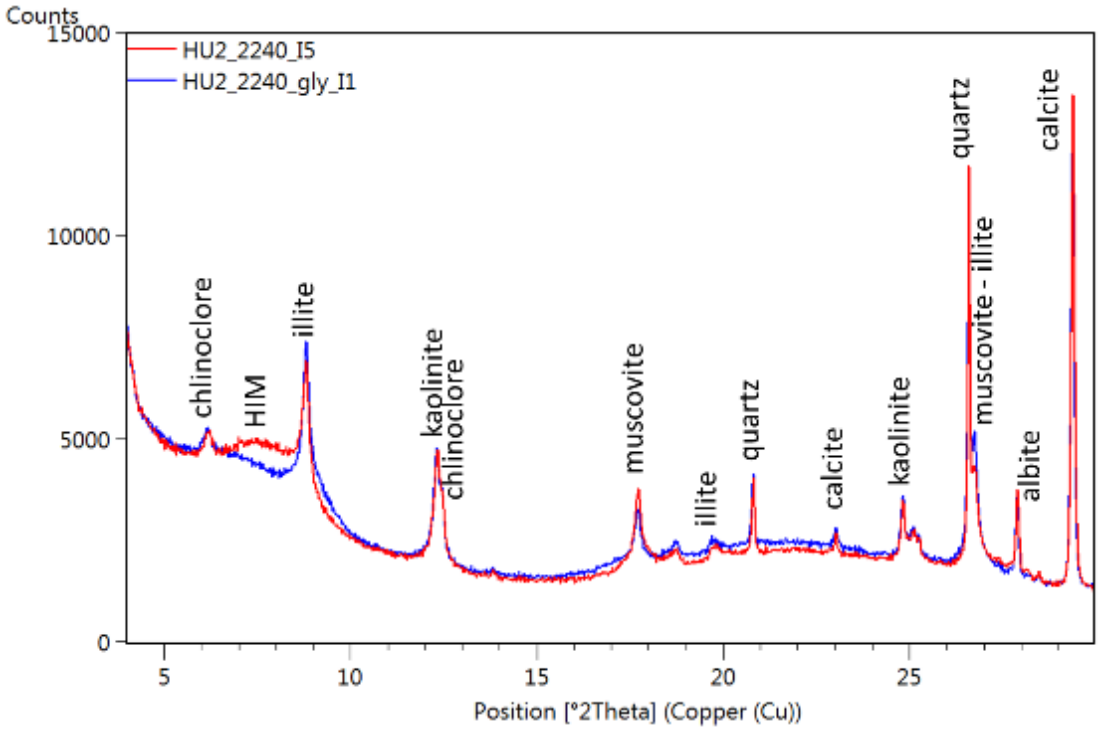

Figure 8: X-ray diffractogram of a sample of the Toarcian black shale from the Humilly-2 well taken at a depth of 2240 m. Red curve: air-dried sample measured without treatment. Blue curve: ethylene-glycol saturated sample to identify the nature of the non-swelling clays in particular illite-smectite mixed-layer clays (HIM: hydroxy-interlayered minerals)

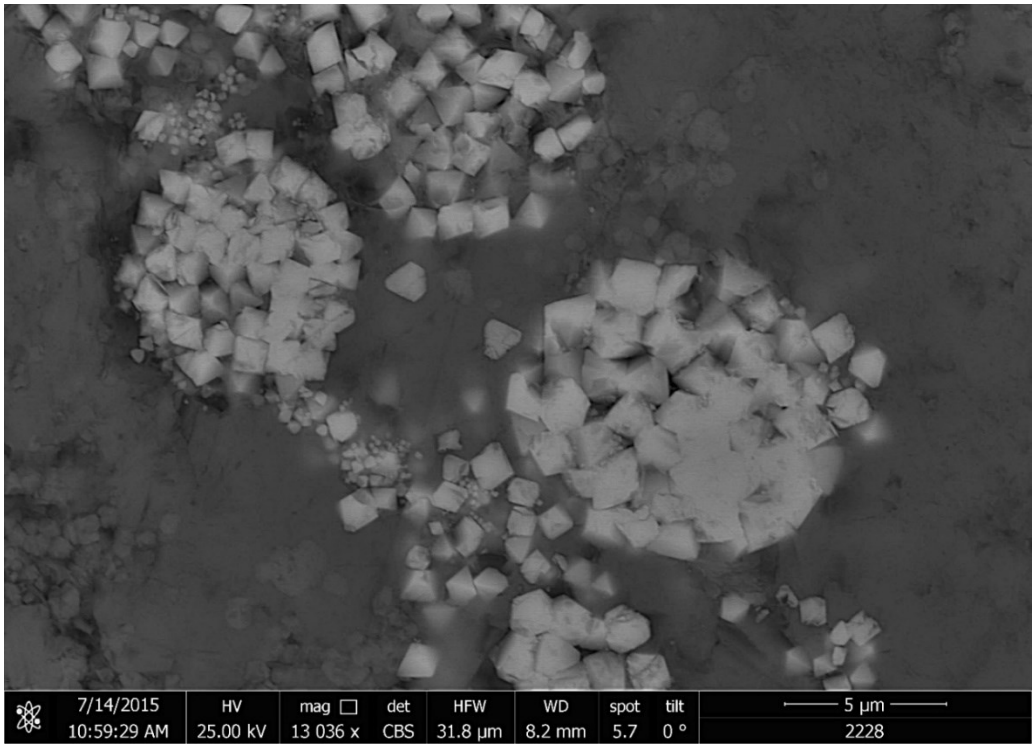

Figure 9: SEM picture of framboid pyrite in the black shale of the Toarcian (sample taken at 2228 m MD from the Humilly-2 well).

b) Geochemistry of the Toarcian shale from the Humilly-2 well

Parallel to the petrographic investigation, total whole-rock geochemistry characterization (ICP-MS) determined both major (Si, Al, Fe, Mg, Ca, Na, K, Ti, P, Mn and Cr) and trace element (metallic elements, U, Th, V and REE) abundance. In the Lower to Middle Jurassic section of the Humilly-2 well (Figure 11), the geochemical trends of SiO_2 and CaO appear anti-correlated. The SiO_2 content sharply decreases in the black shale interval, while the CaO content simultaneously increases to a slight degree (Figure 11). Comparison with the QEMSCAN measurements shows that the geochemical trends in CaO and SiO_2 are fairly well represented by the proportional trends in calcite and quartz (Figure 10).

Phosphate, as well as incompatible and metallic elements (U, Mo, Cu, Zn, Cd, V), are relatively enriched in the Toarcian section of the Humilly-2 well (Figure 11). The high phosphatic content is a common feature of anoxic shales even though the concentration and precipitation processes are still debated (TRIBOVILLARD et al. 2006). In the Toarcian shales from the Humilly-2 well, the phosphatic enrichment is characterized by the occurrence of (fluoro-) apatite of diagenetic origin as can be seen in the sample located at 2228 m MD (Figure 7). The metallic enrichment is clearly visible at the bottom of the black shale interval (Figure 11) and does not prevail towards the top. This observation suggests that anoxic conditions remained active only for short time.

c) Petrography and geochemistry of the Lower Jurassic shale in the Molasse Basin

QEMSCAN analyses were also carried out on the Lower Jurassic shale from the Chaleyriat-1, Chapéry-1, Faucigny-1 and La Chandelière-1D wells. In Figure 12, three different images of these wells are presented to compare the variability of the sample petrography. In the drill cuttings from the Chapéry-1 well, except for the two lower ones at 3722.7 and 3719.8 m (MD), the clay fraction is mostly, if not exclusively, composed of illite (CHY in Figure 12). The silty quartz and calcitic fractions are relatively low compared to those of the Humilly-2 well (Figure 10). The petrography of the Lower Jurassic shales from the Faucigny-1 well (FAY in Figure 12) is similar to that of the shales from the the Humilly-2 well, albeit a higher quartz and a lower calcite fraction (Figure 10 and Figure 12). Between the La Chandelière-1D (LCD in Figure 12) and the Chaleyriat-1 (CYT in Figure 12) wells, the petrography of the Toarcian shales differs. The shales from the former constitute siltsone with calcitic cement, whereas those from the latter are richer in kaolinite and illite than in quartz and calcite.

The average geochemistry of the major elements of the Lower Jurassic shales is summarized in Figure 13. In agreement with the results of the QEMSCAN analysis, the average geochemical composition of the Lower Jurassic shales from the Faucigny-1, Chapéry-1 and Humilly-2 wells are rather similar to each other. In contrast, the average geochemical composition of the La Chandelière-1D and Chaleyriat-1 well samples (both located along the Jura Mountain chain) shows a higher SiO_2 content and in the latter a much higher Al_2O_3 content than all the other wells. The different mineralogical compositions suggest varying distances from the sediment sources. The higher SiO_2 and Al_2O_3 contents in the well samples from the proximity of the Jura Mountains (La Chandelière-1D and Chaleyriat-1 wells) indicates a higher supply of terrigenous material than that from the central part of the basin. Thus, a closer sediment source at the time of deposition can be suggested for the related area, which would agree with their marginal position. In the centre of the basin (location of the Humilly-2 and Chapéry-1 wells), the facies of the Toarcian shales and their petrography are similar, indicating more uniform depositional environmental conditions.

The paleogeography of the Swiss Plateau during the Early Jurassic is an important parameter for predicting and understand the petrographic variation of the organic-rich shales of the Lias. Regional paleogeographic reconstructions of the Early Jurassic (Figure 14) show that the most significant black shale deposits occurred in the area of present-day Germany and France with a southward facies change from organic shale to shallower deposits. However, in the Swiss Plateau an organic-matter enrichment can be observed toward the south, probably as a result of the basin deepening in this direction, permitting more favourable conditions for organic matter preservation.

A balanced cross-section between the Mont-Blanc massifs and the Jura Mountains reveals a total crustal shortening of approximately 46 km along the cross-section (BELLAHSEN et al. 2014; lower part of Figure 14). The reconstruction of the Upper Cretaceous cross-section is evidence of a great distance separating the Jurassic layers of the La Chandelière-1D, Humilly-2 and Faucigny-1 wells (lower part of Figure 14) and thus explains the facies variation in the basin.

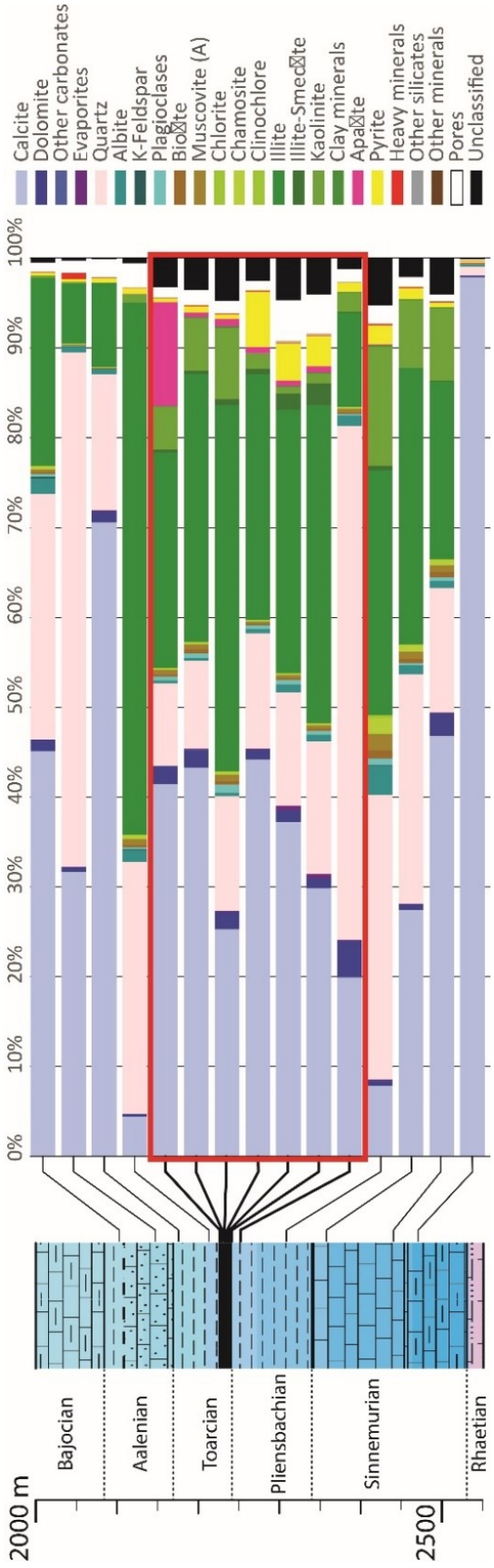

Figure 10: Modal mineralogy chart (in wgt%) of the analyzed samples from the Humilly-2 well. Depth are in m. The black shale succession of the Toarcian is surrounded by a red frame.

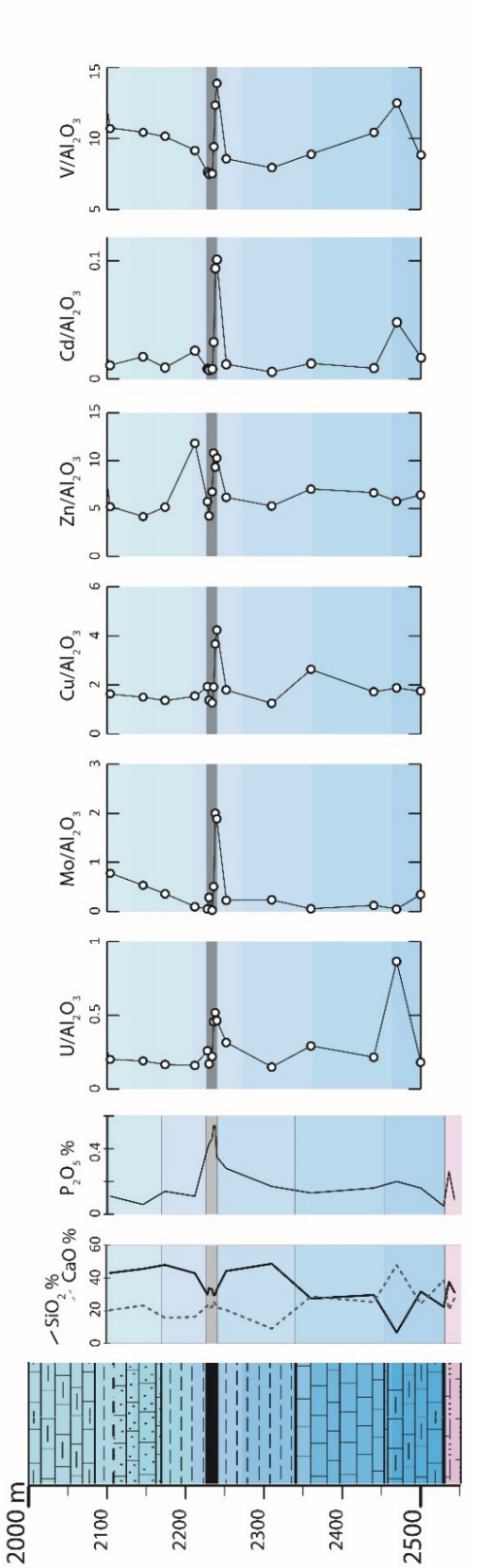

Figure 11: Concentrations of SiO_2, CaO and P_2O_5 (in wgt%) compared with geochemical trends (U, Mo, Cu, Zn, Cd and V in ppm) normalised to aluminium content (Al_2O_3 in wgt%).

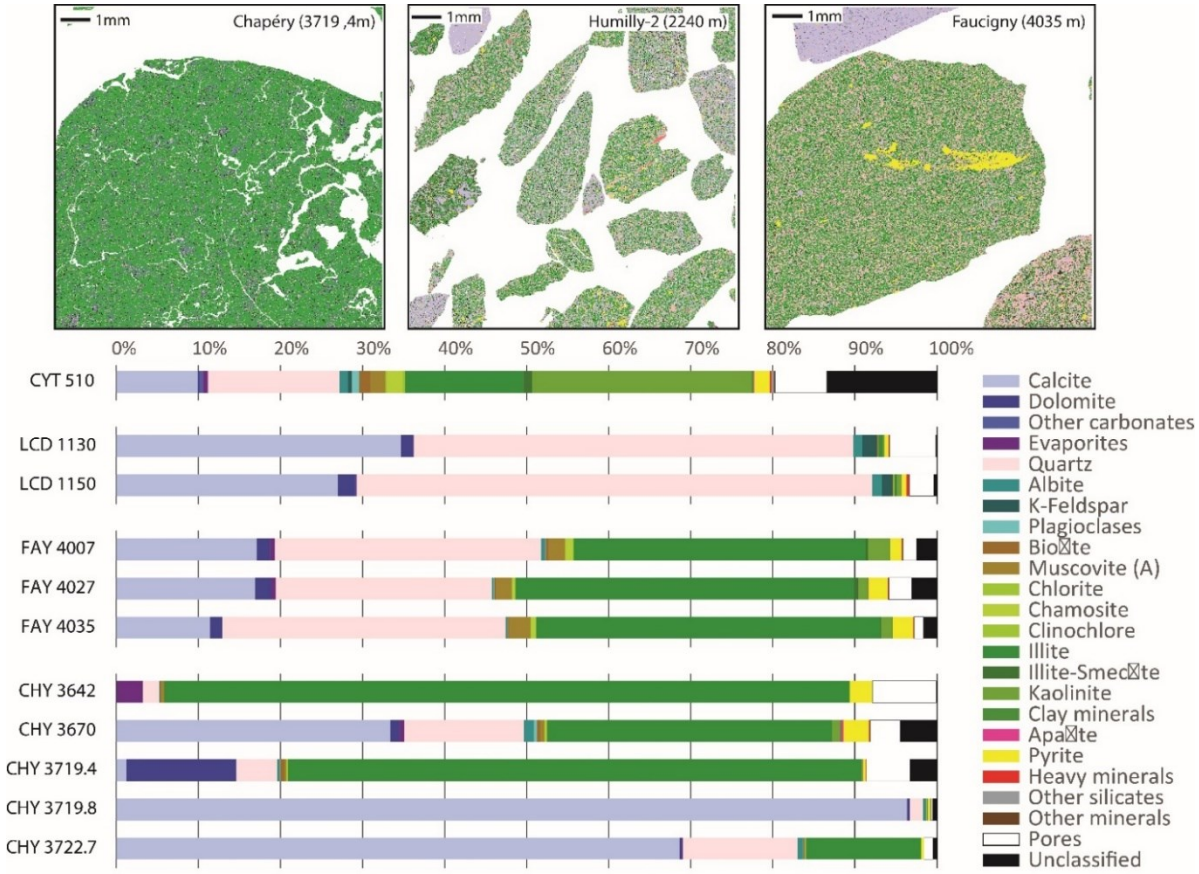

Figure 12: Above: QEMSCAN images of the Humilly-2 well Toarcian cuttings from the Chapéry-1, Humilly-2 and Faucigny-1 wells samples, showing minerals and textures in false colours. The legend is shown in the lower right corner. Below: the modal mineralogy chart of the analysed Lias shale samples from the Chaylerat-1 (CYT), La Chandelière-1D (LCD), Faucigny-1 (FAY) and Chapéry-1 (CHY) wells.

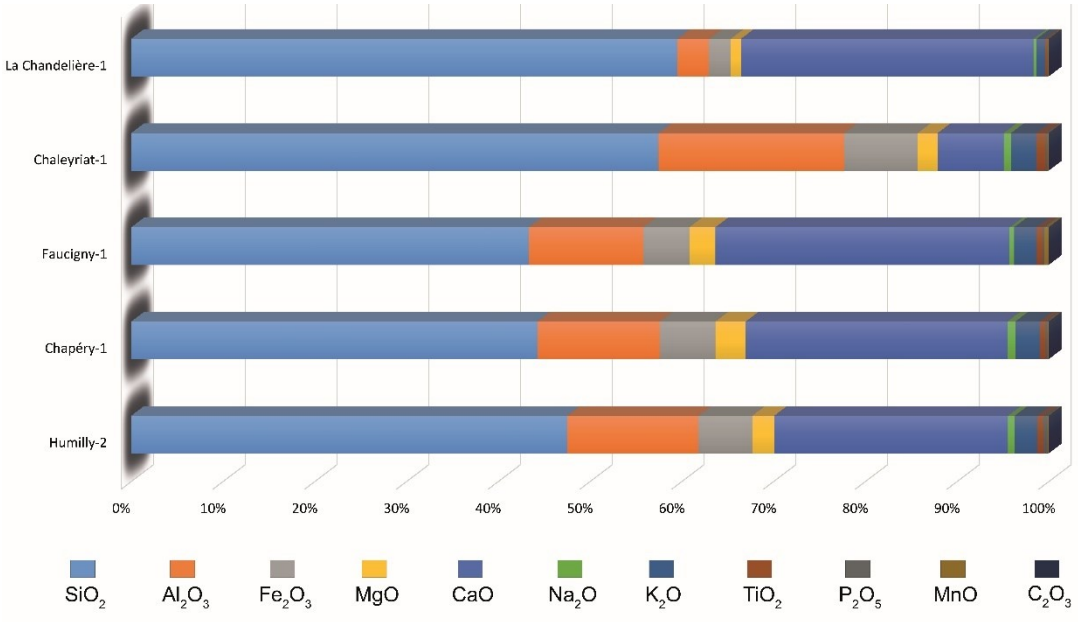

Figure 13: Average geochemical composition (in weight %) of the Lower Jurassic shales from some wells of the studied area.

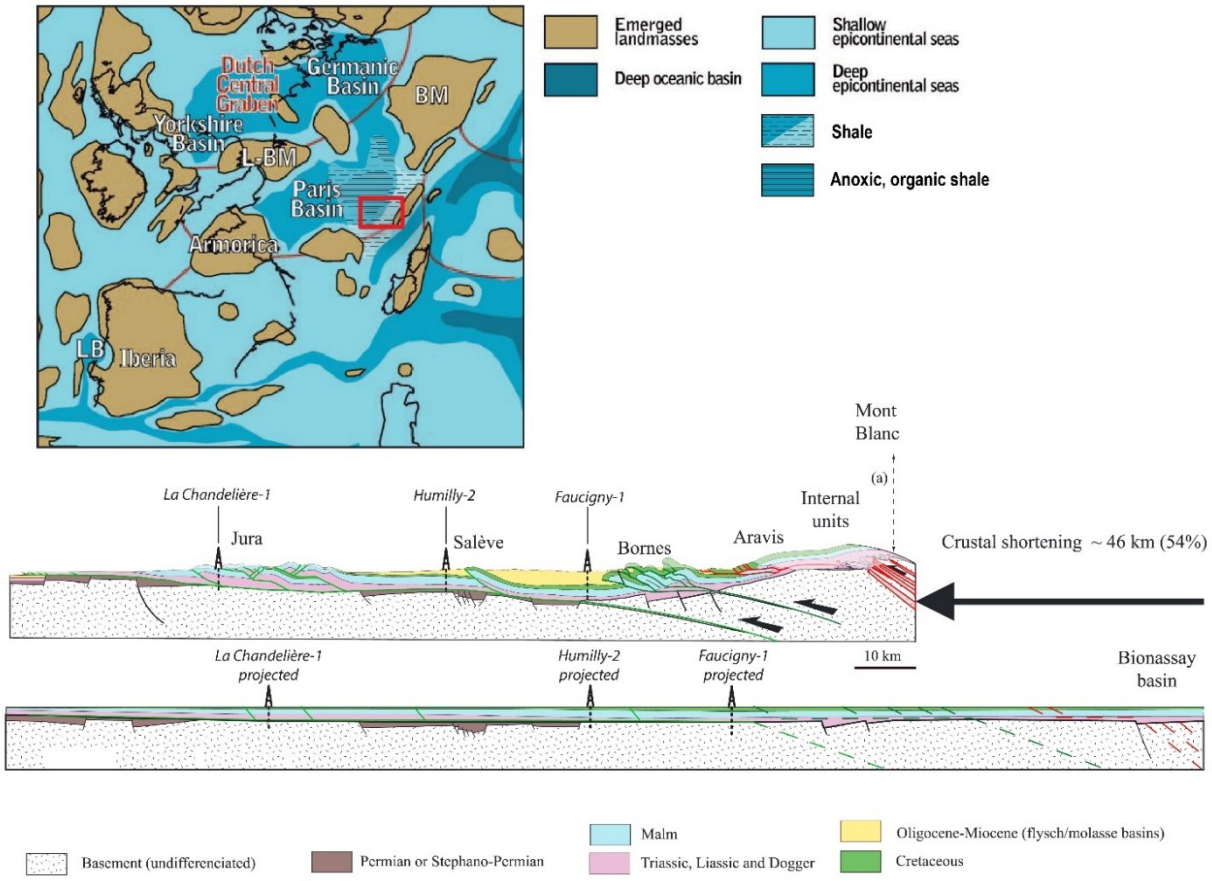

Figure 14: Above: paleogeographic map of the Early Jurassic (after TRABUCHO-ALEXANDRE et al. 2012) showing the estimated position of the present-day Swiss Plateau (red rectangle).
Below: balanced cross-section from the Jura Mountains to Bornes and the southwestern Mont Blanc massifs (after BELLAHSEN et al. 2014) showing the paleogeographic position of the Jurassic layers represented by the La Chandelière-1D, Humilly-2 and Faucigny-1 well samples.

2.2.2. Organic geochemistry

a) Organic matter in the Toarcian shales

The organic matter content was characterized using the Rock-Eval pyrolysis on 47 samples of the Toarcian shales. The Rock-Eval pyrolysis method consists of decomposing the organic matter by heating in the absence of oxygen and then measuring the richness and maturity of potential source rocks. To display the results, we produced a series of standard van Krevelen diagrams, which are used in the literature to characterize the type and maturity of organic matter (ESPITALIÉ et al. 1985a, b; LANGFORD & BLANC-VALLERON 1990).

The amount of total organic carbon (TOC) was measured along the entire stratigraphic column of the Humilly-2 well (Figure 15). In general, the amount of organic material is below 1%. The highest TOC amount was recorded in the black shale interval of Toarcian age, with a maximum peak at 4.3%. High TOC values within the Toarcian shales were measured also in the Chapéry-1 well (4.15%). In contrast, lower TOC values were determined in the well samples from the basin margins. In the Faucigny-1 well samples, a higher TOC amount (1.6%) was observed in the Upper Lias section (neither drill cuttings nor cores of the Lower Lias are available from the Faucigny-1 well), whereas lower values were measured in the Chaleyriat-1 well samples (Figure 15 and Figure 16). TOC data measured of the Lias unit through the analysed wells is presented in the Annex 1. Interpolation of

the TOC values throughout the Geneva Basin region clearly shows this decreasing trend towards the basin margins (Figure 17). The trend may be related to a more favourable setting for anoxic conditions in the central portion of the basin, which in transgressive periods was characterized by low sediment supply and restricted circulation. On the other hand, the marginal areas had strong river and wave energy that favoured the formation of oxidizing depositional environments in which organic matter cannot be easily preserved. Furthermore, the proximity to the sediment sources caused dilution of the organic matter with terrigenous deposits, strongly reducing the potential for forming rocks to generate hydrocarbons.

The Rock-Eval pyrolysis results can also be used as a proxy for the organic matter maturity. Rock-Eval analysis was performed for the Lias and Permo-Carboniferous units, on the samples richest in organic matter (data in Annex 1 and Annex 2). The graph of the hydrogen index (HI) vs. the temperature measured at the top of the residual petroleum potential or S_2 peak (T_{max}) is shown in Figure 18. It indicates that most of Toarcian shale in the southwestern Molasse Basin reached the onset of the oil window but apparently it reached the sufficient maturity to generate gas.

The most striking observation concerns the T_{max} values reached by the shales from the Faucigny-1 well (Figure 18), because they indicate overmature thermal conditions. Thus, there is a large maturation gap between the central part of the basin (beginning of the oil window) and the northern border (Faucigny-1 well). Given the location of the Faucigny-1 well within the subalpine nappe and the depth of the Lias unit in this area (4 km), it may be suggested that the tectonic subsidence resulting from the nappe stacking may account for this change in thermal history. In order to corroborate the thermal maturity pointed out by T_{max}, further analysis, as vitrinite reflectance, is going to be performed (see next chapter).

A diagram of S_2 vs. TOC values is often used to describe the source-rock quality (Figure 19). The Rock-Eval data from the Toarcian shales signify a good to very-good source-rock quality in the centre of the basin, where the Humilly-2 and Chapéry-1 are located. In contrast, the Faucigny-1 well samples exhibit a fair to poor source-rock quality (Figure 19), which is probably related to their over-mature thermal condition (i.e. most of the hydrocarbons probably had been generated and expelled much earlier).

a) Organic matter in the Permo-Carboniferous deposits

Using the Rock-Eval pyrolysis, the organic matter content in 11 Permo-Carboniferous samples was determined. Coal beds sampled from the Charmont-1 and Chatillon-1D wells reveal a high amount of organic carbon. Carbonaceous shales from the Charmont-1 well contain more than 20% organic matter, and coal beds with a TOC of 57.3% and 54.8% were found locally. In the Chatillon-1D well, a conglomerate, Carboniferous in age, containes a thin bed of carbonaceous shale with a TOC of 8.24% (Figure 16).

Plotting the hydrogen index (HI) vs. the T_{max} values indicates that the Permo-Carboniferous samples are mostly composed of Type III (i.e. continental) organic matter (Figure 20). The T_{max} values suggest oil-window thermal conditions for most of the Permo-Carboniferous samples. However, the wide spectrum of maturity indicated by T_{max} even within the same well (Charmont-1) make the reliability of this thermal indicator doubtful. In this case, further measument of vitrinite reflectance can be helpful for corroborating the thermal maturity data.

In the Humilly-2 well samples, there is a positive correlation between the TOC value and the uranium concentration (Figure 21), although the uranium-bearing minerals were identified. This correlation is probably due to the high content of uranium in the deposits rich in organic matter. Uranium content analytical data is presented in the Annex 3.

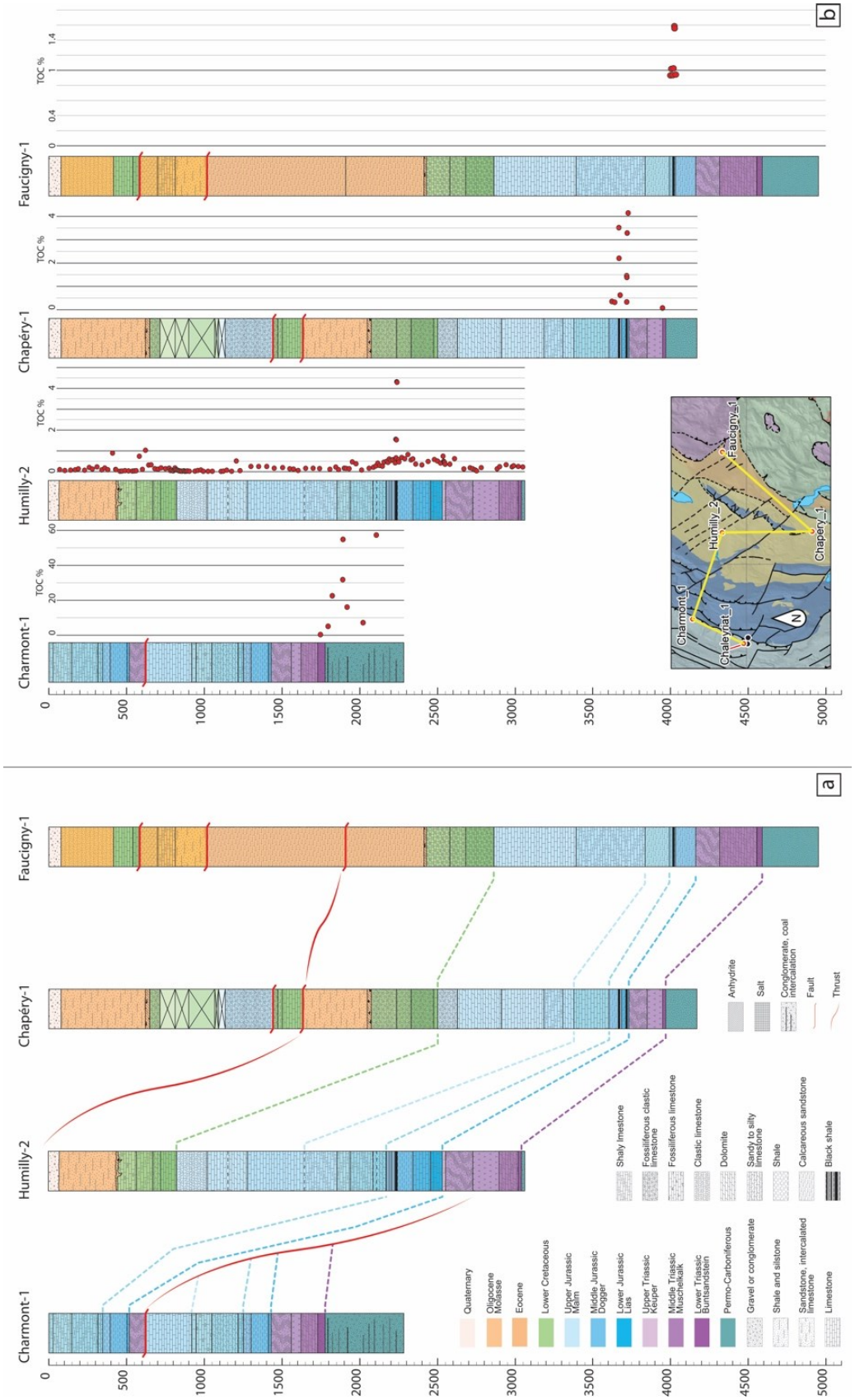

Figure 15: (a) Cross-section connecting the Charmont-1, Humilly-2, Chapéry-1 and Faucigny-1 wells showing the stratigraphic column and the projected geological contact (Figure 6); (b) total organic carbon (TOC) measurements within the stratigraphy. Data for the Lias and Permo-Carboniferous units in Annex 1 and 2.

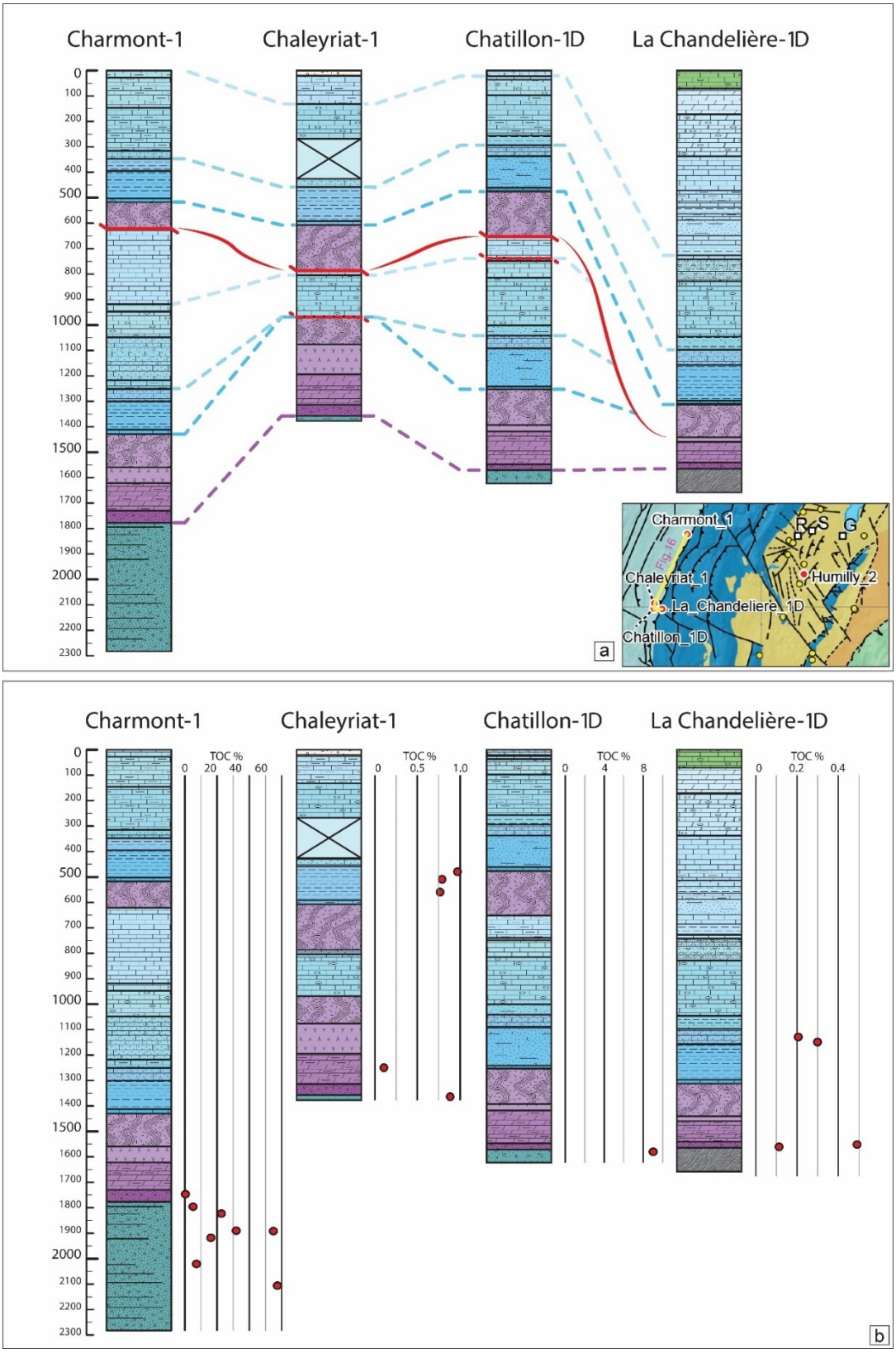

Figure 16: (a) Cross-section connecting the Charmont-1, Chaleyriat-1, Chatillon-1D and La Chandelière-1D wells showing the stratigraphic column and the projected geological contact. Legend of the stratigraphic units in Figure 15; (b) total organic carbon (TOC) measurements within the stratigraphy.

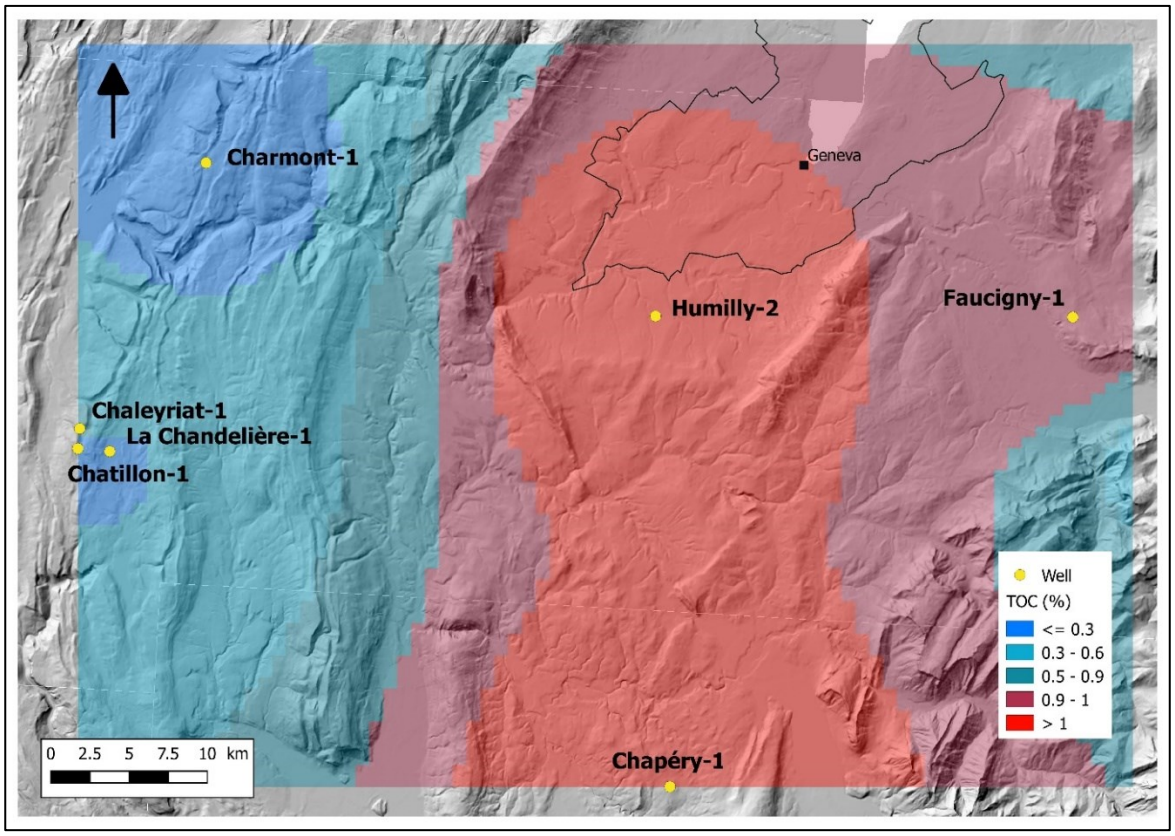

Figure 17: Interpolation of the average TOC values measured in the Toarcian black-shale deposits.

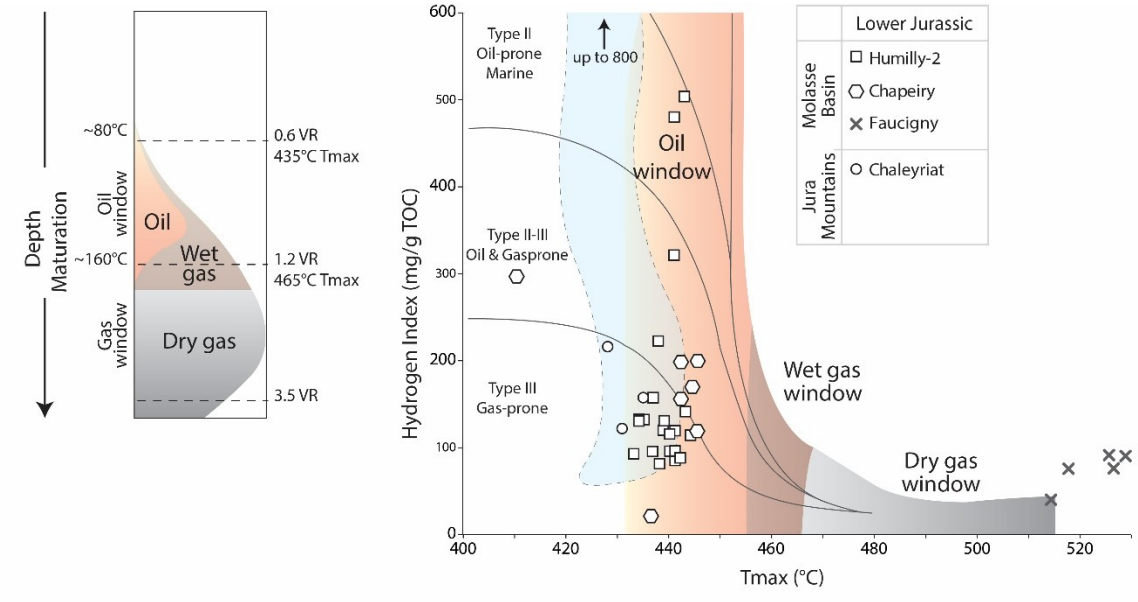

Figure 18: Hydrogen index (HI) vs. T_{max} showing the type and the maturity of organic matter contained within Toarcian shales (plot modified from ESPITALIÉ et al. 1985). Only samples containing a TOC > 0.45 are plotted. On the left, colour legend and thermal condition boundaries of the oil and gas windows; VR: vitrinite reflectance.

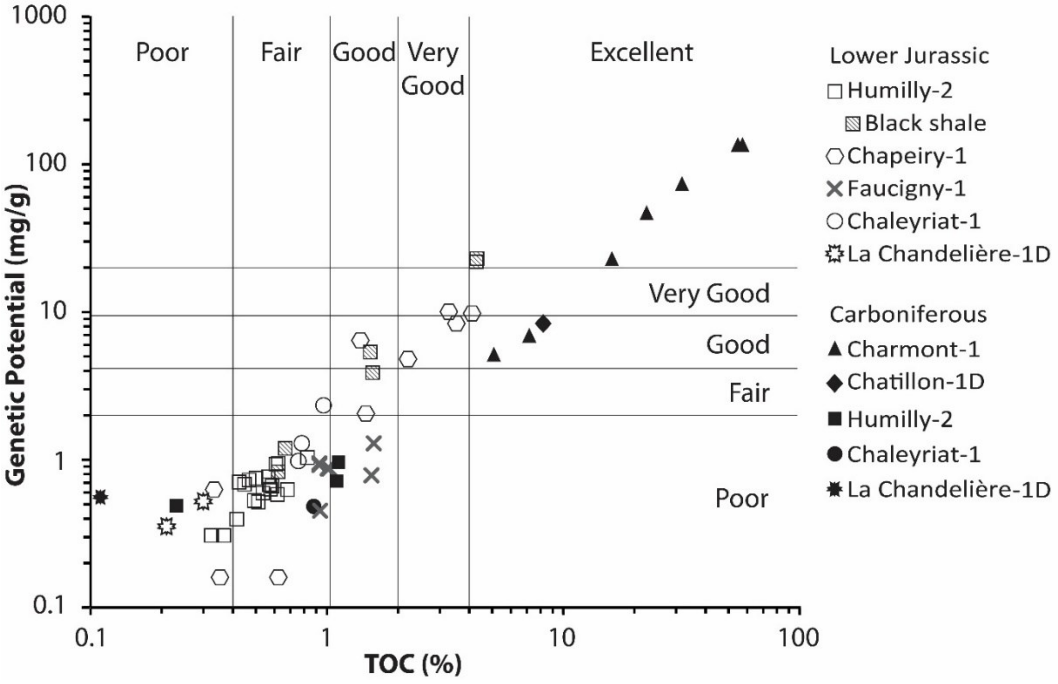

Figure 19: Diagrams showing the predicted source-rock quality based on the S_2/TOC ratio (graph modified from PETERS & CASSA 1994).

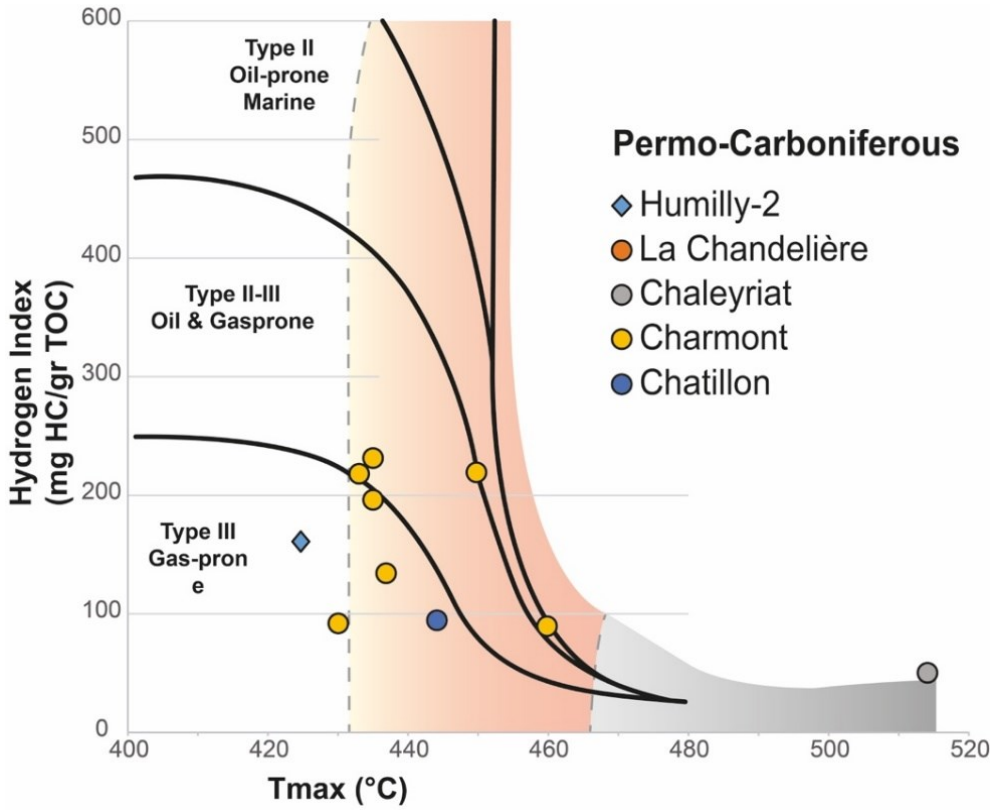

Figure 20: Diagram displaying the type and the maturity of organic matter contained in the Permo-Carboniferous samples. Only samples containing a TOC > 0.45 are plotted

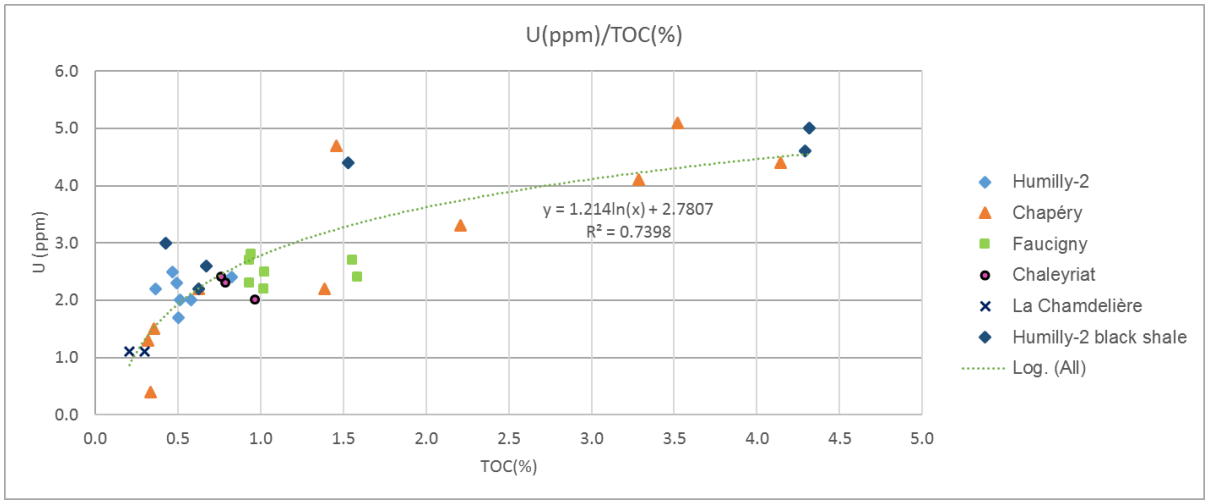

Figure 21: Plot comparing the uranium content (in ppm) of the Lower Jurassic samples and their respective TOC (in %.)

2.2.3. Brittleness index

The petrographic analyses of the Toarcian shales also included calculation of the brittleness index, an index indicating the capacity of a rock to fail from loading (e.g. during stimulation). It should be noted that the brittleness index is an empirical factor without a generally accepted physical interpretation. Underlying deformation mechanisms (fracturing or cracking) and mode of deformation (pervasive distributed fracturing without localization of failure vs. the development of fractures with concomitant loss of load-bearing capacity) are subject to a range of interpretations (e.g. PATERSON & TENG-FONG 2005). In this study we computed a brittleness index from the mineralogical composition of the shales. The QEMSCAN analysis coupled with XRD analysis turned out to be a very powerful tool. The brittleness index (BI) of the Toarcian shales according to WANG & GALE's formula (2003) tends to show a wide variability related to the petrography, and the calculation thus stresses the importance of having accurate petrographic data.

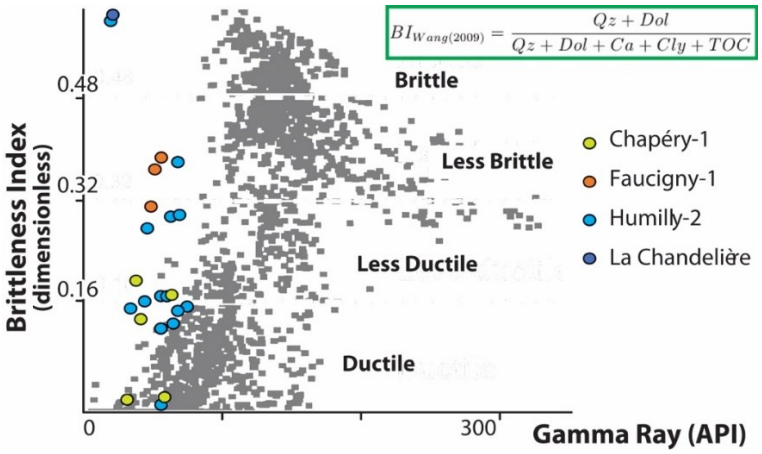

Figure 22: Brittleness index calculated for the Toarcian shales based on WANG & GALE'S formula (2009), which consider the mineral percentage and the Total Organic Carbon contained in the rock (Qz, quartz; Dol, dolomite; Ca, Calcium; Cly, Clays) and comparison with the Barnett shale data (modified from PEREZ & MARFURT 2013).

As mentioned before, WANG & GALE's formula (2003) is one of many others proposed in the literature and may not be the most appropriate for the western Molasse Basin. In Figure 22, Wang and Gale's index is used to

compare our data with those of the Barnett shale (grey background points), which is exploited for shale gas. Mineral composition data and brittleness index of the Toarcian shales are presented in Annex 4.

2.2.4. Permeability

To define an unconventional petroleum play, one needs to identify a source rock as well as a reservoir and a seal. Indeed, a shale formation may serve as a source rock and a reservoir at the same time. This is the case for shale gas accumulation. In the present case, the lack of core plugs in the Toarcian shales (only drill cuttings) does not allow the measurement of their petrophysical parameters.

A PhD thesis at UNIGE on the south-western Molasse Basin (RUSILLON 2017) characterizes petrophysical parameters of potential reservoirs at depth through the measurement of the porosity and the permeability of core samples. Figure 23 shows porosity and permeability of the Tithonian and Kimmeridgian carbonate platforms compared to the entire dataset of reservoirs at depth. A large variability of both the porosity and the permeability values as well as the presence of tight reservoirs, characterized by a low permeability (<0.01 mD), can be recognized.

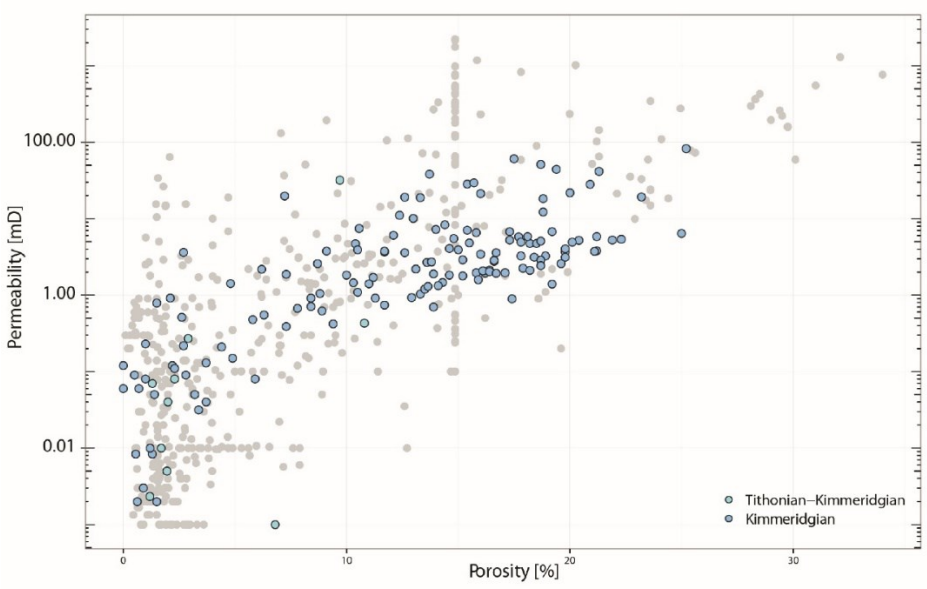

Figure 23: Porosity (%) and permeability graph (milli Darcy, mD) of the Tithonian and Kimmeridgian carbonate platforms in the southwestern Molasse Basin (blue points). These data are compared with the compilation of the complete set of porosity and permeability data from the southwestern Molasse Basin (grey points). Modified from RUSILLON (2017).

2.3. Conclusions and perspectives

Comprehensive analytical measurements in 2015 yielded several preliminary conclusions and established the basis for the work carried out during the 2016/2017 period.

- Source-rock identification:
  - Two potential source rocks are confirmed in the south-western Molasse Basin: (1) coal beds embedded in Permo-Carboniferous sandstone and (2) Toarcian conglomerate and grey to black shales.
  - Permo-Carboniferous coal beds show very high degrees of TOC, locally up to 54%.
  - Toarcian shales show a high TOC, particularly in the centre of the basin, where it reaches 4% in the Humilly-2 and Chapéry-1 well samples.
  - Occurrence of deeper source rocks in the Permo-Carboniferous graben (e.g. Autunian Lower Permian organic-rich lacustrine deposits) is not confirmed at this stage of research.

- Source-rock maturity:
  - The Permo-Carboniferous coal beds in the Jura Mountains have reached the oil (Charmont-1 and Chatillon-1D) and gas (Chaleyriat-1) windows. However, there is no such evidence from the centre of the basin because of the lack of data.
  - Toarcian shales have reached the oil window in the centre of the basin (according to Humilly-2 and Chapéry-1 well data) and have exceeded the gas window near the Alpine front thrust (Faucigny-1 well data).
- Source-rock petrography and geochemistry:
  - The terrigeneous fraction of the Toarcian shales mostly comprises clays (illite>chlorite>kaolinite), calcite and quartz.
  - Associated with the high content of organic matter in these deposits is an enrichment in phosphate as well as incompatible and metallic components (U, Mo, Cu, Zn, Cd, V among others).

In terms of unconventional petroleum geology, the Toarcian shale source rock in the centre of the basin is rich enough in TOC to generate hydrocarbons. According to their maturation values, the hydrocarbon most likely generated is oil. Bitumen deposits identified in the Molasse and Urgonian rocks near the ground surface of the Geneva area (Roulavaz Valley and Gex wells) may be the result of such oil generation and subsequent migration. Biomarker analyses of these samples were performed in the next phase of this project in order to correlate the potential source with the near-surface manifestation. Regarding the Permo-Carboniferous coal beds, further analyses are still necessary to determine whether they activated a petroleum system generating hydrocarbons in the Geneva Basin.

Further potential areas of research are the following:

- analysis of seismic profiles and wells to build a geological model of specific stratigraphic units that host potential unconventional petroleum systems
- sampling other wells (e.g. in the Canton of Vaud) to perform the same analytical workflow as was done for the Humilly-2 well samples
- determining the porosity of the Posidonia shales, which are considered as a potential unconventional reservoir
- production of petroleum play maps that contain keys elements on the generation of hydrocarbons.

3. UNCONGAS Part 2 (2016-2017) Seismic and geochemical surveys

3.1. Summary of part 1 and objectives

In Part 1 of the UNCONGAS project, the unconventional hydrocarbon potential of the deep underground in the Greater Geneva Basin (GGB) was characterized. Past studies point to a thick sedimentary succession comprising several source rocks potentially mature enough to generate oil and gas (LEU & GAUTSCHI, 2014), as modelled for the case in the Canton of Vaud (SCHEGG et al. 1999).

Our study confirms the occurrence of two source rocks in the GGB, represented from the bottom to the top by (1) the *sensu lato* Permo-Carboniferous continental organic matter (contained in coal beds and carbonaceous shales) and (2) the Upper Lias Posidonia shales (Toarcian in age) composed of black to dark grey shales and siltstones. Their organic geochemistry (Figure 24) suggests that both source rocks have already entered the oil window (i.e. potentially generating hydrocarbons at depth) and to some degree the gas window, such as in the cases of the Posidonia shale from the Faucigny-1 well (Bornes Plateau) and the Carboniferous coal beds in the Jura Mountains (Chaleyriat-1 well).

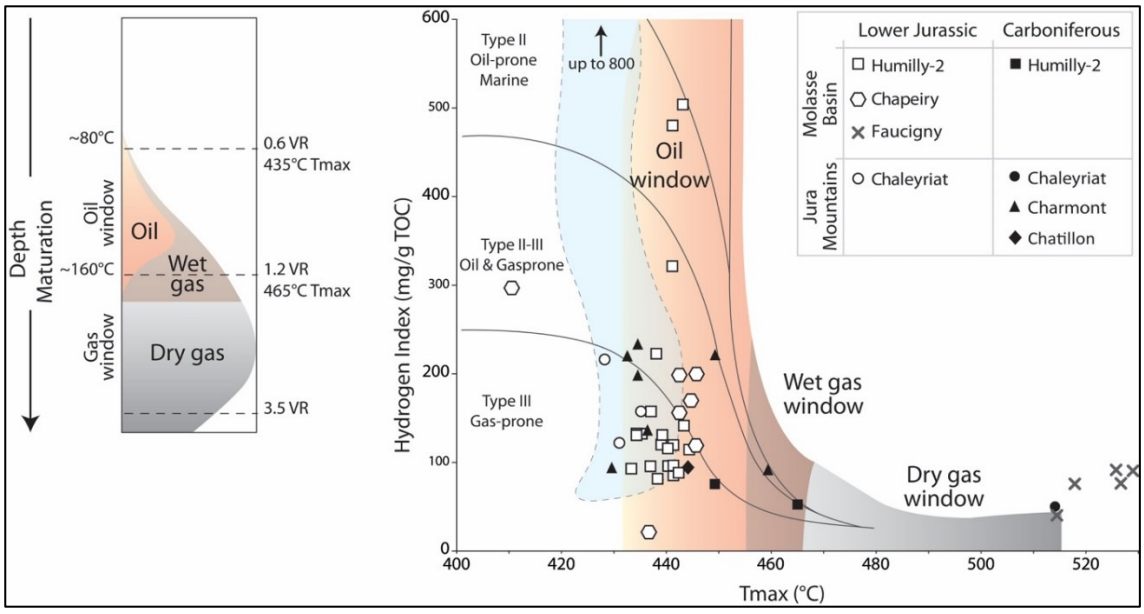

Figure 24: Plot of HI vs. T_{max} outlining kerogen types and source-rock maturity of the two main source rocks below the Greater Geneva Basin. Only the samples richest in organic matter (TOC >0.45%) are plotted. Graph modified from ESPITALIÉ et al. (1986). On the left, colour legend and thermal condition boundaries of the oil and gas windows; VR: vitrinite reflectance.

The petrography of the Upper Lias Posidonia shale (combined with inorganic geochemistry data) shows that in the centre of the basin (i.e. along a Humilly-Chapéry axis), the shales mostly comprise clays (illite>chlorite>kaolinite in proportion), calcite and quartz, correlated with an enrichment in phosphate as well as incompatible and metallic components (U, Mo, Cu, Zn, Cd, V among others). Our data reveal that the petrography varies significantly between the Upper Lias in the Jura Mountains and the Upper Lias in the centre of the basin (Figure 25). It seems intuitive that such a change is linked to the different paleogeographic domains recorded by these rocks.

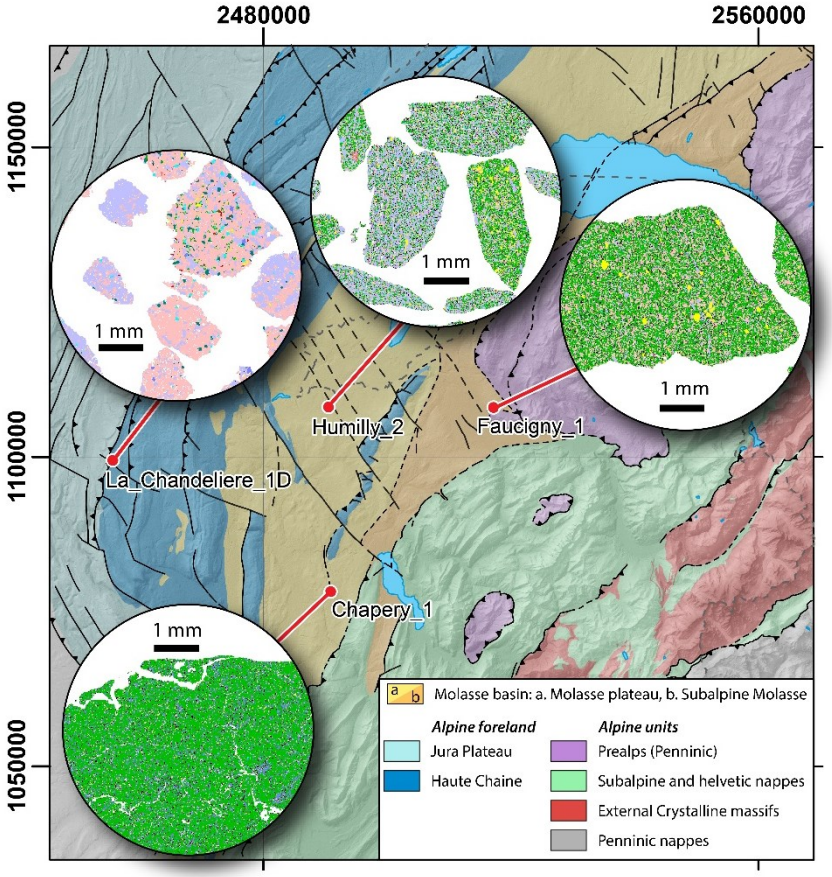

Figure 25: QEMSCAN images of the principal lithology of the Upper Lias samples (Toarcian; Posidonia shale) throughout the basin. A significant facies change is associated with the different paleogeographic domains represented by these samples. QEMSCAN legend in Figure 7.

Part 1 of the UNCONGAS project concludes that the Posidonia shale source rock (Toarcian) in the centre of the basin is rich enough in organic matter to generate hydrocarbons, and its maturity specifically indicates heavy oil. Therefore, we assume that the heavy oil may be the precursor to the bitumen seeps identified near and at the ground surface. Interpretation of the Permo-Carboniferous potential is more difficult, because of the sparse data available throughout the basin.

The objectives of Part 2 of this project are described below:

- Seismic facies analysis, seismic interpretation of deep intervals and well-log correlation to reconstruct the geometries of the basin infill
- Improving the kerogen typing and thermal maturity of the potential source rocks to identify their hydrocarbon potential
- Organic geochemistry of biomarkers of both source rocks and superficial oil and gas seeps to get insight into their origin

In the previous chapter thermal maturity was determined only by Rock-Eval (T_{max}), allowingy a first approximation. In this chapter vitrinite reflectance was additionally measured to improve the reliability of the data. The Rock-Eval data are an input to the interpretation of the kerogen typing. The results presented in this section are published in Do Couto et al. (2021).

3.2. Seismic interpretation

2D seismic profiles provided by NAGRA and SEAG via swisstopo (Figure 26), combined with well data, were used to map the spatial distribution and thickness of the potential source rocks and reservoirs.

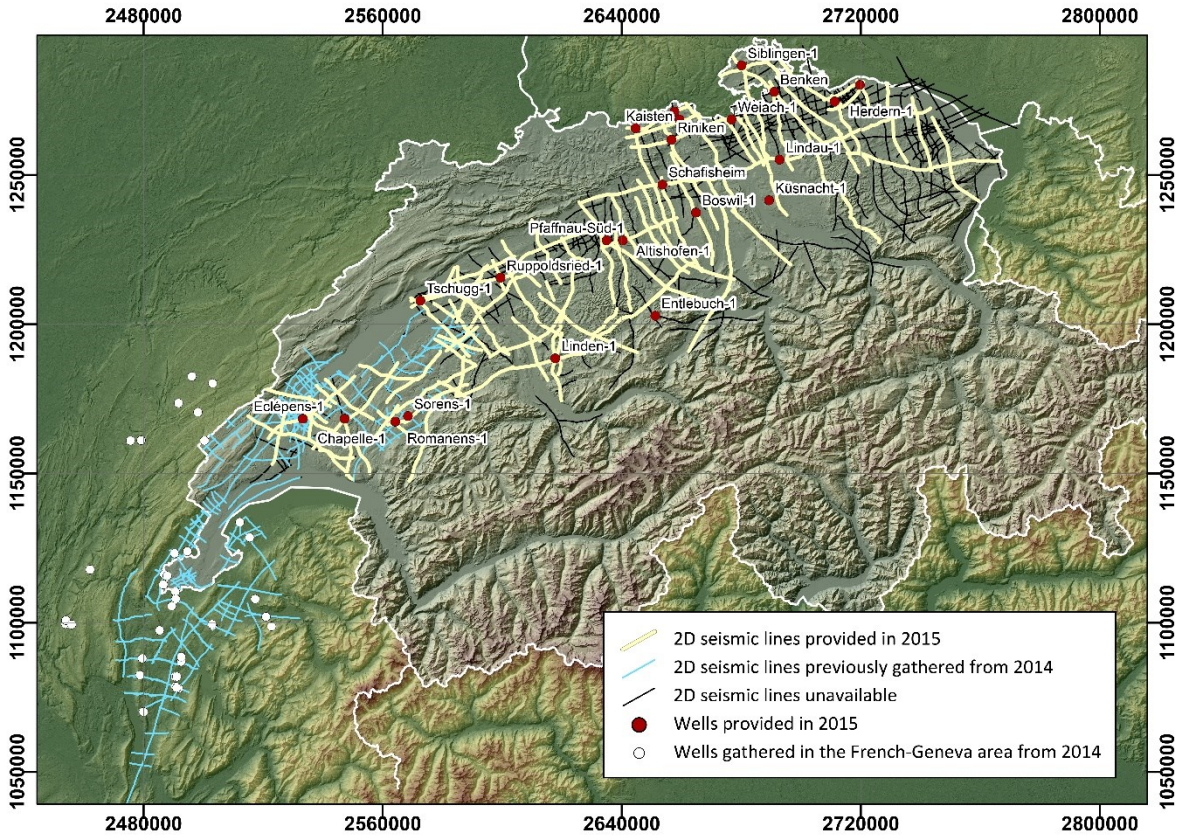

Figure 26: Location map of the 2D seismic profiles received in 2015 and the seismic data gathered over many years at the University of Geneva. Red dots represent the wells received in 2015 and provided by swisstopo.

The main stratigraphic intervals (Table 4) used in the GeoMol project (Landesgeologie 2017) were mapped throughout the Swiss Plateau according to the GeoMol interpretation. In addition to these horizons, two new horizons corresponding to the top and the base of the Posidonia shale (black shales) were mapped where detectable. The seismic interpretation and horizon mapping were then used to determine the spatial distribution and the thickness of the potential source rocks and reservoirs. These results were used to model (BPSM, see chapter 4) the generation and migration of hydrocarbons.

The seismic interpretation and mapping of horizons process involved several steps:

- homogenization of the well tops provided by swisstopo and cantons from Western Switzerland to standardize the regional stratigraphy and to avoid local heterogeneities and discrepancies of basin-wide data (Figure 27 and Table 5)
- check of seismic polarity and vertical miss-ties among all seismic sections with diverse datum elevations
- interpretation and interpolation of the main stratigraphic horizons (Figure 27 and Figure 29)
- structural interpretation throughout the basin
- computing horizon corrections (using the constant shift + exact fit correction method of KingdomSuite©) to avoid missing-ties at the intersections of seismic profiles
- creation of interval velocity grids and TWT- grids (Figure 29)

Table 4: *Interpreted main stratigraphic intervals beneath the Swiss Plateau and their respective colours.*

Colour	Unit	Abbreviation
	Base Cenozoic	B_Cen
	Top Upper Malm	T_UMa
	Top Lower Malm	T_LMa
	Top Dogger	T_Dog
	Top Lias	T_Li
	Top Keuper	T_Keu
	Top Muschelkalk	T_Mus
	Base Mesozoic	B_Mes
	Base Permo Carboniferous	B_PCarb

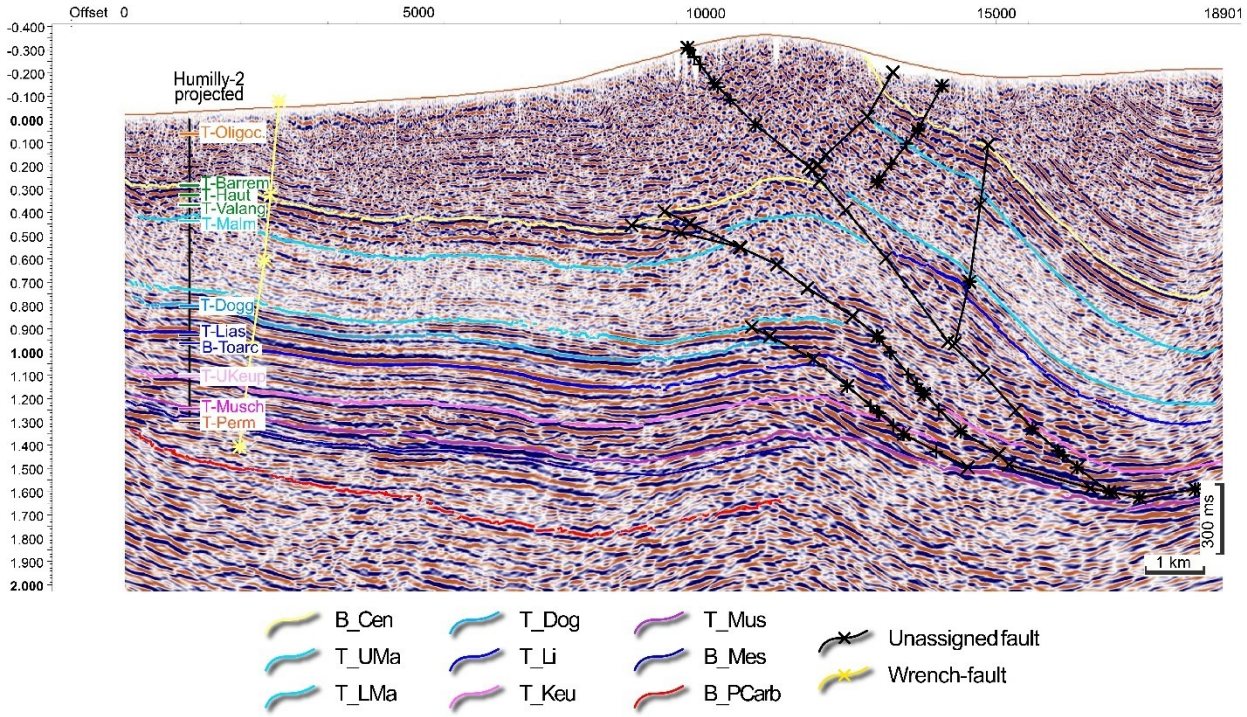

Figure 27: Seismic section 88SVO07, located near the border between France and Switzerland, showing the interpreted main stratigraphic horizons as well as the structural interpretation.

One of the most promising source rocks beneath the Swiss Plateau is the Posidonia shale, which was deposited at the base of the Toarcian during an anoxic event and is recorded throughout the peri-Tethys realm (Monte-Serrano et al., 2015 and references therein). The horizons Top Lias (Lower Jurassic) and Top Keuper (Upper Trias) were mapped in order to appreciate the thickness of the Lower Jurassic and to understand the geometry and distribution of the Posidonia shale at depth (Figure 28). Liassic sediments are thickest towards the southwest, where they reach 442.5 m in the Humilly-2 well (193 ms two-way travel-time or TWT), and they thin towards the N and NE to reach only a few meters in in the Altishofen-1well.

Table 5: *Example of the formation top harmonization from swisstopo for the Altishofen-1 well data.*

Well	Received well tops	New well tops
Altishofen-1	BANDO	Not suitable
	BLias	Top Trias
	BOpa	Top Lias
	BQuaternary	Base Quat
	BTertiary	Base Cenozoic
	BUSM	Base Cenozoic
	BasisLias	Top Trias
	BasisMalm	Top Dogger
	BasisMMK	Top Lower Muschelkalk
	BasisOPA	Top Lias
	BasisQua	Base Quat
	BasisTertiär	Base Ceno
	Bathonien	Top Bathonian
	BCen	Base Cenozoic
	Früher Jura	Top Lias
	Keuper	Top Keuper
	Mittlerer Jura	Top Dogger
	Muschelkalk	Top Muschelkalk
	OMM	Top UMM
	Rhät	Top Rhaetien
	Später Jura	Top Malm
	TOpa	Top Opalinus
	TUBM	Top Alpine LFM
	TUSM	Top LFM
	TAnhy	Top Mid Musch Anhy
	TBr	Top Bed Rock
	TD	Total Depth
	TDo	Top Dogger
	TKeu	Top Keuper
	TLi	Top Lias
	TLMa	Top Lower Malm
	TMus	Top Muschelkalk
	TOMM	Top UMM
	TopChattian	Top Chattian
	TopMalmA	Top Malm
	TopMK	Top Muschelkalk
	TopMMK	Top Mid Muschelkalk
	TopMurchisonae	Not suitable
	TopMuschelkalk	Top Muschelkalk
	TopOPA	Top Opalinus
	TopUSM	Top LFM
	TOpa	Top Opalinus
	TopFels	Top Bed Rock
	TUMa	Top Upper Malm
	TUSM	Top LFM
	USM	Top LFM

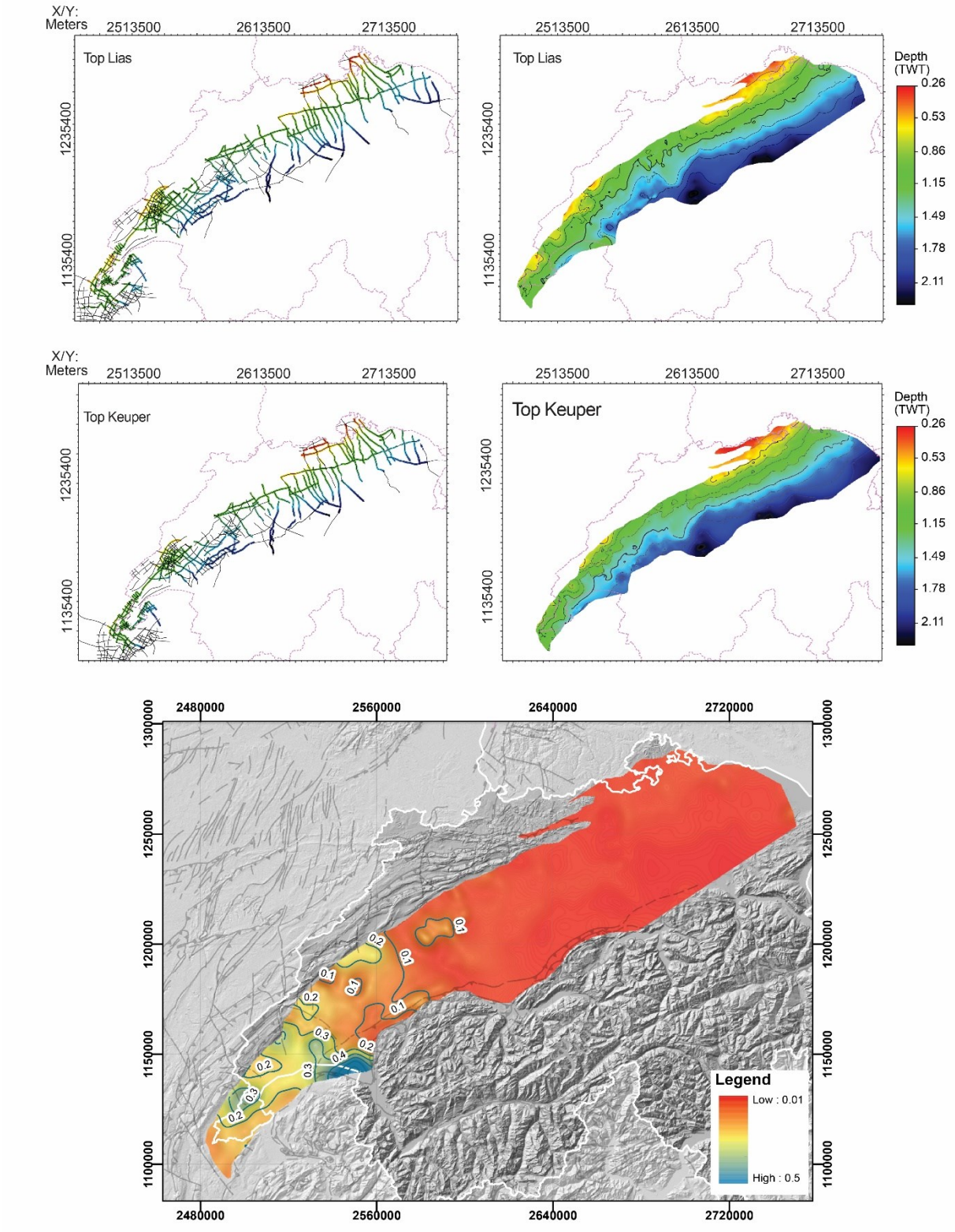

Figure 28: Above: 2D maps of the Top Lias and Top Keuper seismic horizons (left) and their respective grids (right). Below: Isochron thickness map of the Lias with an equidistance of the vertical thickness contours at 0.1 s TWT.

3.2.1. Identification of Permo-Carboniferous troughs

In order to understand the distribution of the Permo-Carboniferous rocks, the deepest seismic reflectors particularly in the southwestern Molasse Basin, were mapped. Until now, no such information has been available. The calculation of seismic attributes such as the pseudo-relief (KingdomSuite©) or the variance (Schlumberger Petrel ®) help to resolve geometries and facies changes of deeply buried units and to recognize deep Permo-Carboniferous troughs (Figure 29).

The identification and mapping of Permo-Carboniferous troughs is still ongoing. The amount of gas that can be generated in the Swiss Plateau depends strongly to the volume of carbonaceous shale and coal rocks constituting the stratigraphic record. Thus, this step is crucial in performing accurate BPSM and reconstructing the petroleum history of the basin.

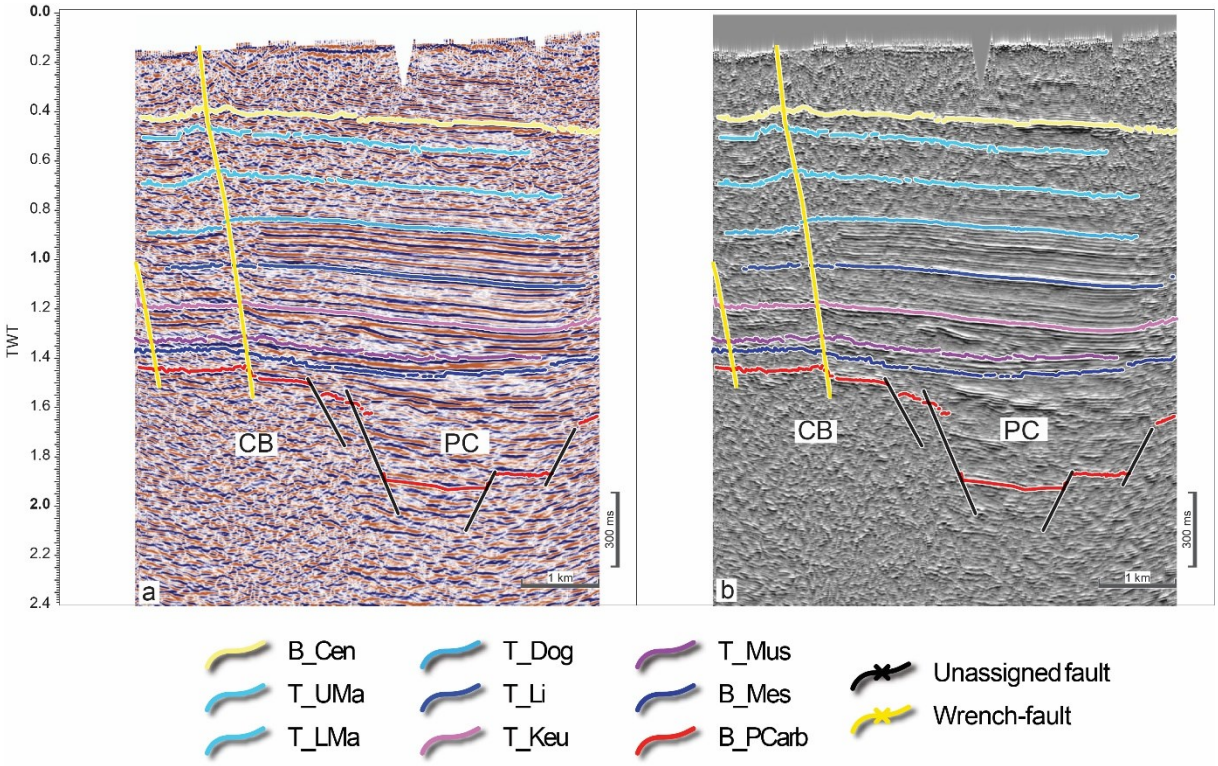

Figure 29: Interpreted seismic profile in time (9006-PSTM, south of Geneva) showing the main stratigraphic horizons and the identified Permo-Carboniferous trough. (a): classical brown to red palette showing the seismic amplitudes changes; (b): Pseudo-Relief display (KingdomSuite©) enhancing the amplitude variations by combining the RMS amplitude of the seismic signal and the reverse Hilbert transform. Note the difference in seismic facies between the Permo-Carboniferous trough (PC) and the crystalline basement (CB)

Parallel to seismic mapping of the main stratigraphic horizons, a well-correlation analysis was performed, focusing particularly on the wireline-log response to the occurrence of black shales. In the Humilly-2 and Chapéry-1 wells, located in the French part of the southwestern Molasse Basin, the Posidonia black shale is easily identifiable by its high natural radioactivity and sonic (acoustic) values (Figure 30 and Figure 31). This can be explained by the large amount of clays rich in radioactive elements such as potassium and uranium (see Part 1). Such observations are not apparent in Faucigny-1 well data, perhaps because of the more intense maturation of the Posidonia shale from this well (Figure 24).

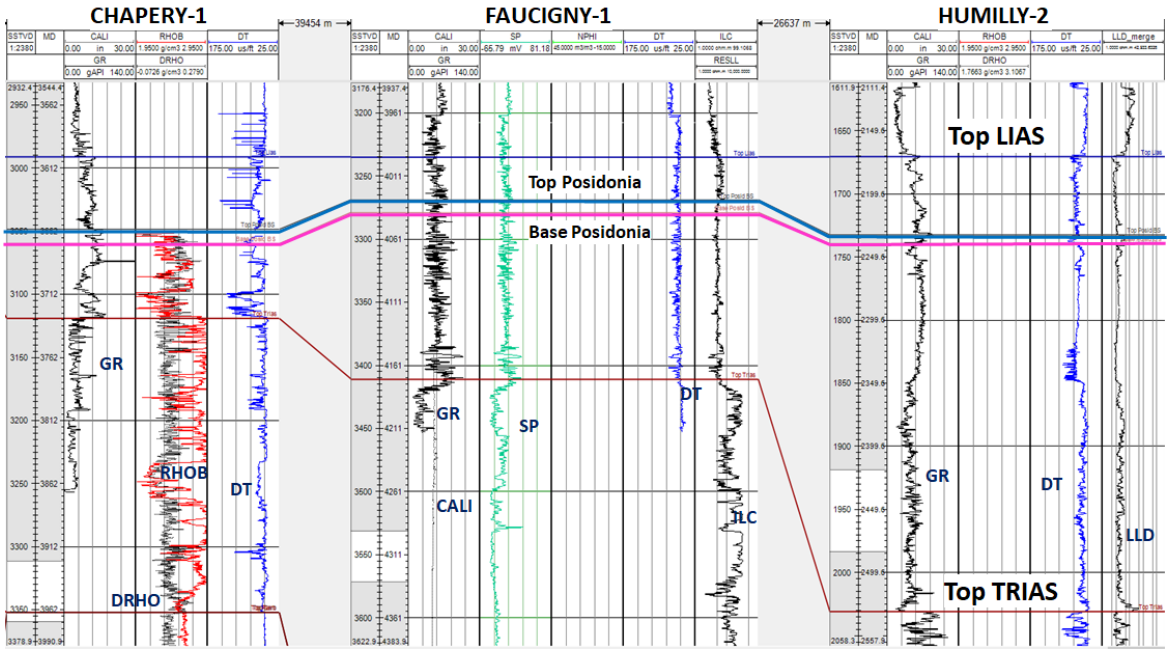

Figure 30: Well-section flattened at the top of the Lias, comparing the Chapéry-1, Faucigny-1 and Humilly-2 well data (location in Figure 6). Radioactivity (gamma rays GR), caliper (CAL), density (RHOB and DRHO), neutrons (NHPI), spontaneous potential (SP), resistivity (ILC, RESLL, ILD, LLD_merge) and the acoustic sonic log (DT) are plotted to illustrate the signal of the Posidonia black shales.

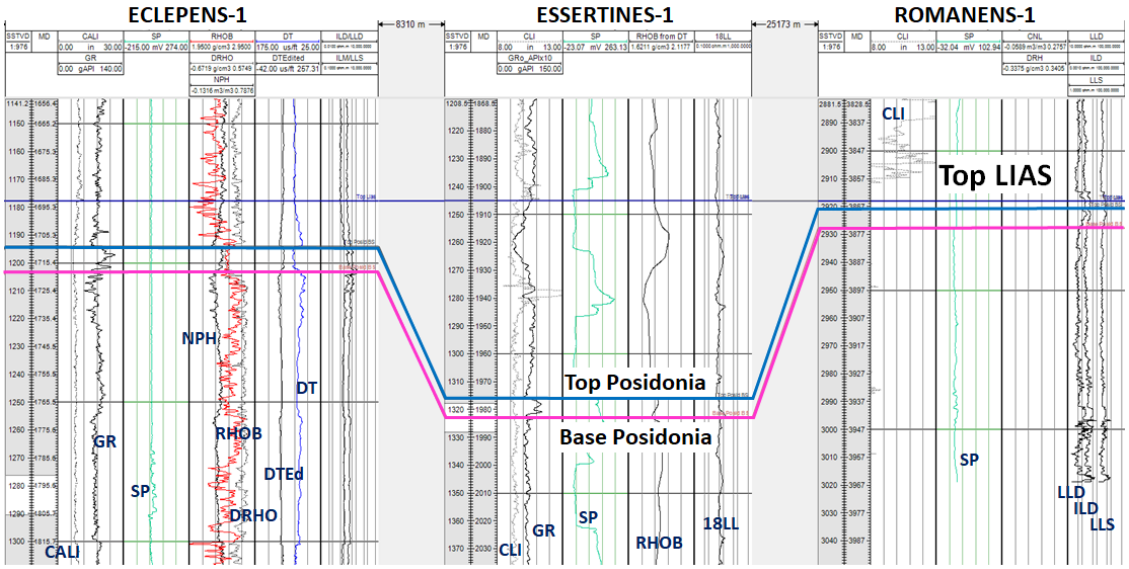

Figure 31: Well-section flattened at the top of the Lias, comparing – from left to right - the Eclépens-1, Essertines-1 and Romanens-1 well data from the Cantons of Vaud and Fribourg. Radioactivity (gamma rays GR), caliper (CALI, CLI), density (RHOB and DRHO), neutrons (NPH), spontaneous potential (SP), resistivity (ILC, RESLL, ILD, LLD, 18LL) and the acoustic sonic log (DT, DTEd) are plotted to illustrate the signal of the Posidonia black shales.

Based on the same approach, we extended our well-log analysis towards the Cantons of Vaud and Fribourg, where the thickness of the Lias units decreases progressively (Figure 30). In Eclépens-1, an interval between ca. 1710 and 1720 m MD is characterized by high radioactive and sonic values (Figure 31), similar to those observed near Geneva in the Humilly-2 data (Figure 30). However, the well log does not indicate a specific black or dark-grey shale layer at this interval and thus makes resampling of cuttings crucial to resolve this question. Black to dark-grey marls and limestones are documented in the Essertines-1 data between 1960 and 1990 m MD, and a "black shale signal" similar to the one in the Humilly-2 data is apparent from 1975 to 1983 m MD (Figure 31). In the Romanens-1 data, sparse occurrences of black to dark-grey marls and shales are visible between 3865 and 3986 m MD. However, it is rather difficult to delimit an interval based on high gamma-ray values and where no sonic log is available (Figure 31). Nevertheless, an interval between 3867 and 3875 m MD contains two thin layers with high gamma-ray signatures that may signify the occurrence of black Posidonia shales (Figure 31). In the case of the Eclépens-1 well data, a resampling of the cuttings is essential.

3.2.2. Seismic facies analysis

The mapping of seismic facies is an important step, so that the seismic character of the Lias containing the black shale (Posidonia) can be identified and followed across the basin to areas with no well information. In addition, seismic facies identification is a key parameter in making inferences on the paleoenvironment, understanding where the Posidonia black shales were deposited and linking to the paleogeography.

The seismic facies of the Lias interval is not homogeneous on a regional scale. South of Geneva, the seismic profile 88SVO07 intersecting the Humilly-2 well shows two different seismic facies (Figure 32):

- An upper seismic package comprising relatively continuous, moderate to high frequency, low amplitude reflections correlated with marls and shales, as established from the cutting description (yellow layer in Figure 32)
- A lower seismic package composed of continuous, low to moderate frequency, moderate amplitude reflections correlated with the shaly limestones of the Humilly-2 well (red layer).

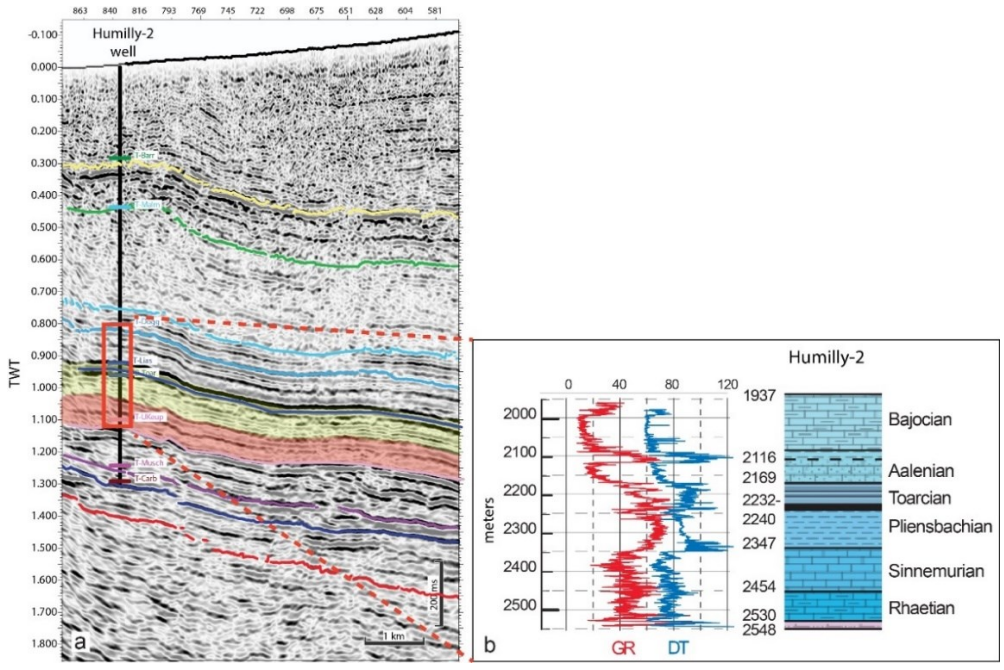

Figure 32: (a) Seismic facies of the Mesozoic stratigraphic section along the seismic profile 88SVO07 compared with the Humilly-2 well log between 1937 and 2548 meters (b). For legend of the Humilly-2 log see Figure 15. In the seismic profile the Lias unit is highlighted, including the black shales (yellow) and Sinemurian - Rhaetian shaly limestones (red).

Several seismic facies were identified during the analysis (Figure 33). Three lithological assemblages belonging to the Lias were encountered in the Eclépens-1 well (Figure 33). They constitute, from top to bottom, (1) very thin clay and marl layers, (2) marly sandstones and (3) layers of clay, marl and shaly limestone. The latter two are shown in Figure 33 (green and purple, respectively) and are correlated with the two seismic facies in seismic profile 79SADH26, which was acquired near the Eclépens-1 well.

The seismic facies are rather difficult to extrapolate because of discrepancies in the seismic signal throughout the whole basin, as pointed out by SOMMARUGA et al. (2012). Nevertheless, the geochemical and petrographic analyses of the Upper Lias layers combined with the identification of seismic facies gives important insights on the basin-wide facies distribution and hence strongly contributes to the unconventional petroleum assessment.

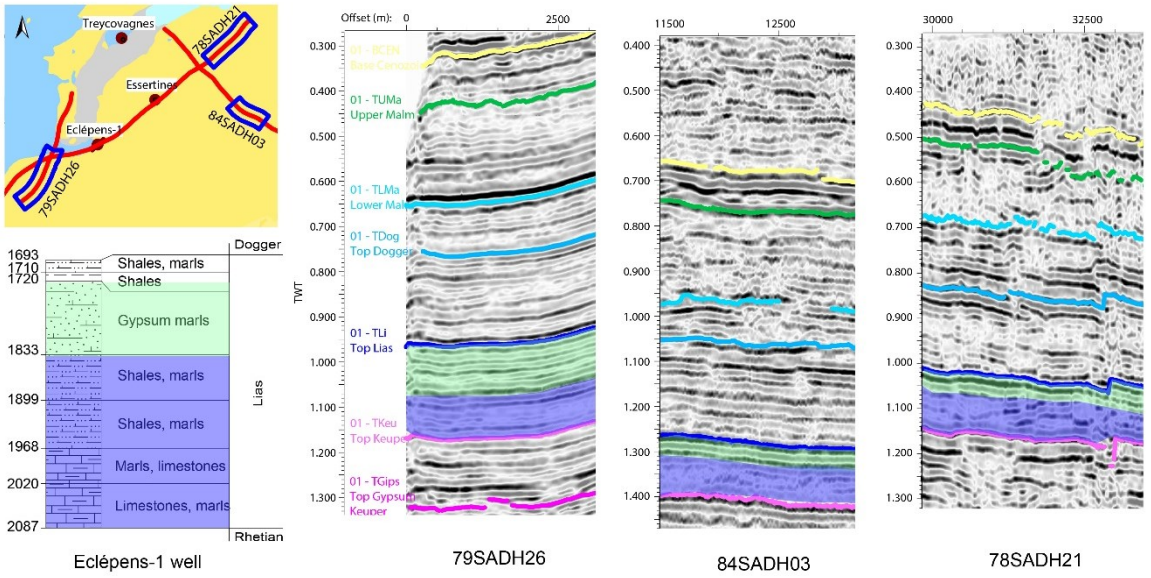

Figure 33: Seismic facies of the Lias section in three seismic profiles from the Canton of Vaud. Two sub-sections comprising shaly sandstone (located below the Top Lias horizon) overlying marls, clays and limestone are correlated with the Eclépens-1 well data. The overall thickness of the Lias section decreases towards the NE (black arrows).

3.2.3. Seismic mapping

Seismic interpretation and mapping depend on the quality of primary data acquisition as well as on the continuously evolving technological, scientific and analytical advances. Therefore, structural and stratigraphic analyses are updated on a continuous basis and reflect the current state-of-the-art. At this stage of the project, most of the main stratigraphic intervals important for BPSM was mapped in the region from the Canton of Geneva to Bern, where the Lias unit (including the Posidonia shale) is thicker. However, the structural analysis remains an important topic to be developed in collaboration with cantonal geological surveys. Our partners analyse subsurface data in the framework of swisstopo's GeoMol project (Landesgeologie, 2017) and additional studies (Musée cantonal de Géologie de Lausanne, Université de Fribourg). The structural analysis is crucial especially with regard to the 2D and 3D BPSM, which enables the simulation of hydrocarbon migration paths along permeability zones. Special attention was paid in distinguishing the horizons Top Lias and Top Keuper, in order to characterize the geometry and spatial variations of the entire Lias stratigraphic record. Before the gridding process, the vertical position of the Top Lias horizon was corrected (mis-tie analysis) using an algorithm of the KingdomSuite© software suite (Figure 34). First, we applied a vertical constant shift to the horizon along selected surveys to produce minimal travel time differences at survey line intersections.

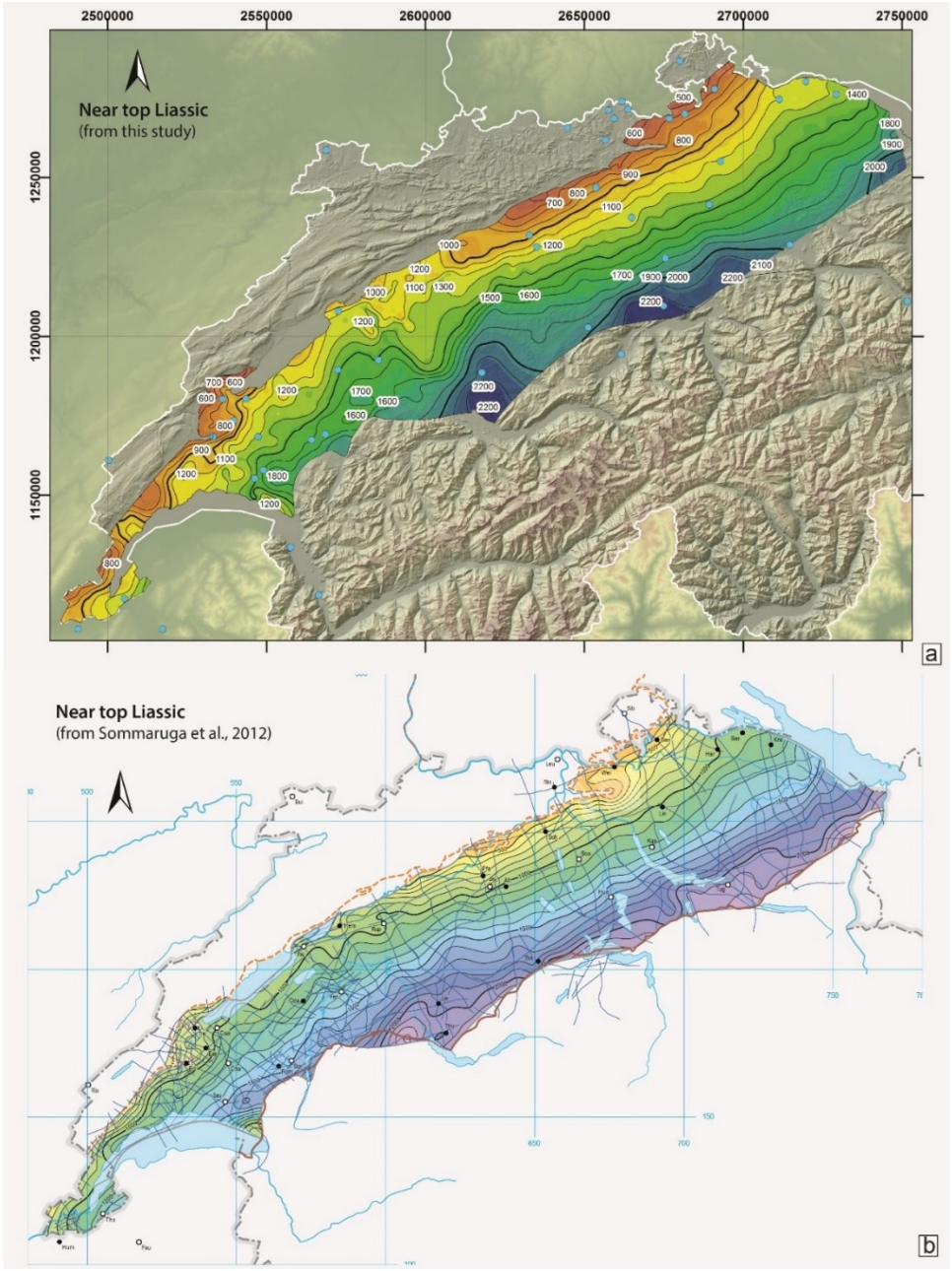

Figure 34: Time-depth map of the Top Lias horizon from this study (a) compared to the Top Lias horizon of the Seismic Atlas of the Swiss Molasse Basin (SOMMARUGA et al. 2012) (b).

We then applied an exact fit correction that computed the average of the two horizon values at each intersection. Both horizons were set to that value, with the correction tapering to zero at a specified distance from the intersection.

In order to perform such a correction, and thus avoid potential artefacts such as discontinuous steps, we chose the seismic profile 73-VD-07 from the Canton of Vaud (tied to the Essertines-1 well) as the reference survey for the mis-tie analysis.

Flex Gridding, a default gridding process of the IHS Kingdom® Suite, was then used to compute a time map of the Top Lias horizon (TWT) by basically combining "minimum tension" and "minimum curvature" geostatistical calculation methods. On a large scale, the resulting TWT map of the Top Lias horizon is similar to the one created by Sommaruga et al. (2012), in which the horizon dips S to SE (Figure 34). However, on a small scale, some discrepancies between the two maps are visible (Figure 34). These discrepancies are most probably due to

(1) our improved stratigraphic interpretations, e.g. between Geneva and Lausanne, whereby a rapid correlation with the seismic results was done in collaboration with the Musée cantonal de Géologie de Lausanne, and (2) the different interpolation process used by SOMMARUGA et al. (2012), which featured a spline interpolation (polynomial law) with the flex gridding.

3.3. Source-rock characterization

3.3.1. Kerogen typing

Hydrogen (HI) and oxygen indices (OI) of the Posidonia shale suggest marine type II and a mixture of marine/continental type II+III organic matter (Figure 35). Rock-Eval analyses of the GGB and surroundings indicate that the Lower Jurassic rocks (including the Posidonia shale) have a highly variable HI (Figure 35). The samples with the highest HI correspond to those richest in TOC, signifying a very high hydrocarbon potential. Lower values of HI and TOC may be associated with a reduction of the oil-potential properties of the organic matter (from a type II to a type III kerogen) or with a maturation trend and a loss of hydrogen with depth during the generation of hydrocarbons (ESPITALIÉ 1985, DOLSON 2016).

With exception of the Humilly-2 samples, most of the Toarcian deposits show a mixture of marine type II and continental type III organic matter (Figure 35). Analysis of the organic matter content permitted the depositional environment to be determined by recognizing the different maceral components of the organic matter. In the Humilly-2 samples, terrestrial and lacustrine macerals were identified (Figure 36), indicating a marginal wetland depositional environment, confirming Rock-Eval data.

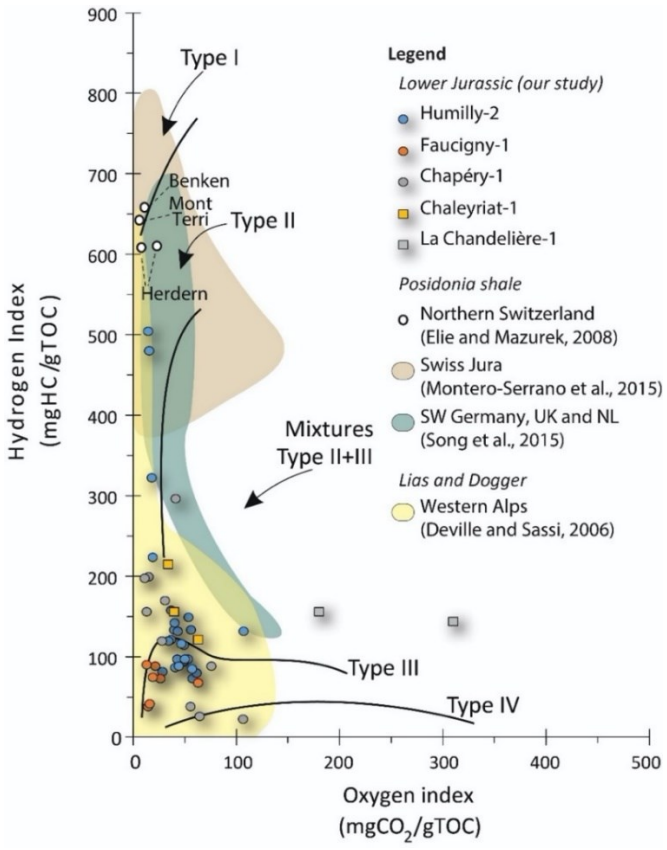

Figure 35: Pseudo van-Krevelen diagram (modified from ESPITALIÉ et al. 1986) showing hydrogen index vs. oxygen index of the Lower Jurassic samples (containing also the Toarcian and the Posidonia shales deposits) from the Greater Geneva Basin (Rock-Eval data in annex). These data are compared with Lower and Middle Jurassic data from other regions in Europe.

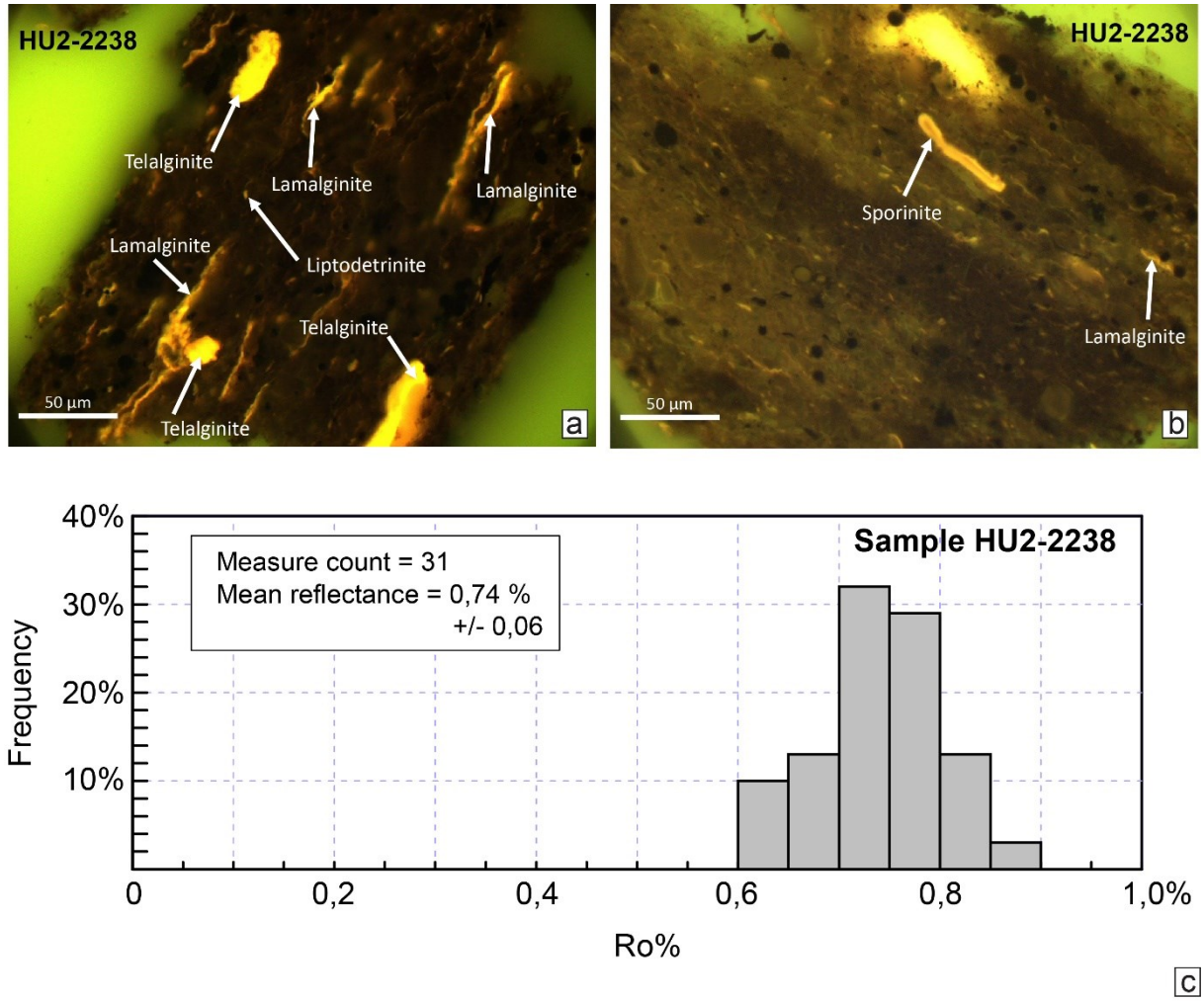

Figure 36: In (a) and (b): optical microscopy, photomicrographs taken under fluorescence mode (image width: 200 µm). The following lacustrine macerals are recognized: telalginite, lamalginite and sporinite, recovered at a depth of 2238 m MD in the Humilly-2 well. In (c): statistical measurements of vitrinite reflectance of the HU2-2238 sample.

The acquired Rock-Eval data are comparable with those from the same formation in southwestern Germany, The United Kingdom, The Netherlands (SONG et al. 2015), the Swiss Jura Mountains (MONTE-SERRANO et al. 2015) and even the Lias-Dogger of the western Alps (DEVILLE & SASSI 2006).

3.3.2. Thermal maturity

In this stage, in order to constrain the thermal maturity of the potential source rocks, further analyses than Rock-Eval (Tmax) were carried out. Vitrinite reflectance is typically used in the petroleum industry as a thermal maturity indicator (the higher the temperature the rock has reached, the higher is the amount of reflected light). Vitrinite reflectance was measured in the two source rocks (Table 6). Most of the measurements reveal that the Upper Lias Posidonia shale is in the oil window (according to TISSOT & WELTE 1984) (Figure 36). In the Chapéry-1 samples, vitrinite reflectance measurements yield 0.72 to 0.77 Ro% (Table 6). No vitrinite was encountered in the Posidonia shale from the Faucigny-1 well, only bitumen (i.e. solid hydrocarbons of organic origin). Bitumen reflectance measured on three samples yield a vitrinite reflectance equivalent of 2.21 to 2.41 Ro%, according to LANDIS & CASTAÑO (1994) and SCHOENHERR et al. (2007). Such values indicate that the Posidonia shale from the Faucigny-1 well is in the gas window (dry gas according to TISSOT & WELTE 1984).

The major difference in the vitrinite reflectance between the Molasse Basin (Humilly-2 and Chapéry-1 wells) and the Bornes plateau (Faucigny-1 well) is most likely due to the contrasting tectonic histories of these two basins.

Table 6: *Vitrinite reflectance (%Ro) results of the Liassic and Carboniferous sections in the studied wells. Only samples with a large amount of organic matter could be measured. The deviation standard (s) of the average value obtained for each sample and the number of vitrinite particles measured are indicated. *: vitrinite reflectance ranges calculated from bitumen (RB) reflectance according to Landis & Castaño (1995) and Schoenherr et al. (2007).*

	Well	Sample	TOC (%)	Tmax (°C)	%Ro (%)	s	RB (%)	Number of particles
Lias	Humilly-2	HU2 -2232	1.56	438	0.72	0.05	-	13
		HU2 - 2236	1.53	441	0.74	0.06	-	14
		HU2 - 2238	4.32	443	0.74	0.06	-	31
		HU2 - 2240	4.29	441	0.74	0.07	-	33
	Chapeiry-1	CHY - 3669	3.52	446	0.76	0.06	-	9
		CHY - 3720.9	1.39	410	0.77	0.04	-	13
		CHY - 3722.7	3.29	442	0.72	0.04	-	13
	Faucigny-1	FAY - 4020	1.03	527	2.21-2.28*	0.14	2.07	22
		FAY - 4026	1.59	527	2.35-2.41*	0.10	2.22	39
		FAY - 4027	1.56	515	2.22-2.29*	0.12	2.09	47
Carboniferous	Humilly-2	HU2 – 3039.8	1.12	449	1.14	0.07		50
	Charmont-1	CHT - 1892	31.81	433	0.60	0.03	-	100
		CHT - 1894	54.85	435	0.64	0.02	-	100
		CHT - 2108.5	57.33	450	0.79	0.03	-	100
	Chatillon-1D	CTL1D - 1578.5	8.24	444	0.76	0.03	-	100
	La Chandelière-1D	LCD - 1553.2	n/a	n/a	0.75	0.04	-	16

3.4. Source-to-oil correlations

Biological markers (also called biomarkers) are complex molecular "fossils" that can be measured in both crude oil and extracted hydrocarbons (PETERS et al., 2005a). Nowadays they are frequently used by geologists as a robust method for correlating the source rock with their expelled hydrocarbons (PETERS et al., 2005a, 2005b and references therein). The use of organic geochemistry and biomarker analysis has become an important tool in the petroleum geology industry. In collaboration with RWTH Aachen and the German Bundesanstalt für Geowissenschaften und Rohstoffe BGR in Hannover, we performed organic geochemical analysis of the saturated hydrocarbons on 12 samples, including Upper Lias shales and Carboniferous coals of the GGB. Ratios of different biomarkers were calculated and used to interpret the depositional environment and the thermal maturity. The Posidonia shale samples (from Humilly-2 and Chapéry-1 wells) exhibit a dominance of short chain n-alkanes (nC14-C19) relative to long chain n-alkanes (nC27-C31), as shown in Figure 37a. Such patterns of n-alkanes reveal a typical algal/phytoplankton-derived organic matter (PETERS et al. 2005b), that confirms the marine type of organic matter suggested by the Rock-Eval pyrolysis. Similar gas chromatogram patterns were found in other Posidonia shale samples in Switzerland (ELIE & MAZUREK 2008). In contrast, Carboniferous coal samples show a dominance of medium-to-long chain n-alkanes (nC20-C27) relative to short chain n-alkanes (nC12-C17), as

shown in Figure 37b. This n-alkanes pattern unveils a typical continental/humic-derived organic matter (PETERS et al. 2005a), in agreement with the Rock-Eval pyrolysis results (Figure 35).

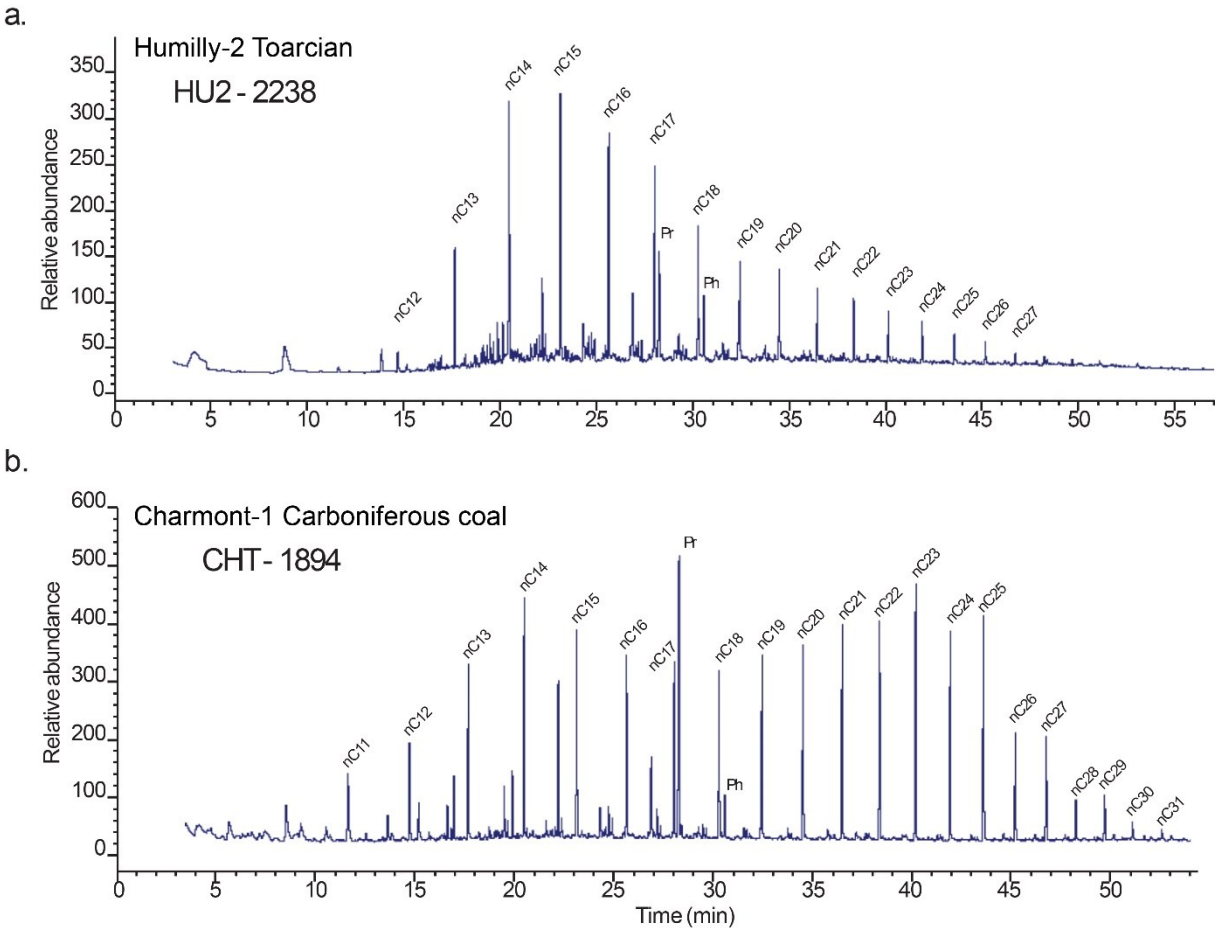

Figure 37: Typical aliphatic fraction total ion chromatogram for (A) Posidonia shale from the Humilly-2 well (Toarcian) and (B) Carboniferous coal of the Jura Mountains from the Charmont-1 well.

Additionally, low Pristane/Phytane ratios of the Posidonia shale from the Humilly-2 and Chapéry-1 wells (0.87<Pr/Ph<2.06; mean value at 1.51), as well as the Pr/nC17 and Ph/nC18 ratios (Figure 38), point to an early mature organic matter (PETERS et al. 2005b), (confirming the vitrinite reflectance data) that was deposited under reducing to anoxic conditions (PETERS et al. 2005b). In contrast, high Pristane/Phytane ratios of the Carboniferous coals from the Jura Mountains (average Pr/Ph=5.23) confirm oxic conditions during deposition and hence a continental origin of the organic matter, as well as an early maturity (PETERS et al. 2005b) (Figure 38). Geochemical data used to reconstruct the plots in Figure 38 and 39 are presented in Annex 5.

Relative distributions of C27, C28 and C29 steranes plotted on a ternary diagram are a proxy used in petroleum geology to differentiate depositional environments of crude oil and source rocks (PETERS et al., 2005b). The relative abundance of C27, C28 and C29 regular steranes of the Lias indicates a phytoplanktonic/open marine source of the organic matter (Figure 39). The regular sterane abundance of the Carboniferous signifies, in turn, a terrigeneous/coastal source of organic matter (Figure 39). The regular sterane abundance of crude oil sampled near Geneva in the Allondon River (bitumen seep oozing in the Freshwater Molasse) denotes a source rock formed by phytoplanktonic/open marine organic matter (Figure 39). Such results suggest for the first time that the source of the bitumen at depth could be the marine organic matter contained in the Posidonia shale, currently mature enough to generate oil (Figure 35). In order to validate this interpretation, further analyses need to be performed on a larger number of bitumen samples.

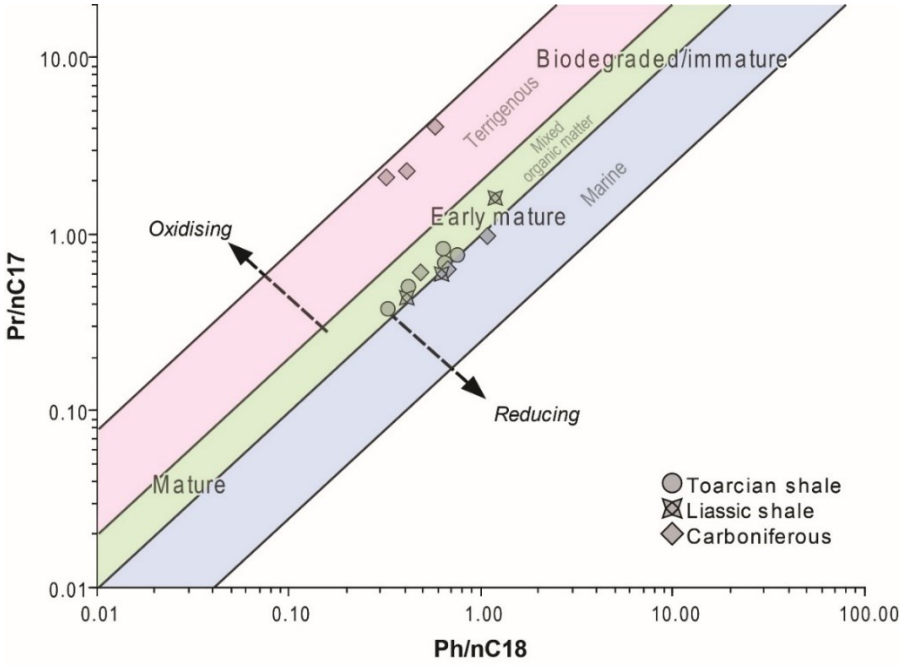

Figure 38: Biomarker diagram showing the ratio between Pr/nC17 vs. Ph/nC18 for selected Liassic and Carboniferous samples. Pr, pristine; Ph, phytane; n, straight chain alkanes.

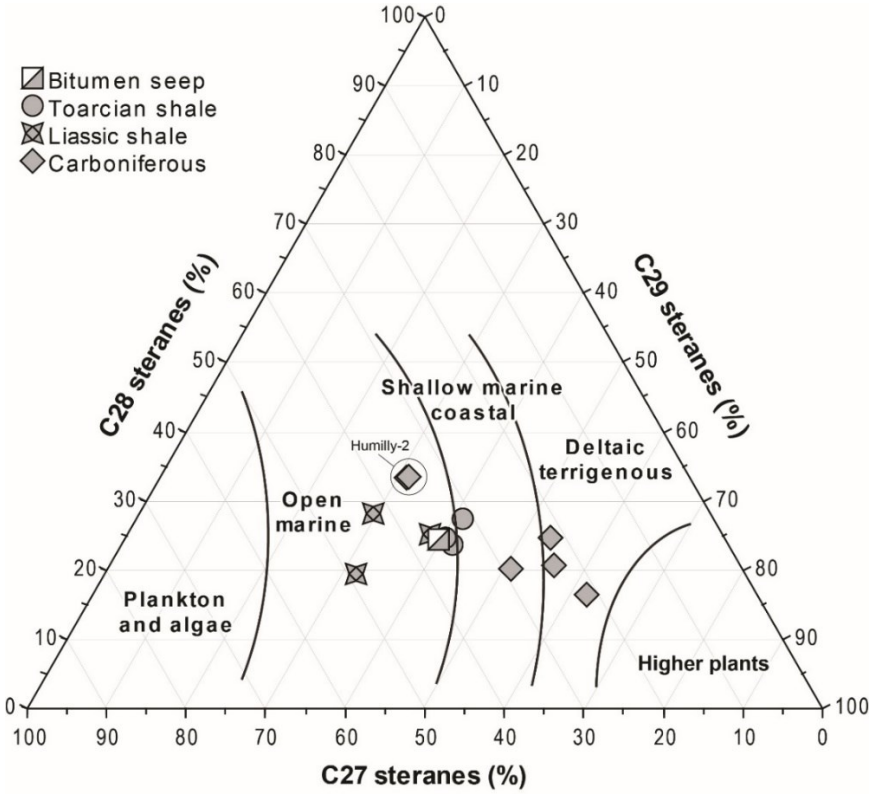

Figure 39: Ternary diagram showing the relative abundances of C27, C28, and C29 regular steranes for Lower Jurassic and Carboniferous samples and the Roulave bitumen seep. The sterane composition of the bitumen seep from the Allondon stream indicates a marine origin, equivalent to the composition of the Lower Jurassic samples

3.5. Gas seeps

In April 2016, a shallow well drilled in the Molasse near Geneva (at Satigny: LV03 - 2'491'332.384, WGS84 - 1'119'345.871, 46° 13' 00.36''N; 6° 01' 49.29''E) encountered a bitumen and gas pocket at a depth of ca. 70 m. Using a syringe, two gas samples (SAT1 and SAT2) were collected from the well head at few minutes of interval, at near atmospheric pressure and injected into a 20 mL headspace vial with a septum-lined crimp cap and filled with helium.

The gas composition (Annex 6) was obtained using a Refinery Gas Analyzer (at BGR, Hannover, Germany). This instrument is a modified gas chromatograph designed for the determination of the molecular gas composition of light-volatile hydrocarbons (methane to hexane) and permanent gases (helium, hydrogen, oxygen, nitrogen, carbon monoxide and carbon dioxide). In addition, stable isotope ratios of carbon and hydrogen were measured using a mass spectrometer. Interpreting the measured composition of the gas may lead to indications of the gas origin (biogenic/thermogenic) and the type and maturity of the related source rock. However, it must be pointed out that interpretations based on a single sample should be taken with caution, especially in the case of gas sampled at low depth, where degradation is frequent. In order to compete and validate the first hypotheses presented in this phase, a more exhaustive sampling campaign is necessary.

The gas composition of the sample from Satigny indicates that the gas is most likely a mixture of thermogenic and microbial methane (Figure 40). The isotopic composition of thermogenic gas is influenced by precursor organic matter (kerogen type) and thermal maturity. By plotting the stable isotopic carbon and hydrogen composition of methane, it appears that the thermogenic gas most likely originates from an early mature source rock (WHITICAR et al. 1986, WHITICAR 1999, Figure 40).

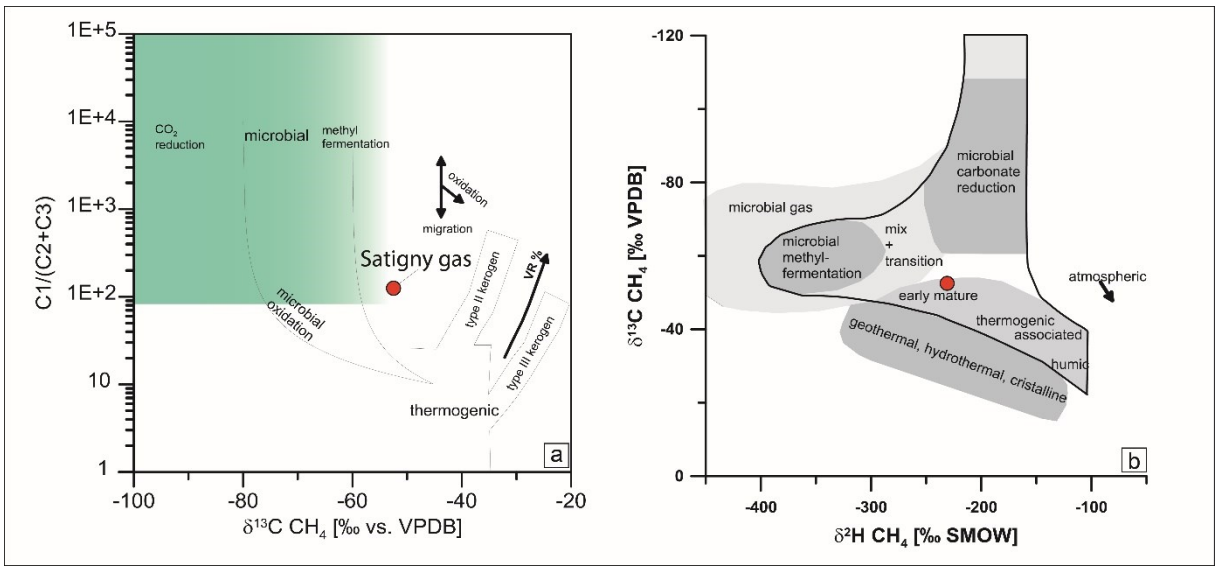

Figure 40: Carbon isotope composition of the gas sampled at Satigny-1 well showing a) biogenic and thermogenic mixing sources that indicate b) an early mature source rock (modified from WHITICAR 1999).

In the literature, an equivalent composition with high isobutane to n-butane ratios (>1) are reported for early mature oil associated with gas from type III (continental) kerogen (CONNAN & CASSOU 1980). However, the low $\delta^{13}C$ value in the methane could also indicate an early thermogenic origin from type II (marine) kerogen, but such a hypothesis cannot explain the "dryness" (low abundance of C2+ hydrocarbons) of the gas. Without additional gas samples and measurements from the basin, it is premature at this stage to conclude whether a mature type II or an early mature type III kerogen is generating the gas. More gas samples from the Molasse Basin will be collected in future campaigns to elucidate the origin of the gas seeps.

The relationship between the stable carbon isotope compositions of ethane and propane can be used to estimate the thermal maturity at which gas was generated, depending on the organic matter precursor. For marine type II

kerogen, the maturity correlation was calculated according to FABER et al. (2015), assuming a $\delta^{13}C$ precursor of -30‰ (blue line in Figure 41). Such a calculation shows that type II organic matter may be the precursor of the gas sampled at Satigny-1, if its maturity corresponds to a vitrinite reflectance of about 2.2 to 2.4 Ro%. In the same way, the maturity correlation for terrigenous type III kerogen was calculated according to BERNER & FABER (1996). The result signifies that a type III organic matter can generate such a gas with a maturity of 0.9 to 1.1 Ro% (red line in Figure 41).

As a preliminary conclusion, it can be stated that the gas geochemistry and isotopic composition indicate a mixture of thermogenic and biogenic origins of the gas from the Molasse Basin. Because of the limited number of available samples, it is not yet possible to predict the precursor of this gas (type of organic matter). A much larger sampling of the numerous hydrocarbon seeps is required to further constrain the precursor of such gases.

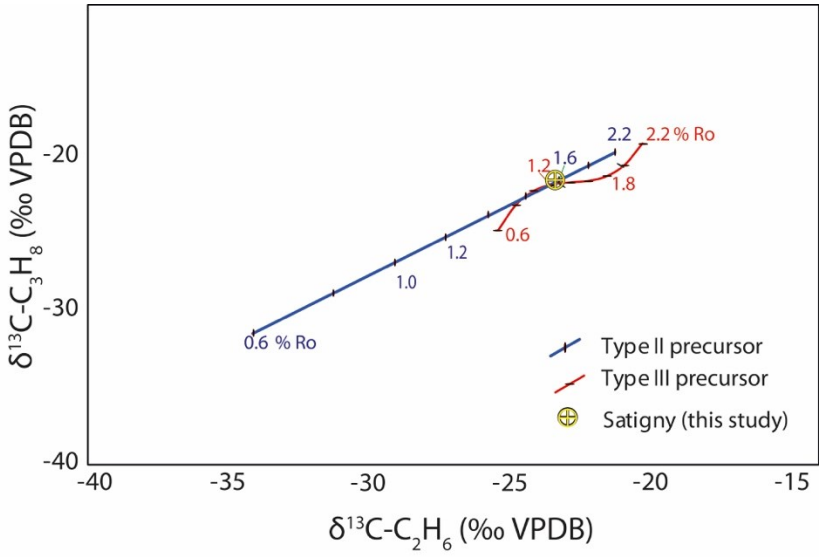

Figure 41: Relationship between stable carbon isotope compositions of ethane and propane to estimate thermal maturity at which gas was generated. Maturity correlation for marine type II kerogen (blue line) is from Faber et al. (2015), assuming precursor $\delta^{13}C$ of -27‰. Maturity correlation for terrigenous type III kerogen (red line) is from BERNER & FABER (1996) (red line), assuming precursor $\delta^{13}C$ of -23‰. Satigny-1 data is plotted in yellow.

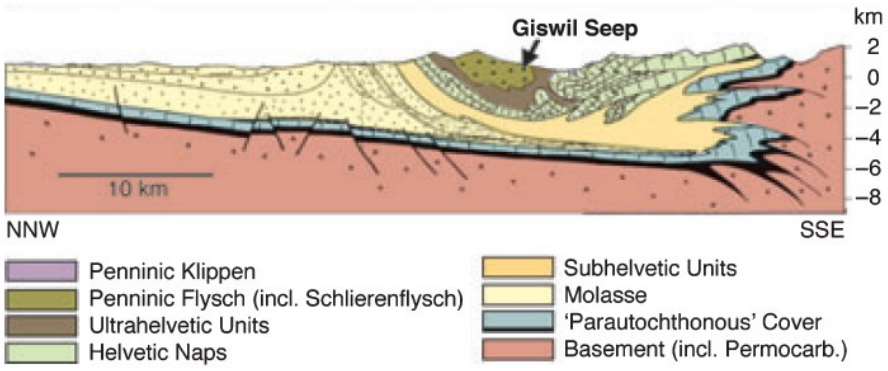

Figure 42: Location of the Wilen and Giswil gas seeps in a NNW-SSE geological cross-section through the Swiss Alps (from ETIOPE et al. 2010).

To better understand the data from the Satigny-1 well, a first screening of the literature on the gas seeps in the Swiss Molasse area was performed. Unfortunately, only a few publications exist, despite the large number of oil and gas seeps reaching the surface (LEU 2012). Carbon isotopic composition of natural gas (measured from the surface, tunnels, cores and boreholes) has been reported by GREBER et al. (1995). These authors note the occurrence of thermogenic and biogenic gases throughout the Swiss Plateau but do not provide their location. In the Northern Alps, two gas seeps near Giswil and Wilen (Canton of Obwald) have been investigated recently (Figure 42). The results indicate that the gas is thermogenic and show some evidence of slight subsurface petroleum biodegradation (WYSS 2001, ETIOPE et al. 2010).

A marine type II kerogen, with a maturity of 1.4 to 1.7 Ro%, has been postulated as the source rock in this region (Figure 43, WYSS 2001, ETIOPE et al. 2010). From this point of view, two potential source rocks are mentioned: (1) the shallow Schlieren flysch (Paleocene-Eocene) or underlying "Wildflysch" and (2) deeper Mesozoic autochthonous sediments (WYSS 2001). Such a conclusion is based on the carbon isotopic compositions of methane and ethane in the Giswil and Wilen samples, which nearly match the empiric law of BERNER & FABER (1996) for marine type II organic matter (Figure 43). The analysis also indicates a maturity of 1.7 to 1.8 Ro% (type II after FABER et al. 2015, Figure 43), which is slightly higher than that postulated by WYSS (2001) (1.4-1.6 %Ro). However, the very low propane (C_3H_8) content in the Giswil sample makes the measurement of its isotopic composition difficult (ETIOPE et al. 2010) and thus creates uncertainties in the interpretation of organic matter precursors. ETIOPE et al. (2010) proposes that the lack of propane may be due to hydrocarbon degradation.

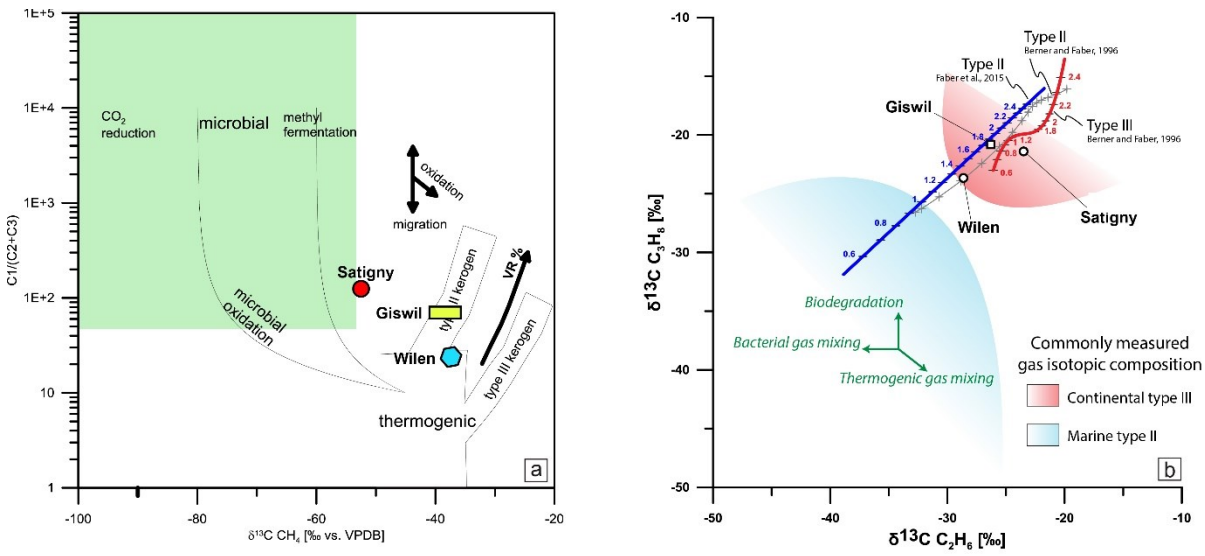

Figure 43: (a) Comparison of the carbon isotope composition of the gas seeps at Satigny, Giswil and Wilen. (b) relationship between carbon isotopic compositions of methane and ethane in the Giswil and Wilen gas samples. The vitrinite reflectance / isotope composition line (maturation line) was obtained using the calibration data for type II source rocks from BERNER & FABER (1996), as interpreted by WYSS (2001). Modified from DO COUTO et al. (2021).

In general, we can assess that without (1) more measurements of gas isotopic composition in gas (at a specific depth), which would clarify the biodegradation and (2) a better maturity estimation of potential source rocks at depth, the conclusions at hand remain uncertain. The mixing of thermogenic and biogenic gas may shift the isotopic composition as well as the biodegradation of a primarily thermogenic gas (JIANFA et al. 2000, LIU et al. 2008, ZHU et al. 2014, OSTERA et al. 2016).

3.6. Conclusions

In the second part of the UNCONGAS project, comprehension of the most relevant hydrocarbon source rocks in the study area was improved. The results allow the assessment of the hydrocarbon potential of these rocks. In detail, the following points were elucidated in this phase:

- The seismic interpretation, together with the well-log correlation, permit to identify a stratigraphic interval in the Lias that corresponds to the organic-rich Posidonia shales. This interval was penetrated by several wells (Chapéry-1, Humilly-2, Faucigny-1, Essertines-1, Eclépens-1, Romanens-1) in the western Swiss Plateau. The effective thickness of this organic-rich interval is about 10 m.
- Geochemical analysis of source rocks and superficial oil and gas seeps, combined with vitrinite reflectance measurements, organic geochemistry of biomarkers and gas isotopic measurements, indicate the existence of an active petroleum system at a depth greater than 2200 m.
- The Posidonia shale may be considered a "shale oil" play, thus representing a source of conventional and unconventional hydrocarbon accumulations in the southwestern Swiss Plateau. However, the insignificant thickness of the organic-rich unit (source rock), the densely-spaced faults and fractures crossing the entire subsurface stratigraphic succession, and the several oil seepages to the surface, strongly suggest that limited volumes of hydrocarbon accumulations are present in the subsurface. Furthermore, the lack of large-scale structural traps stratigraphically above the Posidonia shale and the lack of laterally continuous stratigraphic seals, support this hypothesis. On the other hand, the richness in organic matter of the Lias deposits point to the possibility of an unconventional petroleum system.
- The Permo-Carboniferous unit is deep enough to be able to generate gas. Therefore, these deposits are considered to have the highest potential for gas generation. Nevertheless, intense faulting of the basin and the decollement of the Meso-Cenozoic sedimentary package above the Permo-Carboniferous troughs may prevent large accumulations of gas, at least in the southwestern Swiss Plateau. A conclusive statement regarding this hypothesis requires new subsurface data (i.e. seismic surveys and wells for ground-truthing), which are currently not available.
- The gas seepages found in the Molasse indicate a mixture of biogenic and thermogenic gas, which could be related to shallow immature organic matter degradation and to thermal cracking of deep source rocks, respectively. Because the available data is limited, the type of organic matter precursor of this gas cannot be determined yet.

4. UNCONGAS Part 3 (2017) Petroleum system modelling

4.1. Introduction

Basin Petroleum System Modelling (BPSM) is an excellent tool for reconstructing the thermal history of a basin and to simulate the formation of oil and gas accumulations in the basin. Modelling permits to take into account of a large number of geological variables (e.g. lithology, thickness, geometry, heat flow, compaction factors, fluids circulation, faults, type of organic matter etc), and to quantify their effect on the thermal maturation of the organic matter as well as the hydrocarbon generation, migration and accumulation. Various levels of model complexity can be defined, depending on the amount of available data and time. A 1D model simulates the thermal conditions at a point in the basin, a 2D model is a representation along a profile and a 3D model takes into account the geological property variation in 3D space. In Part 3, 1D models were constructed to provide the first relevant information on the thermal state of the study area. A preliminary 3D model of the Geneva Basin was also produced, but further work is needed to improve its stratigraphic and fault geometries.

Independent of the model complexity, a mandatory step in the modelling workflow is the calibration of the predicted temperature and thermal properties with rock sample measurements using geothermometers (e.g. vitrinite reflectance, illite crystallinity, fission tracks, fluid inclusions). In this phase of the project, the available data were to sparse to validate thermal modelling results.

4.2. One-dimensional (1D) BPSM

4.2.1. Representation of the stratigraphy

We performed BPSM using the PetroMod© software (Schlumberger), which combines seismic, well and geological information to model the evolution of a sedimentary basin. The model is able to predict if and how hydrocarbons accumulated in a reservoir, the source and timing of their generation, migration routes as well as quantities and types of hydrocarbons at subsurface or surface conditions.

An important step for a subsequent simulation is to define the geological events of a specific time period. There are four types of events:

- deposition
- erosion
- hiatus
- thrusting

A 1D BPSM model was constructed for the Humilly-2 well site to obtain a predictive model that allows a consistency check, comparison and correlation of measured maturity data. For this site, all depositional events were added to the stratigraphic column as shown in Figure 44. Furthermore, an erosion event was added to the top of the Lower Cretaceous, to account for the known Upper Cretaceous erosion (SCHEGG et al. 1997). Each formation was attributed one bulk lithology based on the well report.

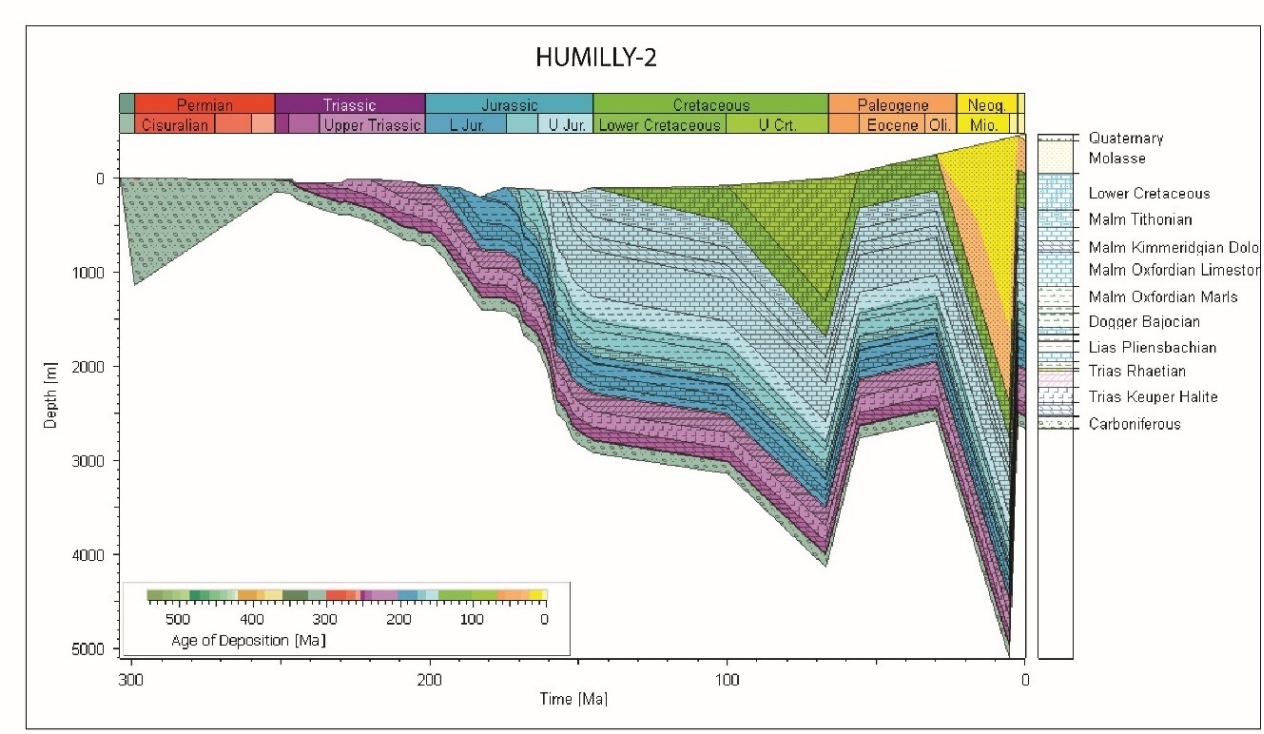

Figure 44: Burial history overview of the Humilly-2 site indicating the formations, lithologies and ages of deposition and erosion.

4.2.2. Boundary conditions of the Humilly-2 well

In addition to the stratigraphic input, the modelling requires the establishment of the following boundary conditions:

- paleo-water depth (PWD)
- sediment water interface temperature (SWIT)
- basal heat flow (HF)

These boundary conditions define the basic energetic conditions for the temperature development of all layers, especially the source rock and, consequently, for the maturation of organic matter through time. There is only one set of boundary conditions for each model. The PWD (paleo bathymetry) was assessed according to the lithology and palaeontological assemblage in the stratigraphic layers and cross-checked with data from the literature (Figure 45). The approach to estimate the temperature of the sediment-water interface was based on that of WYGRALA (1989), which relies on the latitudinal position of the stratigraphic section (Figure 45). Estimation of the basal heat flow (Figure 45) used the McKenzie crustal model, which assumes a uniform crustal stretching (JARVIS & MCKENZIE 1980).

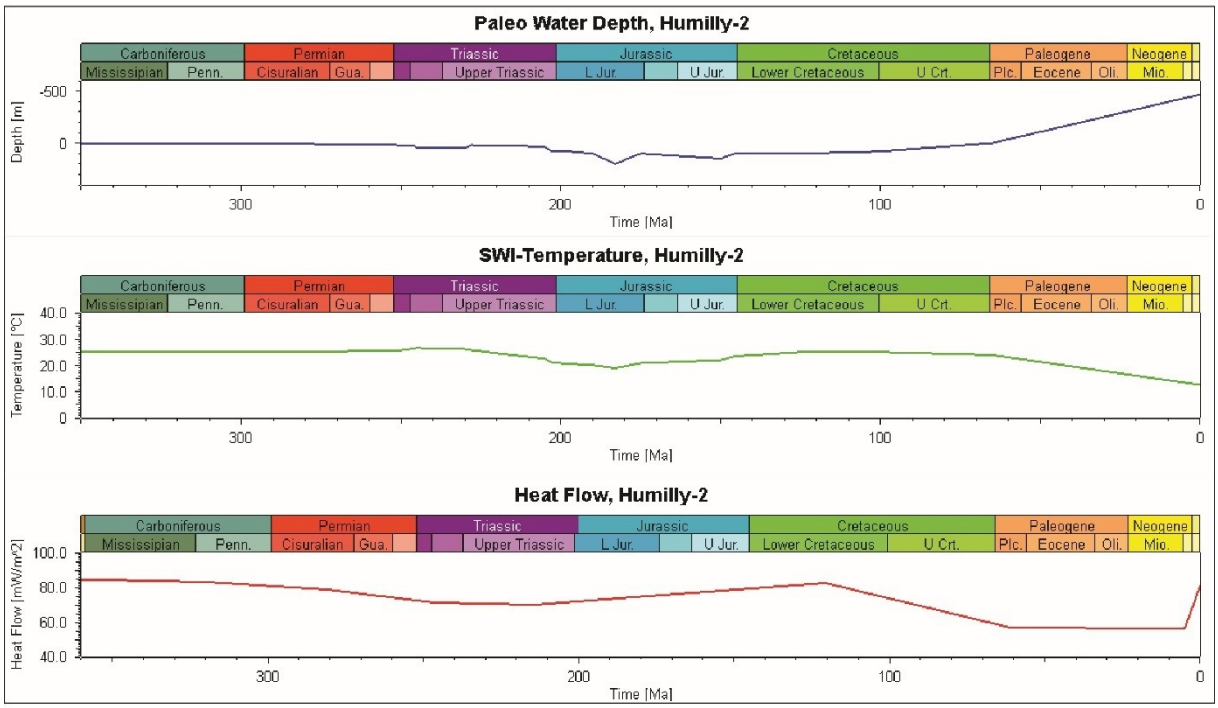

Figure 45: Boundary conditions used to model the stratigraphic succession of the Humilly-2 well site and the tectonic history of the Molasse Basin. SWI: surface water interface temperature

4.2.3. 1D model of the Humilly-2 well

The resulting model of the burial and thermal history of the Humilly-2 well site is in good agreement with the maturity data (Figure 46 and Figure 47). According to the simulation results, the Posidonia shale has reached the early oil window with a vitrinite reflectance of 0.75 Ro%. The model is matches the measured vitrinite reflectance of 0.74 Ro% (Figure 48). The maturity profile of the Humilly-2 well site indicates that the top of the Permo-Carboniferous reaches a vitrinite reflectance of around 0.96 Ro%, with a present-day temperature at around 87°C (Figure 47). This result is consistent with the bottom-hole temperature of 105°C measured in 1969.

Sensitivity tests are useful for understanding and calibrating deviations between measured and simulated values. The differences between the measured and the modelled maturity and temperature data are probably due to the following factors:

- the approximation of the heat flow based on the crustal stretching model
- the thickness Upper Cretaceous deposits prior to their erosion
- the amount of erosion at the base of the Paleogene and the Quaternary

For instance, the McKenzie crustal model is based on uniform stretching taking into account, among other parameters, the thickness of the pre-rifting crust. A slight change in the pre-rift thickness, from 40 km to 37 km thick, causes an increase in temperature of about 6°C at the top of the Carboniferous and an increase in the vitrinite reflectance of the Toarcian Posidonia shale of 0.09%. In addition, surface vitrinite reflectance analysis reveals that the Oligo-Miocene Freshwater Molasse in the GGB can reach 0.43 to 0.47 Ro% (DEVILLE & SASSI 2006). Our 1D BPSM fits quite well with these data and gives a maturity of around 0.39 to 0.42 Ro% (Figure 47). Still, a closer investigation of the erosion rate and the paleo-heat-flow may improve the maturity model.

The 1D BPSM permits the timing of the source-rock maturation to be calculated. For the Humilly-2 site, our simulation shows that the Posidonia shale, rich in organic matter, entered the early oil window at a depth of around 2000-2100 m during the Lower Cretaceous (Figure 46). According to this result, the transformation ratio

(i.e. the percentage of generated petroleum compared to the maximum potential petroleum generation in a source rock) of the Posidonia shale reaches 45% today.

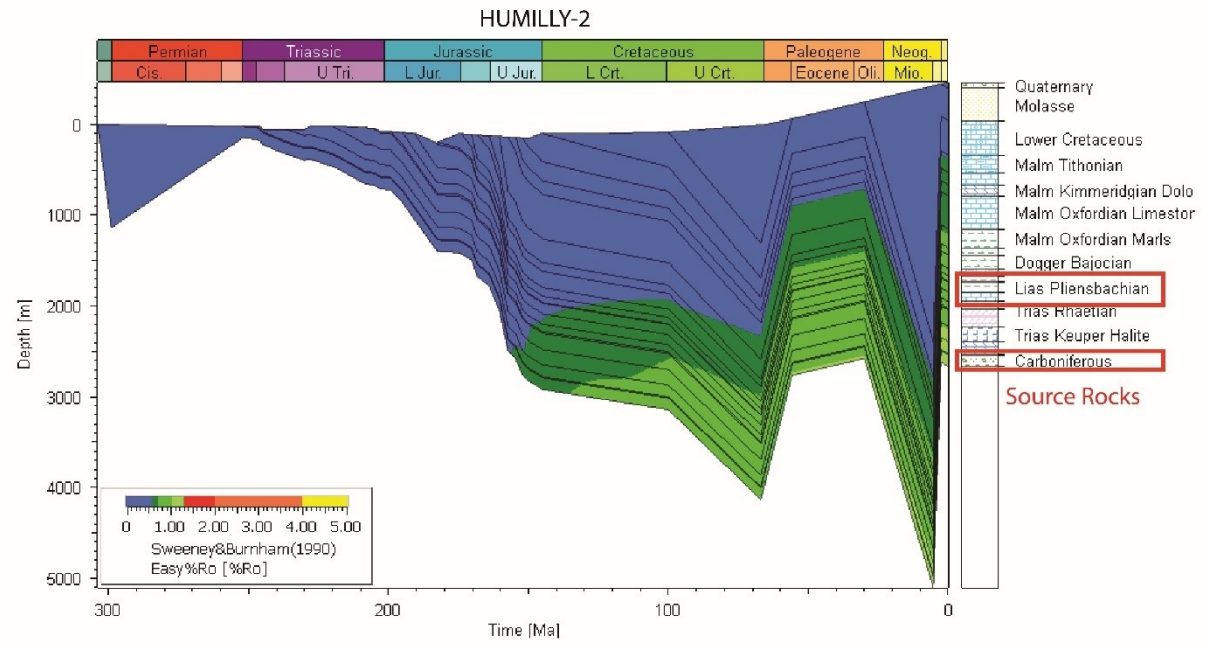

Figure 46: Burial history of Humilly-2 well site displaying the early oil (dark green) and main oil (light green) maturity fields according to SWEENEY & BURNHAM (1990).

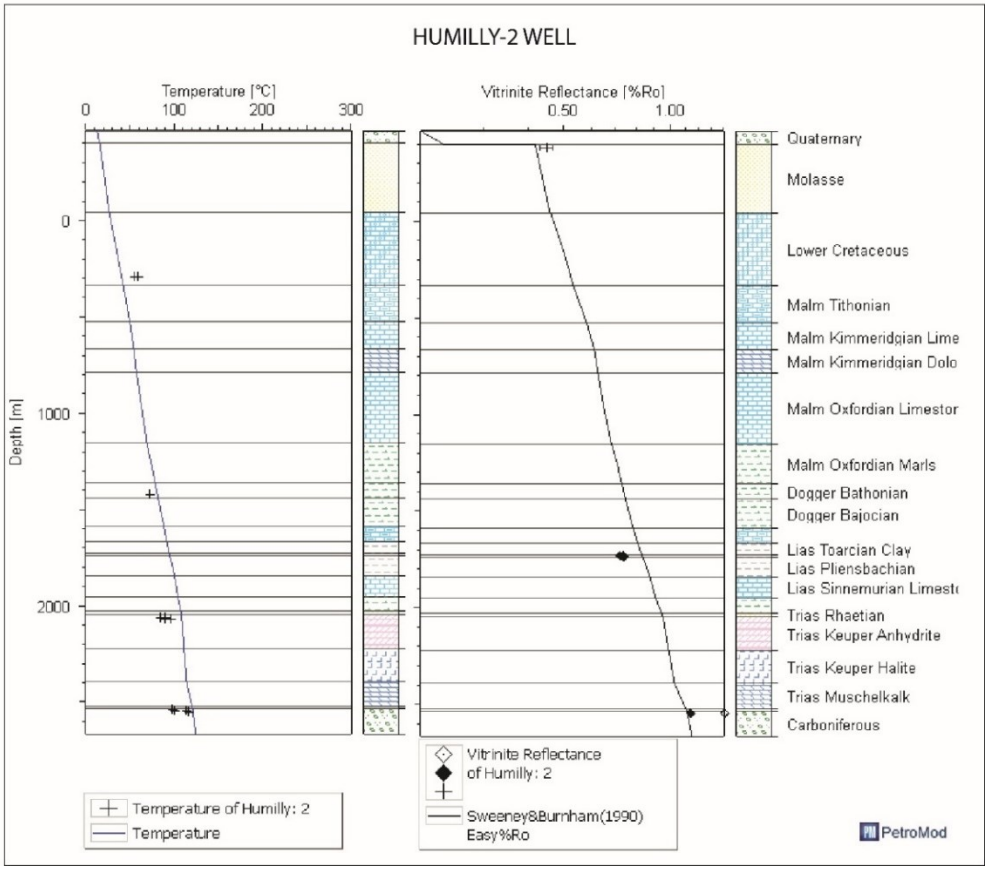

Figure 47: Results of the Humilly-2 well site simulation showing the temperature reached in the stratigraphic succession (left) and the calculated maturity (right).

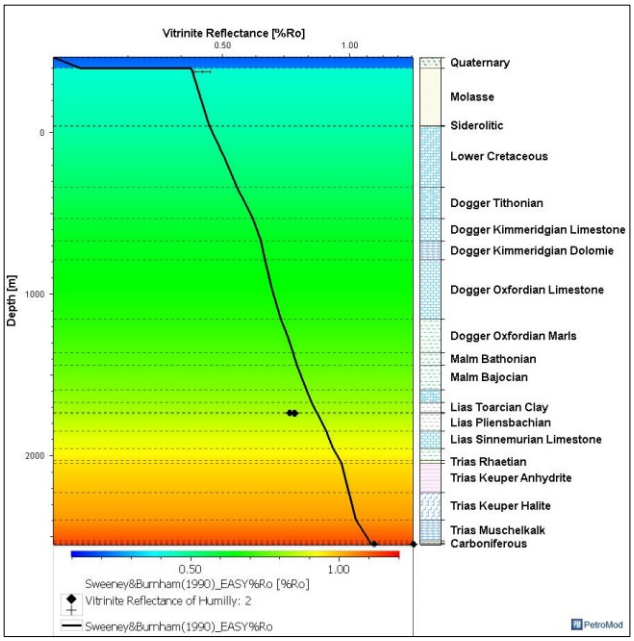

Figure 48: Calibration of the thermal model with the sparse vitrinite reflectance (%Ro) data.

4.2.4. 1D model of the Eclépens-1 well

A 1D BPSM simulation was performed also for the Eclépens-1 well site and was based on well reports, estimates of erosion rates (SCHEGG et al. 1997, 1999) (Figure 49). As for the previous model, the heat flow was computed using the uniform crustal extension model of McKenzie (1978).

Results of the primary simulation suggest that, in the Eclépens-1 area, the Toarcian Posidonia shale entered the oil window during the Lower Cretaceous. They also predict a present-day maturity at 0.73 Ro%, similar to that calculated by SCHEGG et al. (1997). The simulation yields a current transformation ratio of the Toarcian Posidonia shale of around 35%, lower than that of the Humilly-2 model. However, the type of organic matter and the organic content of the Toarcian Posidonia shale source rock are not known in the Eclepens-1 samples, and the measurements of TODOROV et al. (1993) used in the simulation come from northern Switzerland. Therefore, a change in the organic content and geochemistry could also imply a shift in the hydrocarbon transformation timing (TISSOT & WELTE 1984). Geochemical analyses of the Posidonia shales in the Eclépens-1 well will be performed in the future to better constrain the model.

The Eclépens-1 well terminated in the Keuper unit and did not reach the basement (Figure 49). About 12 kilometers to the north, the Treycovagnes-1 well traversed the entire Mesozoic interval to reach more than 470 m of Permian sediments constituting conglomerates alternating with medium-grained sandstones and red shales intercalations. An organic-rich formation of the Permian, known as the Autunian shales, represents a very good lacustrine source rock (LEU 2014). To simulate the behaviour of the basin, we modelled a synthetic well based on the stratigraphy of the Eclépens-1 site (Figure 50) and added the basal stratigraphy of the Treycovagnes-1 site from the Upper Keuper to the Permian. Seismic interpretation allowed to identify a series of Permo-Carboniferous troughs below the Mesozoic cover in the Eclépens-Essertines-Treycovagnes area (Figure 50b, SOMMARUGA et al. 2012). Thus, in addition to the known stratigraphic succession, a series of Permian shales and Carboniferous sandstones with coal beds were included at the base of the synthetic well to account for the potential organic matter. Results of the simulation suggest that (1) the Permian lacustrine source rock comprising red shales should have reached the condensate/wet gas window (0.9< Ro%<1.35; Figure 50a) since the Lower Cretaceous and that (2) the Carboniferous should have reached the dry gas window (>1.35 Ro%; Figure 50a).

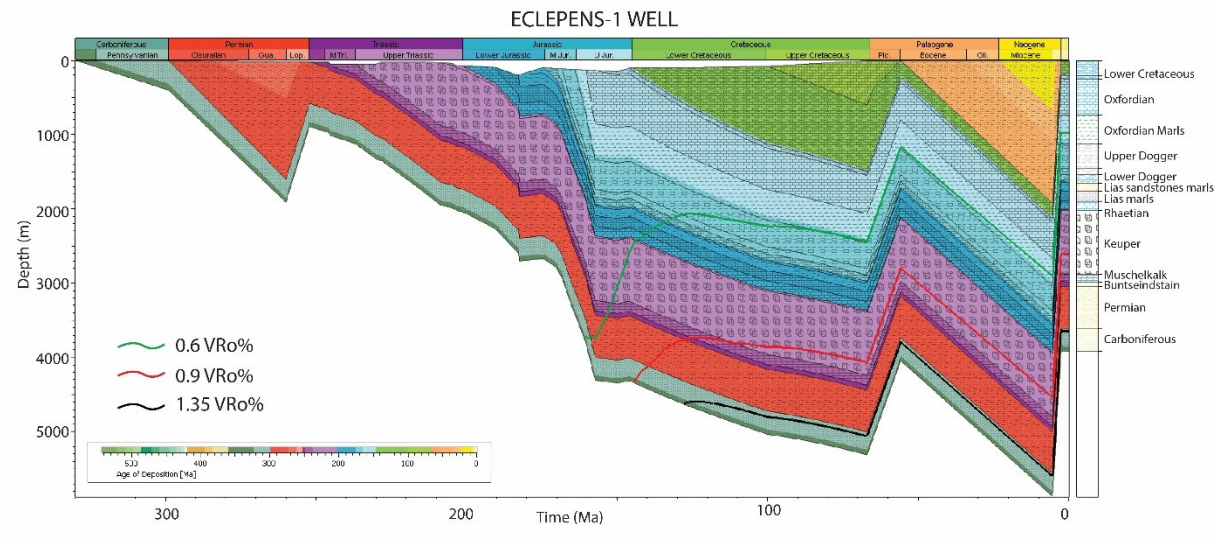

Figure 49: Burial history of Eclépens-1 displaying the entry into the oil window (red line) according to SWEENEY & BURNHAM (1990).

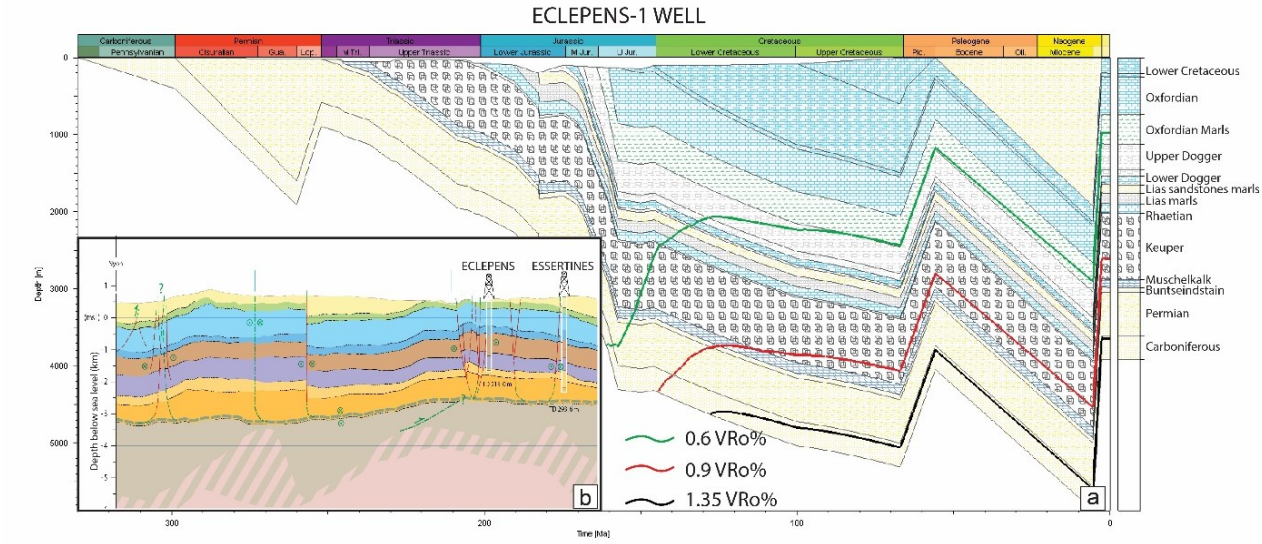

Figure 50 (a) 1D model of the Eclépens-1 well. Entry into the oil window (green line), condensate/wet gas window (red line) and the gas window (black line) according to the modelling results. (b) interpreted seismic profile intersecting the Eclépens-1 well and showing a Permo-Carboniferous trough at depth (SOMMARUGA et al. 2012).

4.3. 3D model of the Geneva Basin

In the last phase of the project, a 3D geological model of the GGB was constructed, integrating large sets of geophysical, geological and outcrop data. The geometry and thickness of the different layers constituting the stratigraphic record of the basin were determined. The available structural data (fault planes) were also implemented in the model (Figure 51).

By incorporating literature data, the thermal gradient recorded in the basin history was reconstructed and modelled. Modelling results suggest variations in temperature over time, which in turn constrain zones of hydrocarbon generation throughout the basin (Figure 52). Oil-window and gas-window thermal conditions were inferred

for the Toarcian and Carboniferous layers, respectively. These units, rich in organic matter (see Pert 2), are potential source rocks of the system. Therefore, hydrocarbons generated from these rocks may be found in extensive portions of the basin. They may be encountered when exploring for non-hydrocarbon resources (such as geothermal reservoirs) and thus pose operational hazards.

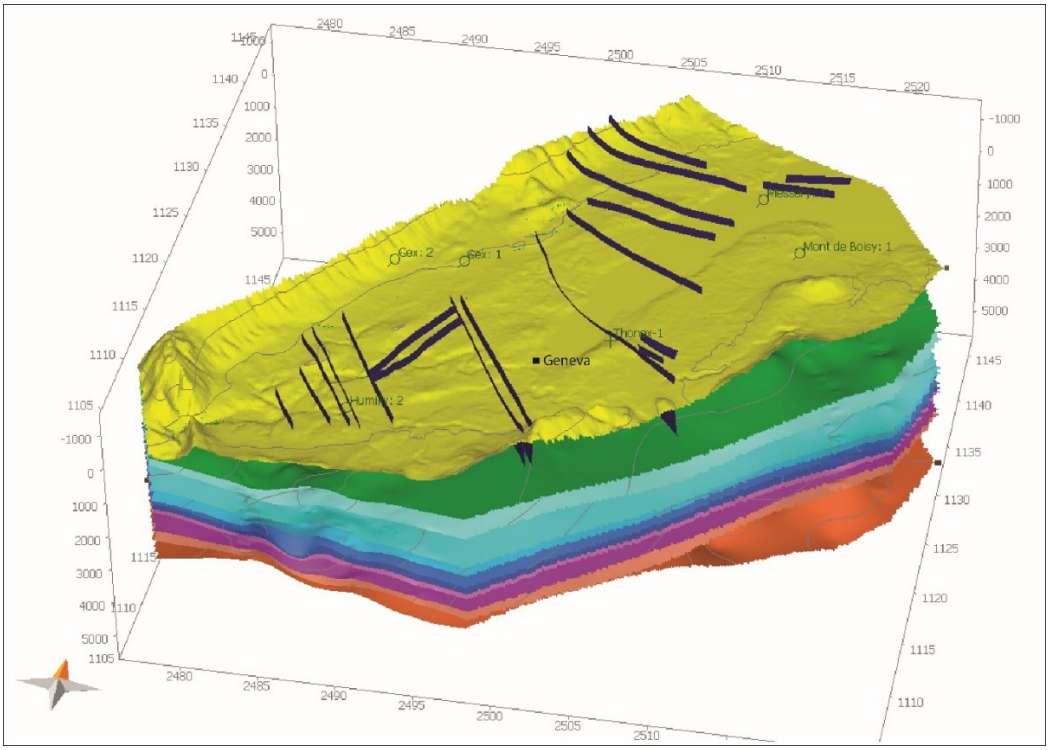

Figure 51: Geometrical model of the Geneva Basin (data from GeoMol).

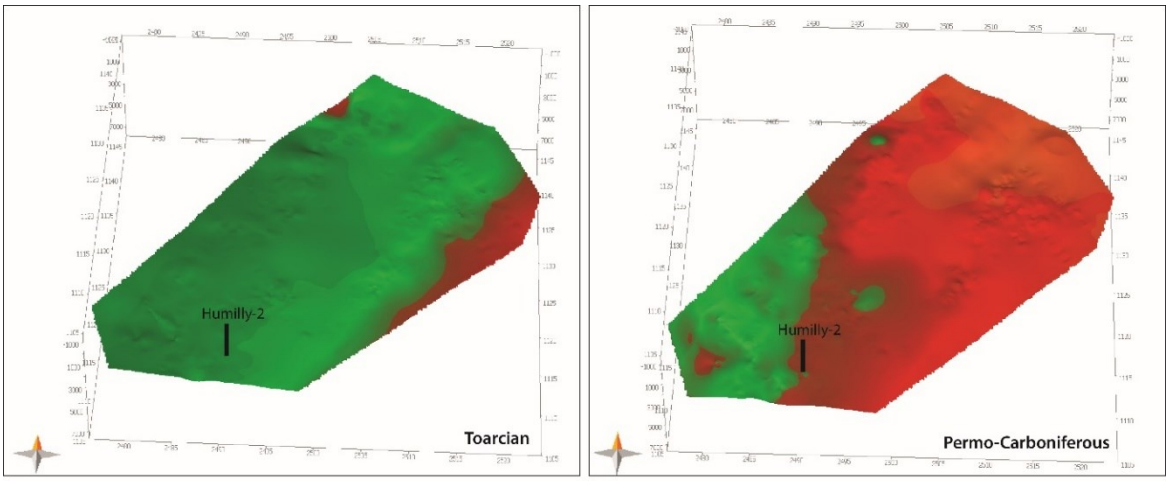

Figure 52: Maturity maps (green - oil window; red – gas window) calculated by the model for the Toarcian and Carboniferous layers.

Permeability variations throughout the basin were considered to model the hydrocarbon migration paths. Migration paths are an important consideration when modelling the initial amount of hydrocarbons in place and hy-

pothesizing the size of potential oil and gas accumulations (Figure 53). The results show that preferential migration paths occur mostly along modelled fault planes. Thus, oil and gas circulation would also be expected to occur in these areas.

The thermal history reconstructed in the 3D model is better constrained than that in the 1D model, because it is based on more data and variables. As a result, the validation of the 3D model with vitrinite reflectance performed more reliable results. The measured vitrinite reflectance is consistent with the theoretical values given by the model (SWEENEY & BURHNAM 1990). However, the limited number of samples available for vitrinite measurements is insufficient to perform a fully reliable calibration. Future work will involve additional sampling for vitrinite reflectance measurements and implementation of new geothermometers, such as illite crystallinity, fluid inclusions and fission tracks.

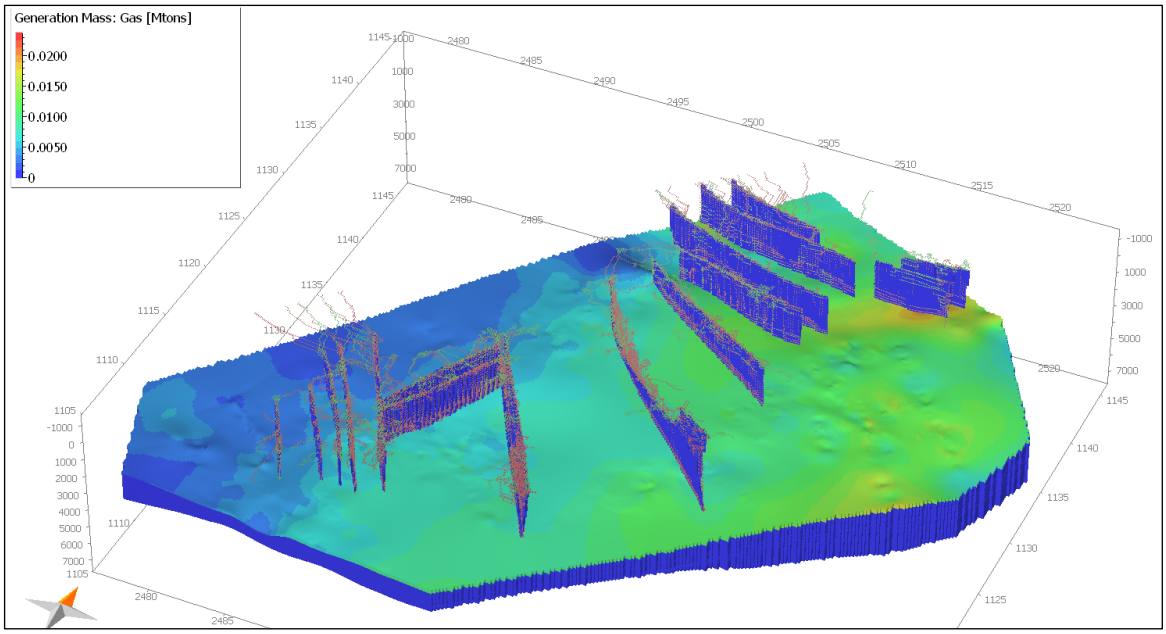

Figure 53: Generation mass of gas (Megatons) in the basin and modelled hydrocarbon migration paths.

4.4. Reconstruction of maturity gradients in the Swiss Plateau

Currently, only sparse vitrinite reflectance data are available from the Lias and Carboniferous deposits of the Geneva Basin, which are richest in organic matter. Thus, the limited number of temperature-control points at depth are insufficient to calculate a reliable thermal gradient for the region. Future analyses of organic-rich samples will provide the necessary data, but in this phase, a more reliable estimate of the maturity gradient was possible by implementing measured data from the literature.

4.4.1. Western Swiss Plateau

Literature vitrinite reflectances measured in the Oligo-Miocene Molasse, which outcrops close to the studied wells, were used to extrapolate a maturity gradient to depth (Figure 54a; DEVILLE & SASSI 2006). A range of 0.42 to 0.47 Ro% fits the maturity profiles of the Humilly-2 and Chapéry-1 wells, whereas a range of 0.54 to 0.58 Ro% fits in the case of the Faucigny-1 well (Figure 54b).

Calculated maturity profiles are compared to those suggested for the Canton of Vaud (SCHEGG et al. 1997, GORIN et al. 1993). Considering only the wells that reached the Early Jurassic intervals (Eclépens-1, Essertines-1 and Treycovagnes-1), the interpolated vitrinite reflectance of the Posidonia shale may attain 0.7 to 0.8 Ro% (Figure 54b), similar to the maturity of the Humilly-2 well samples (0.74 Ro%, Figure 48). Except for Savigny, where the well is the only one in the Canton of Vaud penetrating the Subalpine Molasse, the maturity profiles of SCHEGG

et al. (1997) are relatively homogeneous and similar to the ones we interpolate for the Humilly-2 well samples (Figure 54b). The Essertines-1 results are slightly different from the others, as it indicates a higher maturity trend. Such a difference may be due to a higher post-Molasse erosion rate, thus a higher original burial depth (SCHEGG et al. 1997). This hypothesis will be tested with BPSM at a later stage. At the Chapéry-1 site, vitrinite reflectance of the Posidonia shale is lower than in other parts of the basin, taking into account the depth of the formation (Figure 54). These differences, observed in a relatively restricted area, can hardly be explained by assuming a variation in the geothermal gradient. A possible explanation could be the deep circulation of hot fluids that produce local thermal anomalies. Further investigations are planned to explore this hypothesis.

At the Faucigny-1 site, the maturity of the Posidonia shale is very high compared to that of the other well samples (Figure 54b). Vitrinite reflectance of the surface samples also shows an increase in maturity of the Subalpine Molasse (Figure 54a, DEVILLE & SASSI 2006). In this area, intense tectonic loading occurred during the early Oligocene, as a consequence of the emplacement of the Prealpine nappes (DEVILLE & SASSI 2006). Thus, a higher burial rate in this area was likely and probably caused the higher thermal conditions.

In the Thônex-1 well, the thermal gradient was calculated by interpolating geothermometric data from the Molasse deposits (SCHEGG & LEU 1996). A coalification gradient of 0.33 Ro%/km was calculated from these data, considering a surface Ro% value of 0.4. According to the GeoMol 3D model of the Lias unit in the Geneva-Savoie area (available at **https://geneve.geomol.ch**), a depth between 2400 and 2500 m below surface or below sea level can be estimated for this area. Thus, a maturity for these layers of 1.1 Ro% is expected, much higher than that measured in the Humilly-2 well samples. Further investigations are necessary to constrain these data and to explain the variation in thermal history.

4.4.2. Central and eastern Swiss Plateau

Compared to those in eastern Switzerland and southern Germany, the maturity gradients in the western and southwestern Molasse Basin appear to be lower (Figure 55). Early Jurassic samples from Weiach were not analysed, but the calculated maturity profile suggests an approximate value of 0.6 Ro% (LEU & GAUTSCHI 2014). Given the general maturity profiles in northeastern Switzerland and southern Germany, the Posidonia shale may have reached the condensate/wet gas window at a greater depth, such as in the case of Tettnang, Germany (MAZUREK et al. 2006).

Maturity data from the Permo-Carboniferous units are too scarce in the Swiss Plateau to allow determination of maturity trends. Previous studies of the Permian and Carboniferous deposits in Weiach (MAZUREK et al. 2006) show that the Permian is in the oil window and the Carboniferous in the condensate/wet gas window (0.9< Ro%<1.35).

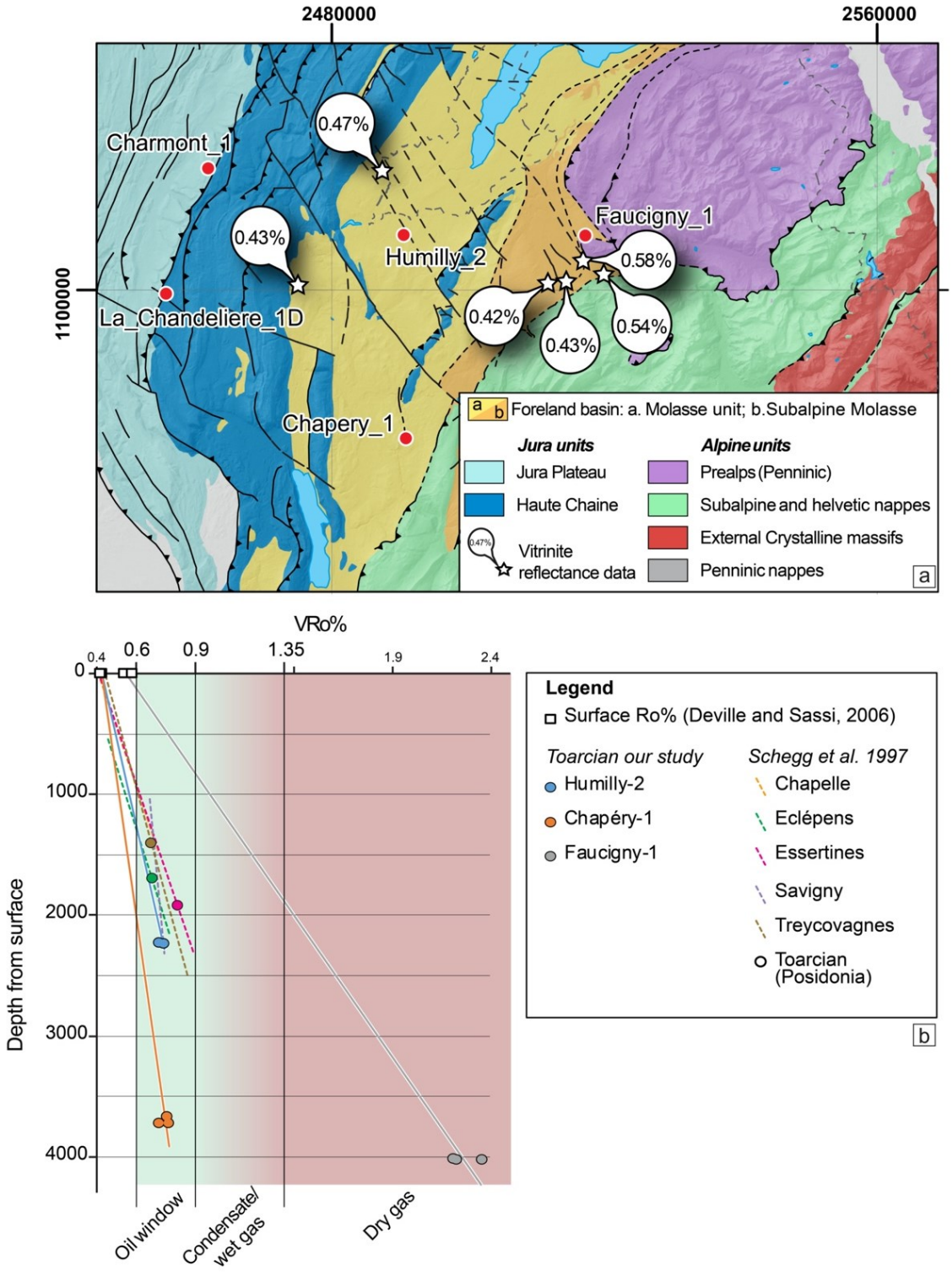

Figure 54: (a) Geological map of the Geneva Basin with the vitrinite reflectance data of surface samples (DEVILLE & SASSI 2006). (b) Maturity profiles in the Geneva Basin from data provided in this study (cuttings from the Humilly-2, Chapéry-1 and Faucigny-1 wells). For comparison, literature data from the wells Chapelle-1, Eclépens-1, Essertines-1, Savigny-1 and Treycovagnes-1 are shown (SCHEGG et al. 1997).

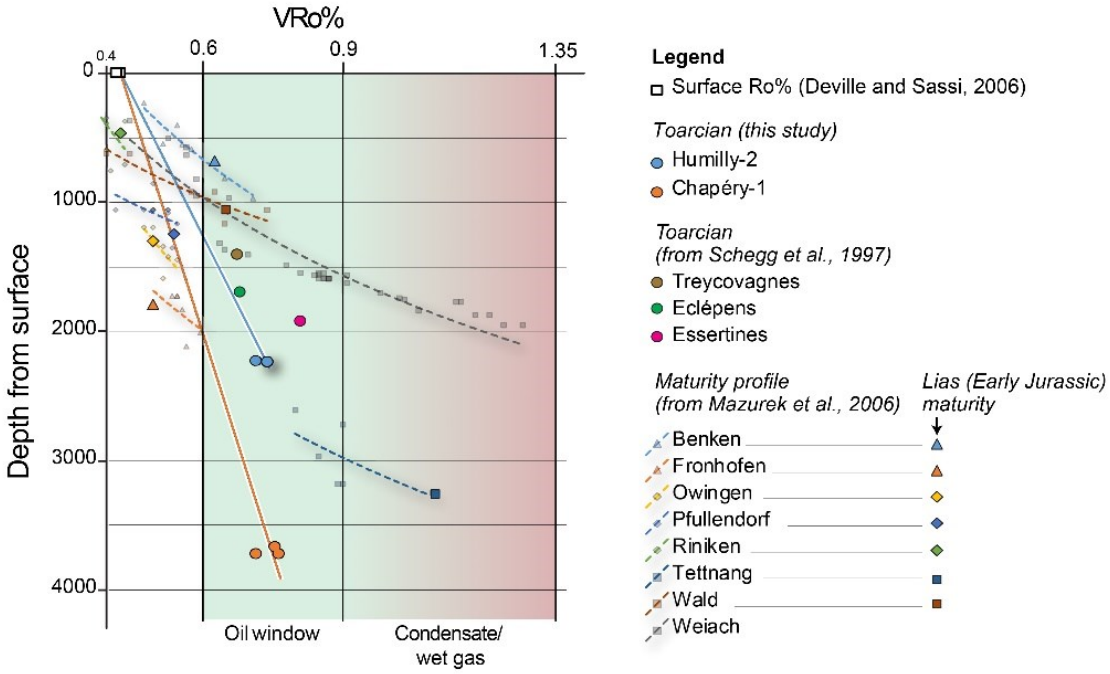

Figure 55: Maturity profile in southwestern Switzerland based on cuttings from wells Humilly-2 and Chapéry-1. For comparison, data from northeastern Switzerland and southern Germany are also displayed.

5. UNCONGAS Part 4 (2017) Hydrocarbons volume estimate

5.1. Introduction

To assess the likelihood of encountering hydrocarbon accumulations during geothermal exploration of the Swiss Plateau, it is necessary to estimate the amount of oil and gas potentially stored in the subsurface. To answer this essential question, several parameters need to be considered and evaluated, such as: (1) the source rock volume and its hydrocarbons potential, (2) the source rock expulsion efficiency and (3) the reservoir capacity to store oil and/or gas. Generally, in an initial exploration phase only some of these data are available, so several assumption need to be made. Therefore, estimations from the initial exploration stages are mostly probabilistic in nature and contain major uncertainties. In subsequent exploration phases, when more data are collected, uncertainties in resource estimates are gradually eliminated. If hydrocarbons are encountered and volumes are tested in the later phases, resources may actually be converted into producible reserves.

This project is currently in the first resource estimation phase. Estimation of the possible volumes of hydrocarbons stored in the Swiss Plateau was performed with the following workflow:

- calculation of the volume of rocks able to generate hydrocarbons
- estimation of the amount of hydrocarbons generated by the source rocks
- estimation of the gas and oil initially in place

Data from previous regional studies (e.g. GeoMol) as well as from analytical studies in this project (see previous parts) were used for the calculations. The latter focused mostly on the Geneva Basin, in which detailed geochemical and petrographical analyses were performed on source-rock and reservoir samples from well cores. Furthermore, the geometries and thicknesses of the stratigraphic layers were modelled at a higher resolution for the Geneva Basin than for the rest of the Swiss Plateau, where data are less abundant. Thus, in the UNCONGAS project, data and interpretations from the Geneva Basin were extrapolated to the rest of the study area, keeping in mind the high uncertainty associated with extrapolations using sparse data. The extrapolations were based on a range of scenarios, in which each parameter was characterized by a range of estimates. The scarcity and scattering of the data meant that several assumptions had to be made. More data will be acquired in future work, also from the rest of the Swiss Plateau, so that more realistic estimates will be possible.

5.1.1. Source-rock volume

To date, the Toarcian black-shale unit could be differentiated only in few well logs, mostly located in the western part of the Swiss Plateau. Therefore, the thickness of these deposits in the rest of the study area towards the Lake of Constance need to be estimated.

The volume of the Permo-Carboniferous source rock is even more uncertain. Seismic surveys and drilling campaigns report difficulties in identifying any Permo-Carboniferous deposits and determining their extent and thickness. The volume presented in this study is based on literature data proposing a variety of scenarios and interpretations, a methodology that we also follow.

5.1.2. Source rock volume calculation

In the Swiss Plateau two source rocks were identified: 1) the Lower Jurassic Posidonia black shale unit (Toarcian) and 2) the coal and organic-rich shales of the Permian-Carboniferous deposits. The Jurassic source rock forms part of the substratum of the Swiss Plateau basin containing the Molasse deposits. Therefore, it extends throughout the entire area with variable thickness. The Permo-Carboniferous source rocks accumulated in confined grabens, which formed during the Varisican post-collisional orogenic (mountain-building) phase. To present, the position and the geometry of these troughs beneath the Mesozoic substratum remain highly uncertain because of the scarce and low-quality data (seismic, logs, cores) from this depth. Most of the available data on the geochemical properties of these source rocks come from the Geneva Basin area. These properties were extrapolated to

the entire Swiss Plateau, in terms of organic-matter richness, type and hydrocarbon potential, although this assumption greatly simplifies the large heterogeneity of the organic matter that could exist throughout the basin.

b) The Posidonia shales (Lias, Toarcian)

In order to calculate the volume of the Posidonia shales in the Swiss Plateau, it was necessary to first determine the extent and thickness of the entire Lias unit. The boundaries of this unit were mapped on the basis of 2D seismic data in the context of the GeoMol project (Landesgeologie 2017). Thus, grids of the Top Triassic and Top Lias horizons were calibrated throughout the entire study area using the stratigraphy of 17 deep boreholes from the Swiss Plateau (Figure 56), for which these two stratigraphic markers had been identified. The tops of the Lias and Triassic surfaces were obtained and used to calculate the top Lias surface in depth (Figure 57) and the thickness of the Lias stratigraphic unit throughout the entire Swiss Plateau (Figure 58), with the aid of the Schlumberger Petrel software. Finally, a gross rock volume of 1.15 x 1012 km3 (or 1150 km3) was determined.

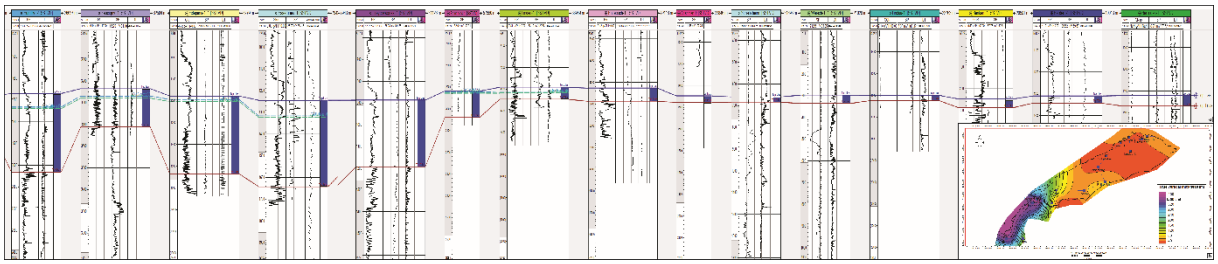

Figure 56: (a) well logs used to calibrate the seismic data interpolation, where the Lias unit boundaries were defined. Where possible, the Toarcian black-shale unit was identified (thin blue lines). (b) the inset shows the interpolated depth map (meters) and the well locations. Original figure at big scale in Annex 7.

In estimating the volume of oil and gas generated by these rocks, only the thermally mature portion of the volume was considered. The maturity boundaries proposed by LEU & GAUTSCHI (2014), based on vitrinite reflectance, were used to delimit the area where the Lias unit is in the mature state (Figure 57), thus currently able to generate hydrocarbons. In this area, the thermally mature Lias unit has a volume of 1.13 x 1012 m3, which can be considered as the gross volume of the source rock and/or reservoir.

To correctly estimate the amount of hydrocarbons generated by these deposits, it was required to determine the volume of rock containing a relevant amount of organic matter, which is also expressed as “net volume”. In the case of the Lias deposits, the net volume corresponds to the Posidonia black-shales deposits. The Posidonia black-shales signal can be recognized only in few well logs via gamma-ray traces (Figure 56). With these well data, the Posidonia black-shale thickness was determined and used to construct the corresponding thickness map (Figure 59 and Table 7). However, because of the lack of data in the central-eastern part of the Swiss Plateau, the interpolated values in these areas cannot be considered as completely reliable. Future data acquisition campaigns should be carried out to constrain the models of these deposits throughout the entire Swiss Plateau.

In this phase of the project, probabilistic estimates of the net volume of source rock were made. The ratio of net (Toarcian black-shale unit) to gross (Lias unit) volumes was calculated for the well logs with the easily recognizable units (Table 8). Thus, we consider three end-member hypotheses of the net/gross ratio, and we extend it to the entire Swiss Plateau area. The percentages of hydrocarbon-prone source rock (net volume) with respect to the total Lias unit are the following: a minimum of 2%, an average of 5% and a maximum of 7%. The net volumes corresponding to these three hypotheses for the entire Swiss Plateau are shown in Table 8.

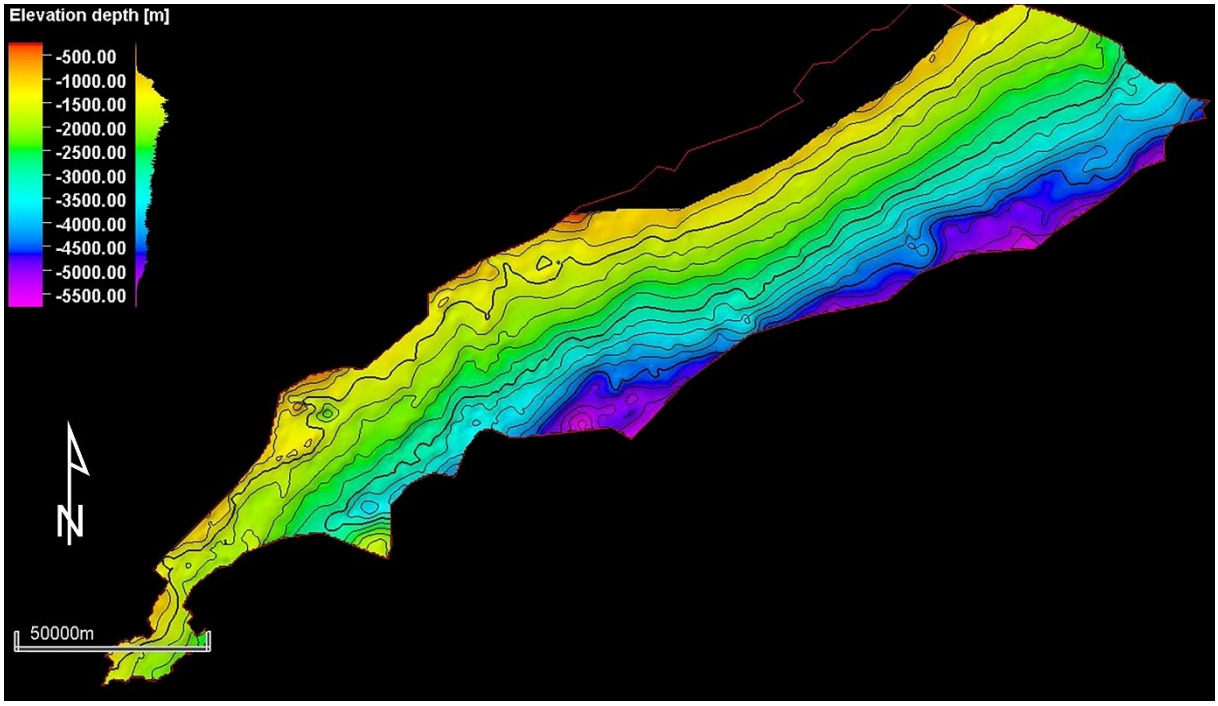

Figure 57: Depth map in meters to the top of the Lias unit, produced by interpolation of 2D seismic and well data. Only the mature area was used in the calculation. Maturation limits are based on vitrinite reflectance data from LEU & GAUTSCHI (2014).

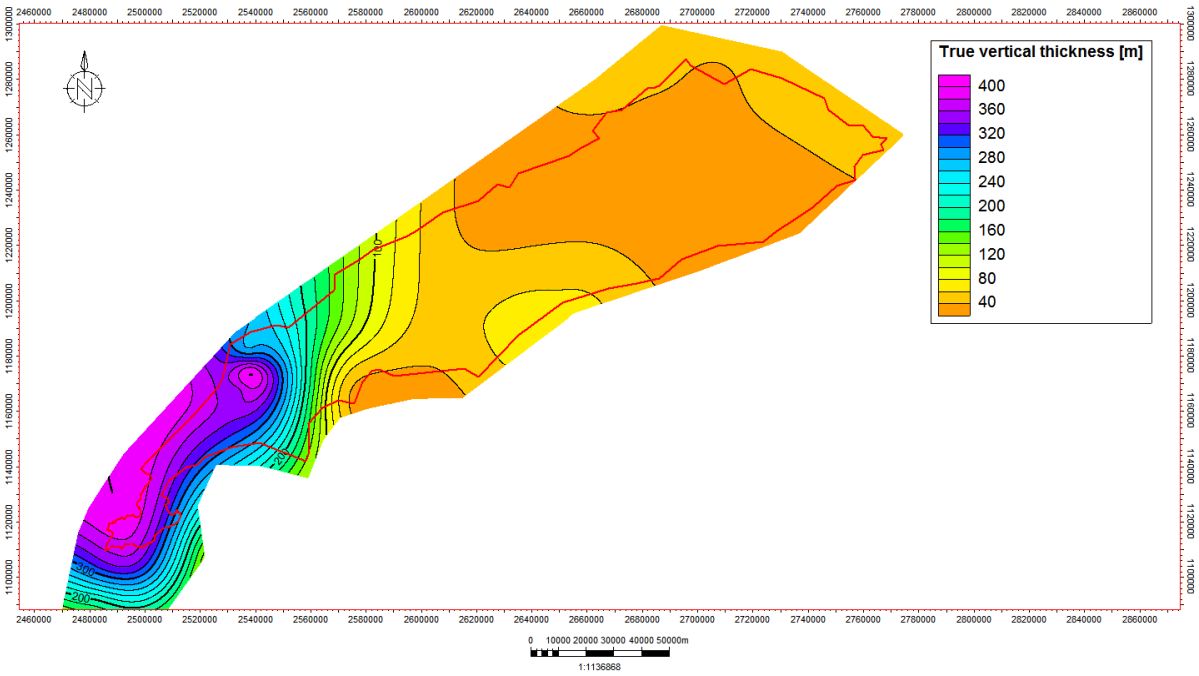

Figure 58: True vertical thickness variation (isopach map in meters) of the Lias unit in the Swiss Plateau (area of study indicated by the red line)

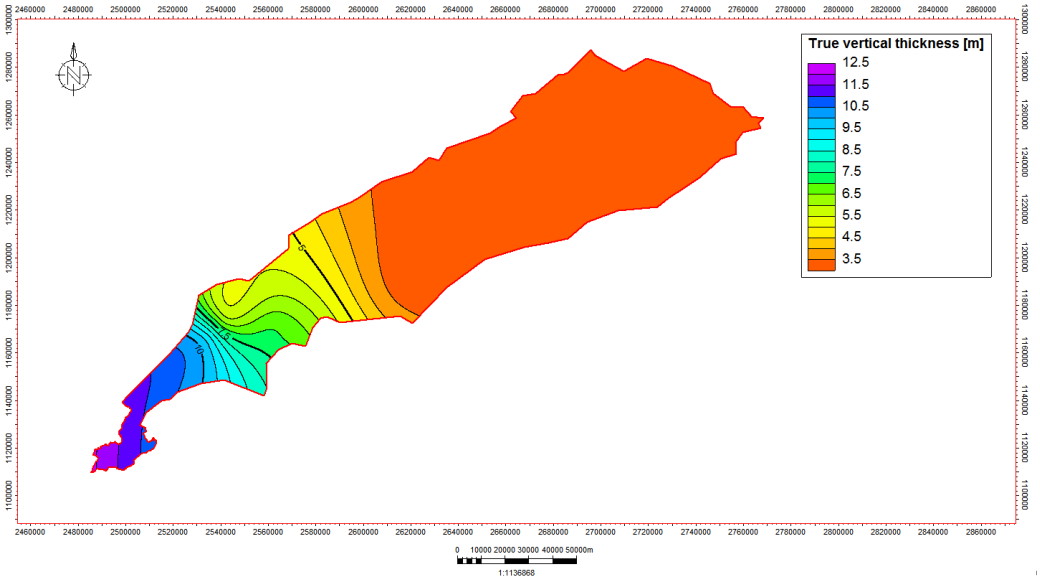

Figure 59: True vertical thickness variation (in meters) of black shales contained within the Toarcian (Posidonia black shales) throughout the Swiss Plateau

Table 7: *Percentage of the net to gross volumes calculated for the wells in which the Posidonia shale unit (Toarcian) was recognized. Thickness measured in well –logs (Figure 57).*

Well name	Lias thickness (m)	Posidonia shales thickness (m)	%
Chapery-1	128	9	7.0
Eclépens-1	359	9	2.5
Essertines-1	397	6	1.5
Faucigny-1	176	10	5.7
Humilly-2	360.5	7	1.9
Linden-1	56	4	7.1
Romanens-1	121	7	5.8
Treyçovagnes-1	308	6	1.9

Table 8: *Bulk rock volume (BRV) and net volumes estimated for the Toarcian black-shale source rock in the entire Swiss Plateau area.*

Net-to-gross ratio (%)	BRV (m^3)	Net volume black shales (m^3)
7	1.13×10^{12}	79.1×10^{9}
5	1.13×10^{12}	56.5×10^{9}
2	1.13×10^{12}	22.6×10^{9}

c) Permo-Carboniferous deposits

The calculation of Permo-Carboniferous source-rock volumes is even more challenging than in the case of the Lias unit because until now, only sparse data are available on the areal distribution of the troughs and grabens with accumulations of these deposits. Thus, any estimate is highly uncertain.

A series of Permo-Carboniferous grabens at various depths is distributed throughout the Swiss Plateau, just above the surface that defines the basal Mesozoic unconformity. The shape, extent and depth of these grabens were estimated (Figure 60) by taking into account the results of PAOLACCI's PhD thesis (unpublished) and Leu (2014), which mostly involved seismic interpretation. Based on well data and stratigraphic interpolation, a variable thickness was assigned to the different grabens, ranging from 300 m to 5 km. Thus, the volume of the deposits in the Permo-Carboniferous grabens was calculated to be 2.7 x 1012 m^3, which correspond to the source rock «gross volume». This value can be considered as a highly uncertain approximation. As in the case of the Posidonia shales, future data acquisition campaigns would have to target Permo-Carboniferous grabens to improve any resource estimates.

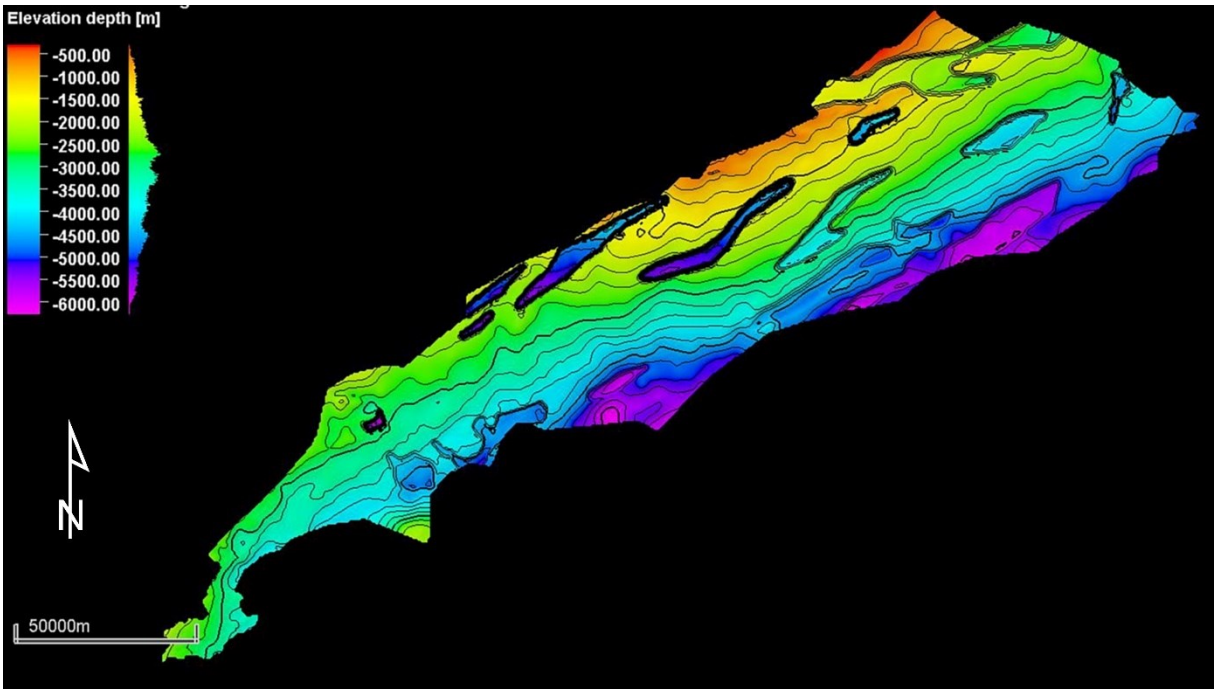

Figure 60: Base of the Mesozoic surface and location of the Permo-Carboniferous grabens.

In order to estimate the amount of hydrocarbon-prone organic matter (e.g. organic-rich shales, coals) in the Permo-Carboniferous troughs, the most significant outcrop and well data were considered. The best-exposed outcrop is located in the Salvan-Dorénaz Basin (CAPUZZO & WETZEL 2004), where organic-rich shales and coal form packages about 40-50 m thick, which are typically repeated along the stratigraphic section. The stratigraphic record of the Weiach-1 well (northern Switzerland) was also considered, since it traverses the entire Permo-Carboniferous series to reach the crystalline basement (NAGRA, 1986). By computing the net-to-gross ratio from the well log, the bituminous shale and coal thickness and the proportion with respect to the entire Permo-Carboniferous stratigraphic record were measured (Table 9).

Table 9: *Permo-Carboniferous stratigraphic record from the Weiach-1 well and percentage of deposits that can be potential source rocks (coal and bituminous shales) with respect to the total Permo-Carboniferous unit thickness*

	Total thickness (m)	Source-rock thickness (m)	Source-rock proportion (%)
Permo-Carboniferous unit	1029	135	13
Permian source rock		65	6
Carboniferous source rock		70	7

In addition, the well-documented coeval deposits in the North Sea area were also considered. In this area, the packages of coal and carbonaceous shales are around 40 m thick (see GR and DT signal of the well log in Figure 61, DOORNENBAL & STEVENSON 2010). The total thickness of these packages measures between 320 and 160 m

(see well 48/10b-4, 44/21-3 and 44/19-3 in Figure 61), which in this basin represents 20% and 10%, respectively, of the entire Permo-Carboniferous interval. These data are consistent with the proportions in Switzerland.

For the purpose of starting with a preliminary estimate, a volume of organic-rich deposits between 10% and 20% of the entire accumulation in the Permo-Carboniferous grabens was considered. The resulting net volumes are presented in Table 10.

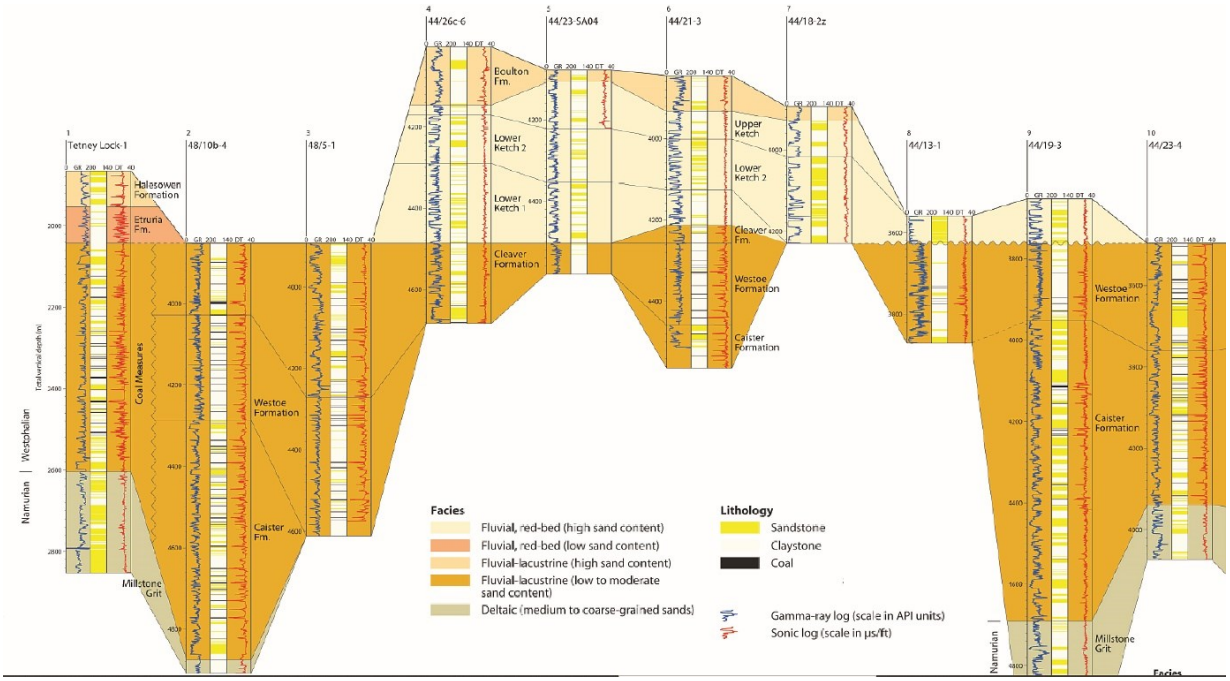

Figure 61: Examples of coal-bearing Carboniferous intervals from the southern North Sea used as a possible analogue for estimating the percentage of organic-rich shale and coal intervals in the Swiss subsurface; modified from DOORNBAL & STEVENSON (2010).

Table 10: *Estimated volumes of the Permo-Carboniferous deposits and the related source-rock layers.*

Total volume (m^3)	Proportion of source-rock deposits (%)	Volume of organic-rich deposits (m^3)
2.7×10^{12}	20	5.4×10^{11}
2.7×10^{12}	10	2.7×10^{11}

5.2. Calculation of the hydrocarbons generated by the source rock

The first step in estimating the accumulated reserves in a basin is to calculate the amount of hydrocarbons that were generated and expulsed by the source rock during the entire basin evolution. This volume depends on the amount and type of organic matter contained in the source rocks, as well as on the thermal transformation rate of the latter. By knowing the volume of the source rock and the geochemical properties of its organic matter, the original source-rock generative potential can be calculated. To determine this value, the calculation method proposed by SCHMOKER (1994) was used.

SCHMOKER's method calculates the volume of hydrocarbons generated by a source rock by taking into account the kerogen type, the kerogen transformation kinetics and the time-temperature history to which the kerogen has been exposed. An empirical measurement of the conversion of kerogen to hydrocarbons based on the hydrogen

index (HI) is adopted here. The HI (from Rock-Eval analysis) indicates the hydrocarbons produced per gram TOC by the thermal degradation of kerogen. Thus, this index represents the potential of a source rock to generate additional hydrocarbons. The difference between the original HI (prior to any hydrocarbon generation) and the present HI can be equated to the hydrocarbons generated by a source rock per unit mass of organic carbon (SCHMOKER 1994). TOC and HI data were obtained from the Rock-Eval analysis of the Geneva Basin deposits (see previous sections) and then extrapolated to the entire Swiss Plateau area. To better constrain and validate the results here, more geochemical data are needed from the entire Swiss Plateau area.

SCHMOKER's approach comprises three steps (Figure 62):

- calculating the mass of organic carbon in the source rock (M)
- estimating the mass of hydrocarbons generated per unit mass of organic carbon (R)
- determining the total mass of hydrocarbons generated (HCG)

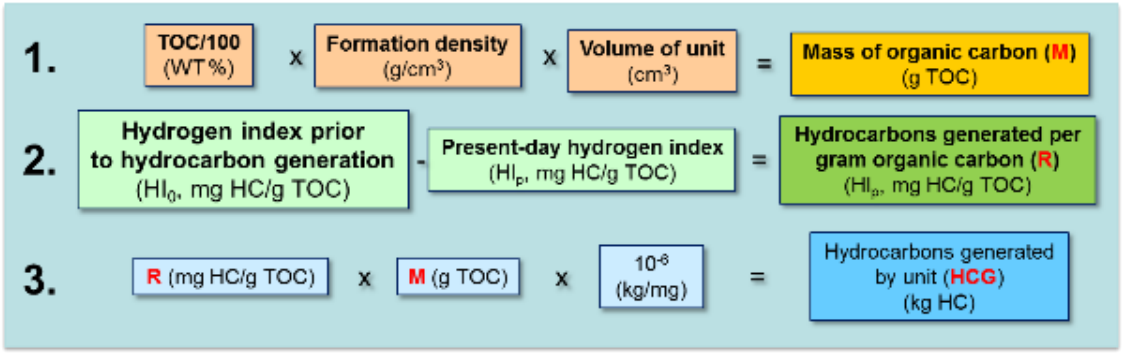

Figure 62: Workflow proposed by SCHMOKER (1994) to calculate the hydrocarbons generated by a source rock

Estimating the mass of hydrocarbons generated by the rock (step 2) is always the critical part of the mass balance calculations, because it is difficult to estimate the original amount of organic matter in the rock before its thermal transformation. ESPITALIÈ et al. (1986) propose a method to estimate this variable by means of a diagram that permits to reconstruct the original HI of the source rock, knowing the type of kerogen and its present thermal state (Figure 63). Thus, three representative end-members of the Rock-Eval data from the Lias and Permo-Carboniferous deposits of the Geneva Basin (taken from the Humilly-2, Chapeiry-1 and Charmont-1 wells) were plotted on the ESPITALIÉ's HI-vs.-T_{max} graphs and restored to the original immature values.

In the case of the Toarcian deposits, three end-member types of source rocks were considered: a Type II kerogen, a Type III and a mixed Type II / Type III kerogen (blue diamonds in Figure 63). These three different types were identified on the basis of the HI, T_{max}, S_2 and TOC values. As indicated in Figure 63, the Type II kerogen has a clearly higher HI index (ca. 450) compared to that of Type III (HI <200). The mixed Type II / Type III shows intermediate HI values (ca. 300). All three kerogen types display similar T_{max} values, indicating oil thermal maturity conditions.

For the Permo-Carboniferous deposits, three end-member source rocks were chosen: a coal sample, a carbonaceous shale and a Type III kerogen (red diamonds in Figure 63). The greatest difference among the selected samples is in the TOC) whereas the HI is somewhat similar because all the samples comprise terrestrial organic matter. This type of organic matter is transformed mostly into gas when it is thermally mature.

By applying the equations in Figure 62, the generated hydrocarbon mass (kg) was determined for three end-member source rocks and for the different net-volume scenarios of the source rocks. In the case of the Toarcian deposits, three volumetric scenarios were considered (net source rock volume equal to 7%, 5% and 2% of the entire Lias unit), whereas only two scenarios were considered for the Permo-Carboniferous units (net source rock volume equal to 10% and 20% of the entire gross unit). The obtained hydrocarbon mass calculated was then converted into volume of generated gas (m^3) by considering an oil density of 0.8 gr/cm^3 for the Toarcian marine

black shales and a gas density of 0.7 gr/cm^3 for the Permo-Carboniferous terrestrial source rock. The calculation results are presented in Table 11 and Table 12.

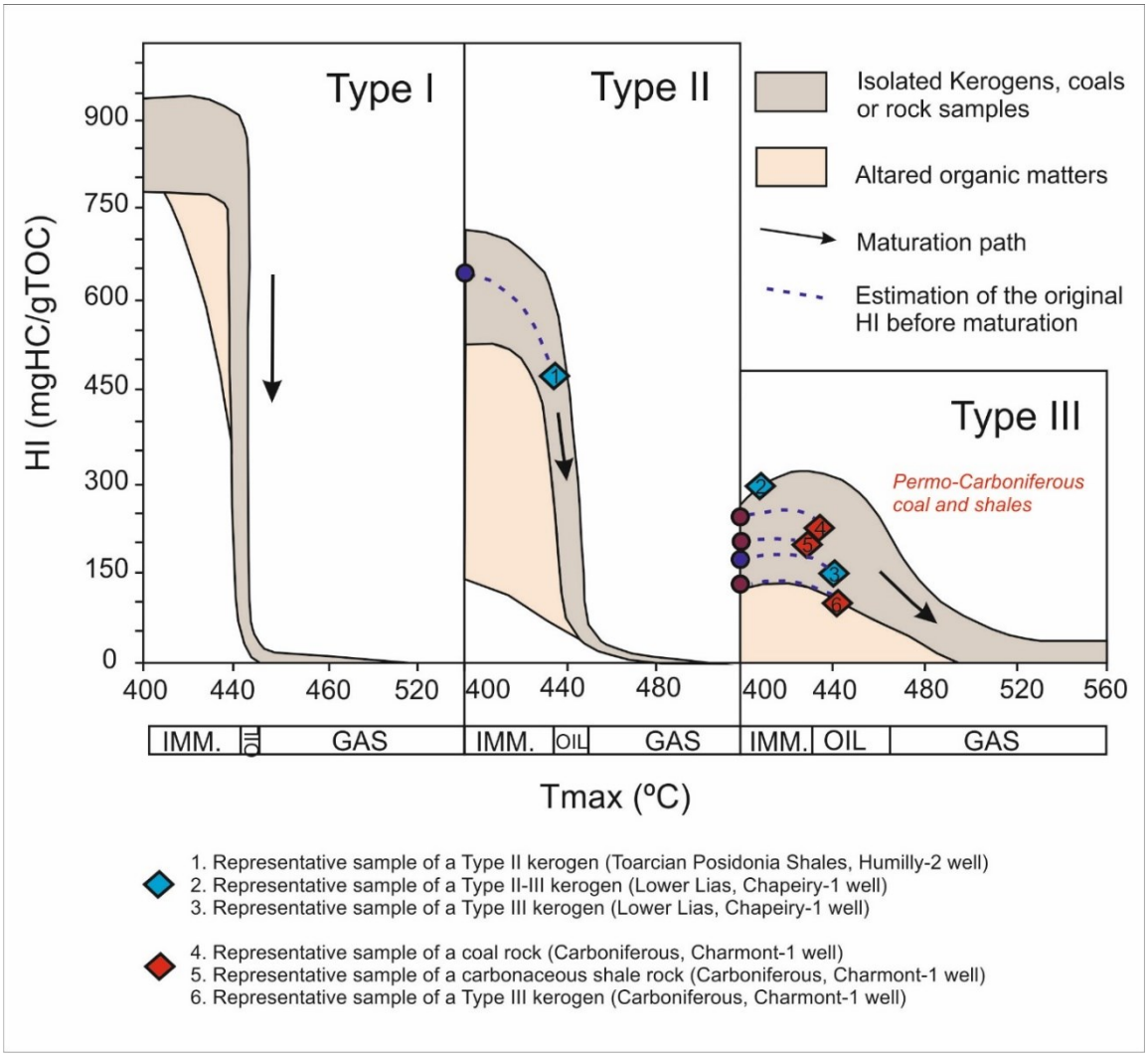

Figure 63: HI vs. T_{max} Rock-Eval indices graph used to determine the type of kerogen in the source rock and its thermal maturity. The original hydrocarbon potential of the rock can be determined by restoring the initial HI (ESPITALIÉ et al. 1986). Only representative samples of the Lias (blue diamonds) and Carboniferous (red diamonds) source rocks are plotted (Rock-Eval data the annexes 1 and 2)

Table 11: *Estimation of the oil generated by the Posidonia black-shale unit (Toarcian) using Schmoker's method. Different cases in terms of source rock volume and kerogen type are proposed.*

	Black Shales Volume (m^3)	Density (g/cm^3)	TOC (%)	HIx (mgHC/gTOC)	HIo (mgHC/gTOC)	HC generated (ton)	HC oil generated (Billion m^3) (10^9 m^3)	HC oil generated (Billion barrels - bbl) (10^9 bbl)
Considering the black-shales volume **7%** of Lias								
Type II kerogen			4.3	505	640	1.24E+12	155	973
Mixed Type II-III	7.90E+10	2.67	1.4	297	450	4.50E+11	56	352
Type III kerogen			4.2	156	170	1.23E+11	15	94
Considering the black-shales volume **5%** of Lias								
Type II			4.3	505	640	8.82E+11	110	691
Mixed Type II-III	5.70E+10	2.67	1.4	297	450	3.22E+11	40	251
Type III			4.2	156	170	8.79E+10	11	69
Considering the black-shales volume **2%** of Lias								
Type II			4.3	505	640	3.53E+11	44	276
Mixed Type II-III	2.30E+10	2.67	1.4	297	450	1.29E+11	16	100
Type III			4.15	156	170	3.52E+10	4.4	28

Table 12: *Estimation of the volume of gas generated by the Permo-Carboniferous unit using Schmoker's method. Different cases in terms of source rock volume and kerogen type are proposed.*

	OM-rich deposits Volume (m3)	Density (g/cm3)	TOC (%)	HIx (mgHC/gTOC)	HIo (mgHC/gTOC)	HC generated (tons)	HC gas generated (Billion m3) (10^9 m3)	HC gas generated (Tcf)
Considering the OM deposits volume **20%** of the Permo-Carboniferous								
Coal			55	231	250	1.52E+12	2170	77
Carbonaceous Shales	5.41E+11	2.69	23	196	205	2.97E+11	424	15
Type III kerogen			5	92	130	2.83E+11	404	14
Considering the OM deposits volume **10%** of the Permo-Carboniferous								
Coal			55	231	250	7.60E+11	1090	39
Carbonaceous Shales	2.70E+11	2.69	23	196	205	1.49E+11	213	8
Type III kerogen			5	92	130	1.42E+11	203	7

The volumetric estimates of hydrocarbons generated in the Swiss Molasse Basin are discussed in this section. In the case of the Toarcian source rock, the results show that mostly oil was produced, since in the study area these deposits have reached the oil-window thermal conditions. A maximum volume of 155 billion m^3 of oil could be generated, considering the most favourable case that the Toarcian black shales comprise 7% of the entire Lias unit and that the related organic matter is formed by a high-quality Type II kerogen. On the other hand, a minimum volume of 4.4 billion m^3 of oil could be generated, considering that the Toarcian black shales form only 2% of the entire Lias unit and that its organic matter corresponds to a low hydrocarbon-prone Type III kerogen.

In the case of the Permo-Carboniferous source rock, the study concludes that it generates mostly gas, because its deposits are currently under the gas-window thermal conditions and constitute mostly gas-prone terrestrial organic matter. A maximum volume of 2'170 billion m^3 of gas could be generated by these rocks in the best-case scenario, whereby the organic-rich layer is coal that forms 20% of the entire Permo-Carboniferous unit. In contrast, a minimum volume of 203 billion m^3 of gas could be generated in the case that the source rock comprises only 10% of the entire Permo-Carboniferous unit and that a low hydrocarbon-prone Type III kerogen is involved.

In Figure 64, the hydrocarbon volumes generated by the two source rocks in this study are represented by bar diagrams. In addition to the minimum and maximum values, the median and the percentiles at 75% and 25% are presented. The volumes are expressed in billions of barrels (billion bbl) in the case of oil, generated by the Toarcian source rock and in trillion cubic feet (Tcf) in the case of gas, generated by the Permo-Carboniferous source rock (see also Table 11 and Table 12)

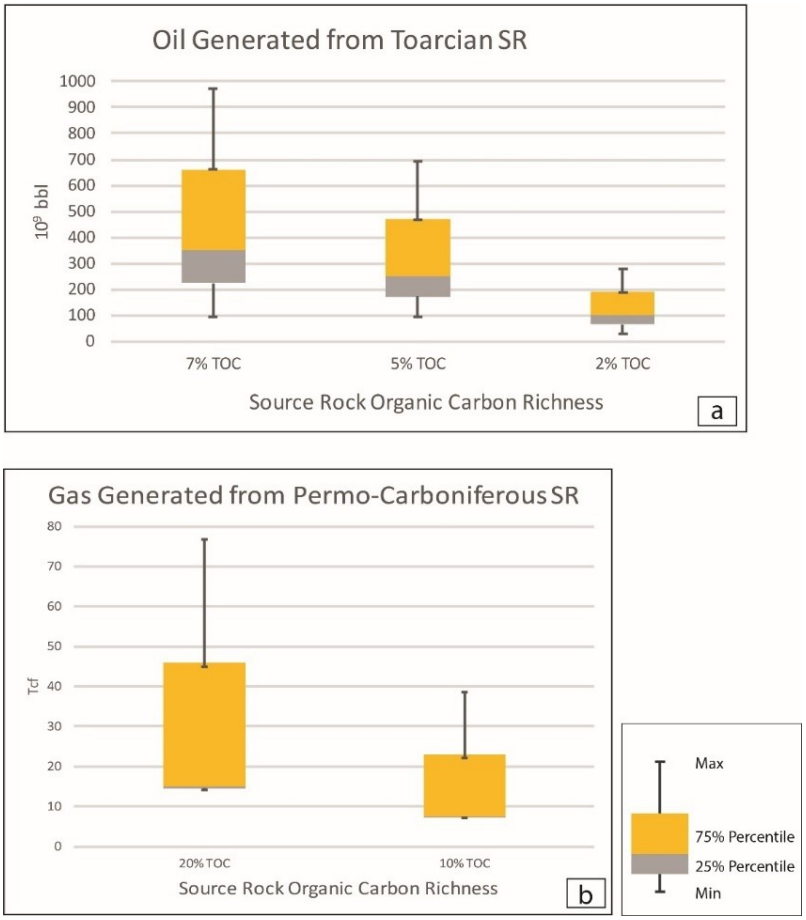

Figure 64: Bars diagrams showing potential volumes of generated hydrocarbons (a) oil, (b) gas. Volumes refer to the estimate calculated in Table 11 and Table 12.

The volumes in Figure 64 represent the amounts of hydrocarbons that potentially could be generated in the Swiss Molasse Plateau, considering the type of organic matter forming the source rock, its thermal maturity and its

volume. However, it is not known how much of these hydrocarbons has been effectively expulsed and accumulated somewhere else and how much has been retained within the shales and organic-matter microporosity. The expulsion efficiency of the source rock is the key variable that controls this ratio.

Diverse methods are proposed in the literature to estimate the amount of petroleum expelled from thermally mature source rocks, taking into account (1) the volume of the rock, (2) the rock density, (3) the original content of organic matter and (4) the expulsion factor (e.g. PETERS, 2006). The expulsion factor is the ratio of the carbon mass expelled from a thermally mature source rock as petroleum to the original kerogen of the immature source rock (PETERS 2006, LEWAN et al. 2002). Determining this variable could be highly challenging, as it strictly depends on the behaviour of the rocks under various physical and chemical conditions. Thus, the petrophysical and geochemical properties of the source rocks need to be investigated accurately.

5.3. Calculation of the available volume for hydrocarbon storage

The calculation of available volume for hydrocarbon storage (AVHS) follows the methodology for determining the volume of hydrocarbon in place. However, in this work, we use the terminology of AVHS to refer to the entire stratigraphic units of the Swiss Plateau and not just to the trapping structures. The AVHS for a given area is controlled, to a large extent, by two key characteristics of the unconventional rock formation: the volume of rock with storage capacity and the amount of porosity. Furthermore, pressure and temperature govern the volume of gas in solution with the reservoir oil, defined by the reservoir's formation volume factor. In addition to free gas, organic-rich shales can hold significant quantities of gas adsorbed on the surface of the organics (and clays).

The calculation of hydrocarbon initially in place is made by using established reservoir-engineering equations and conversion factors to calculate AVHS (available volume for hydrocarbon storage):

$$AVHS(oil) = \frac{(BRV * N{:}G * Phi * So)}{Bo}$$

$$AVHS\ (gas) = \frac{(BRV * N{:}G * Phi * Sg)}{Bg}$$

- Definitions of the equation variables are given below: BRV is the bulk rock volume corresponding to the calculated gross volume of the rock interval and is based on areal extent and thickness from 2D-seismic interpretation and well calibration. The BRV in this study is essentially based on the GeoMol results and literature information.
- N:G is the net-to-gross ratio, which for unconventional reservoirs characterizes the net organic-rich thickness of the shale and coal-bearing intervals within the entire two stratigraphic intervals (Toarcian/Lias in this study). For conventional reservoirs (i.e. Permo-Carboniferous), it refers to the portion of the stratigraphic interval that can store hydrocarbon. The net-to-gross ratio is expressed either in percent or as a fraction and is usually estimated from a combination of logs, such as gamma-ray, density and neutron.
- Phi is the porosity, a dimensionless fraction expressing the volumetric proportion of voids, obtained from the well log or core samples. This shale property is influenced by the thermal maturity and its depth of burial.
- So, Sg and Sw are the oil, gas and water saturations, respectively, and are expressed as dimensionless fractions of the porosity filled with gas (Sg) instead of water (Sw) or oil (So). The porosity is multiplied by Sg to give gas-filled porosity. Sw defines the fraction of the pore space filled with water, often the residual or irreducible reservoir water in the natural fracture and matrix porosity of the shale. Liquids-rich shales may also contain condensate and/or oil (So) in the pore space, further reducing gas-filled porosity.
- Bo and Bg are the oil formation and gas volume factors used to adjust the oil volume in the reservoir, typically containing gas in solution, to oil volume in stock-tank volumes (given in barrels or m^3)1 at

[1] A rule of thumb: 2π barrel or bbl ~ $1m^3$

surface conditions. This property depends on reservoir pressure, temperature and thermal maturity values. The procedures for calculating Bo are provided in standard reservoir engineering publications (MCCAIN 1990). In this work, Bo and Bg were not used in the calculation (hence their value is 1), since we focused on calculating volumes in place in the subsurface and not at surface conditions.

To estimate the volumetric storage potential of the Toarcian and the Permo-Carboniferous units, three scenarios were considered (Table 13). For the latter, a combination of different values of N:G, Phi and hydrocarbon saturation were used and the BRV was kept constant. These data are based on well logs and measurements on core material (unpublished data from the University of Geneva in the context of the «Géothermie 2020» and «Géothermies» projects; HEFNY et al. (2020), MAKHLOUFI et al. (2018), MOSCARIELLO (2016, 2019), MOSCARIELLO et al. (2020), RUSILLON (2018).

Table 13: *Calculation of the volume available for hydrocarbon storage in the Lias and Permo-Carboniferous units.*

Toarcian shale oil reservoir Parameters for volume of oil in place				
BRV (m^3)	N:G	Phi	So	AVHS oil
1.13E+12	0.07	0.05	0.7	2.8E+09
1.13E+12	0.05	0.02	0.5	5.7E+08
1.13E+12	0.02	0.01	0.2	4.5E+07
Carboniferous low K gas reservoir Parameters for volume of gas in place				
BRV (m^3)	N:G	Phi	So	AVHS oil
2.70E+12	0.7	0.2	0.5	1.89E+11
2.70E+12	0.5	0.1	0.4	5.40E+10
2.70E+12	0.2	0.05	0.3	8.10E+09

In addition to the free gas in place, shale reservoirs can hold significant quantities of gas adsorbed on the surfaces of organics (and clays) in the formation. In order to measure the adsorbed gas, an isotherm curve (also known as the Langmuir isotherm) was established for the prospective area of the basin, using available data on TOC and on thermal maturity. These data were used to determine the Langmuir volume (V_L) and the Langmuir pressure (P_L). Adsorbed gas in-place was then calculated using the following formula, where P is original reservoir pressure.

$$GC = \frac{V_L * P}{P_L + P}$$

The absorbed gas content (GC), typically given in cubic feet of gas per ton of net shale, was converted to gas concentration using current or typical values for shale density. Density values for shale are typically around 2.65 gm/cc and depend on the mineralogy and organic content of the shale.

The estimates of V_L and P_L for adsorbed gas in place are based on available data in the literature. In general, V_L is a function of the temperature, organic richness (TOC) and thermal maturity (Ro) of the shale (Figure 65). P_L expresses how readily the adsorbed gas on the organics in the shale matrix is released as a function of a finite decrease in pressure.

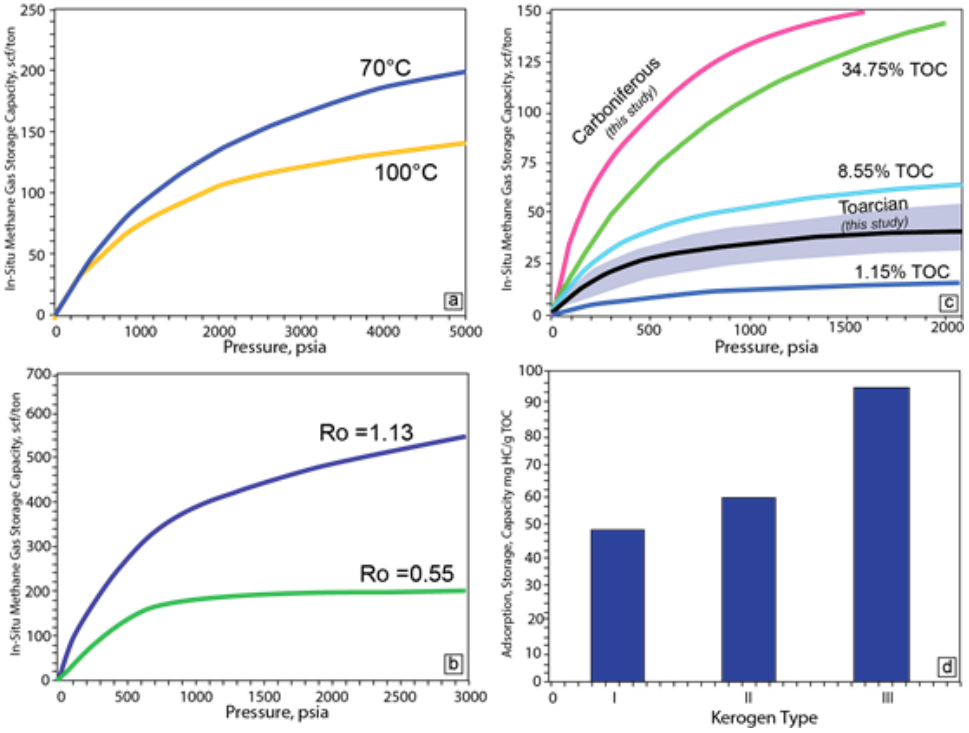

Figure 65: Influence of temperature (a), thermal maturity (b), TOC (c), and type of kerogenes (d) on the ability to gas adsorption (modified from Weatherford laboratories, Houston, personal communication). In (c) the Carboniferous and Toarcian units mean TOC value determined in this study (see previous chapters) is used to extrapolate the related curves.

Based on the properties of the organic-rich shale intervals in this study, it was therefore possible to estimate the in-situ gas storage capacity (standard cubic feet/ton) and the volume of absorption storage capacity (mg HC/g TOC). However, given the sparse information about reservoir pressure in our basin, a quantitative estimate of the additional adsorbed gas was not possible.

5.4. Conclusions

Volume estimates performed herein give a first idea of the amount of hydrocarbons that have been generated and that potentially could be stored in the Swiss Molasse Plateau. A summary of the obtained values is illustrated in Figure 66. The conceptual terms used in analysing the two source rocks of the basin are indicated. The wide range between minimum and maximum values is visible and reflects the major uncertainties (e.g. in BRV, TOC, Phi distribution), existing at present. Furthermore, the hydrocarbon potential of the source rocks is based on extrapolations of data only from the Geneva Basin. Further analyses throughout the entire Swiss Plateau will be performed in the future, in order to obtain more realistic estimates.

The results indicate that in the Swiss Plateau, the amount of hydrocarbons that could be stored in the Toarcian unit ranges between 0.045 and 2.8 billion m^3. Considering the amount, the type and the thermal maturity of the organic matter forming this unit, the amount of oil that could be generated ranges between 155 billion m^3 and 4 billion m^3, which is much higher than the volume that could be stored. This means that only a portion of the hydrocarbons that has been generated by the Toarcian black shales potentially could be stored in this stratigraphic unit, whereas the rest has migrated. This is also the case for the Permo-Carboniferous unit where, according to our preliminary calculation, the gas volume that potentially could be generated is between 2,170 and 200 billion m^3, considerably higher than the storage potential of the sandstone bodies comprising the Permo-Carboniferous unit (between 8 to 189 billion m^3). In both cases, the presence of faults and dipping stratigraphic surfaces could have forced the generated hydrocarbons to migrate to the upper surfaces and/or to accumulate in other reservoir units and structural traps. By taking into account the geometries of the geological units of the basin and their

tectonic and thermal histories, petroleum system modelling would allow a more accurate reconstruction of the hydrocarbon generation, migration and accumulation in the basin.

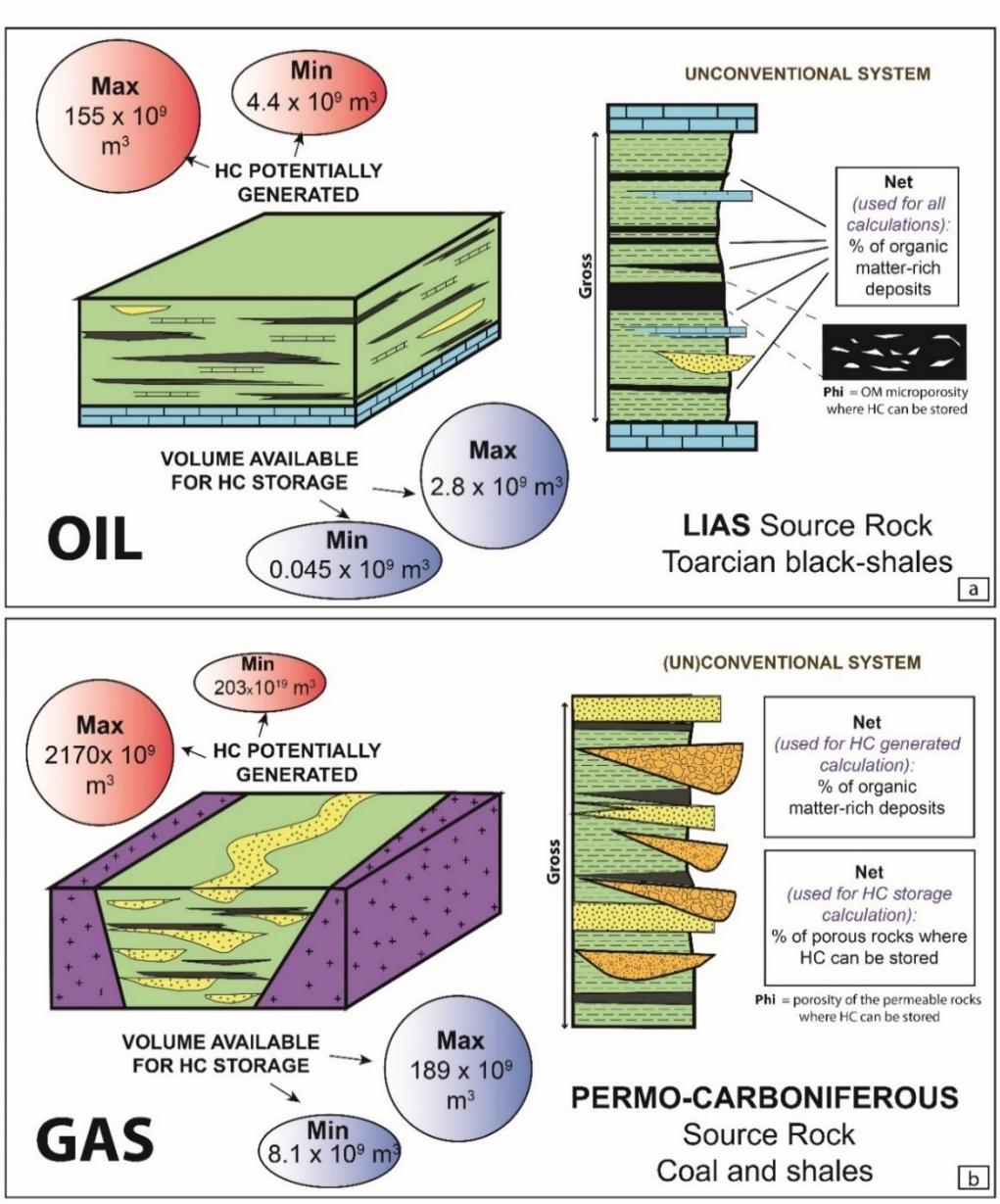

Figure 66: Synthesis of the hydrocarbon volume estimates in this study, (a) oil, (b) gas; HC = hydrocarbons, OM = organic matter.

6. Outlook and perspectives

The methodology applied in the study of the Geneva-Savoie area yields important insights into the potential of oil and gas generation. The workflow we have developed, based on a multidisciplinary approach, needs to be applied to other areas of the Swiss Molasse Bain. For example, in the Canton of Vaud (Essertines-1-Eclépens-1-Treycovagnes-1 well area) bitumen seepages have already been sampled for geochemical analysis and preliminary BPSM simulations suggest that both oil and gas is currently being generated (Eclépens-1, Figure 50). In addition, two wells penetrating the Toarcian Posidonia shale (Courtion-1 and Romanens-1) and the occurrence of various structural traps (SOMMARUGA et al. 2016) make the southern part of the Canton of Fribourg an interesting area for investigation with a similar approach.

In general, both thermogenic and biogenic hydrocarbons are frequently encountered in wells drilled for other purposes (e.g. in Wellenberg, Oftringen, St. Gallen). The concurrence has major implications not only in terms of resource potential but also in terms of fundamental questions regarding the planning, design and execution of an exploration campaign, be it regionally extensive seismic surveys or detailed well planning. Much can be gained from a detailed understanding of the thermal history of the Swiss Molasse Basin in terms of other resource potentials, such as geothermal and saline aquifers for gas storage. Similarly, the occurrence of hydrocarbon source rocks as well as the expulsion and migration paths to reservoirs have a major impact on operational safety during subsurface activities. However, only very few well data have been published to date concerning the organic geochemistry of the source rock in the Swiss Plateau (MATTER et al. 1988, ELIE & MAZUREK 2008, LEU 2014). In order to evaluate the petroleum potential, samples from key intervals in the Lias and the Permo-Carboniferous units should be analysed for organic geochemistry (Rock-Eval pyrolysis) and maturity of the source rocks at depth. In western Switzerland, vitrinite reflectance analysis (SCHEGG et al. 1997) should be repeated, since the analytical tools and measuring techniques have evolved substantially. In central and eastern Switzerland, vitrinite reflectance measurements should be performed systematically. Some data from this area are already available (Benken-1, Herdern-1 and Weiach-1 wells; Nagra 2002) and will serve to calibrate the next BPSM simulations.

The methodology and workflow now need to be applied to regions of Switzerland where data and samples from additional wells are available. Currently, the Permo-Carboniferous, the Triassic and the Jurassic units are central to unravelling the history of the Swiss Molasse Basin in terms of its resource potential. In detail, the following wells should be the focus of this future study:

- *Toarcian Posidonia shale:* Berlingen-1 (TH), Courtion-1 (FR), Eclépens-1 (VD), Entlebuch-1 (LU), Essertines-1 (VD), Hermrigen-1 (BE), Lindau-1 (ZH), Linden-1 (BE), Romanens-1 (FR), Schafisheim (AG), Thun-1 (BE), Treycovagnes-1 (VD)
- *Permo-Carboniferous:* Entlebuch-1 (LU), Kaisten-1 (AG), Riniken-1 (AG), Treycovagnes-1 (VD), Weiach-1 (ZH)

We requested access to the well of NAGRA (Kaisten, Riniken, Schafisheim, Weiach-1) and SEAG (Berlingen-1, Eclépens-1, Entlebuch-1, Lindau-1, Linden-1, Romanens-1), in which we plan to sample the potential source rock and reservoirs. Similar efforts are underway for the Cantons of Vaud, Fribourg and St. Gallen.

The following workflow steps of the UNCONGAS project will be applied to the entire Swiss Molasse Basin: 1) sample analysis, 2) seismic Interpretation, 3) basin modelling, and 4) common risk segment maps.

1) Sample analysis

This step covers the following activities (Figure 67):

- Petrographical characterization of the source rocks based on QEMSCAN analysis (qualitative and quantitative analysis of minerals) and XRD analysis (recognition of the clay fraction). Results will be correlated with the seismic facies analysis in order to identify preferential lithologies rich in organic matter
- Organic (Rock-Eval pyrolysis, vitrinite reflectance, biomarker investigation) and inorganic (ICP-MS) geochemical investigation of source rocks
- Oil and gas composition including carbon isotopic composition of gas in order to reveal their provenance

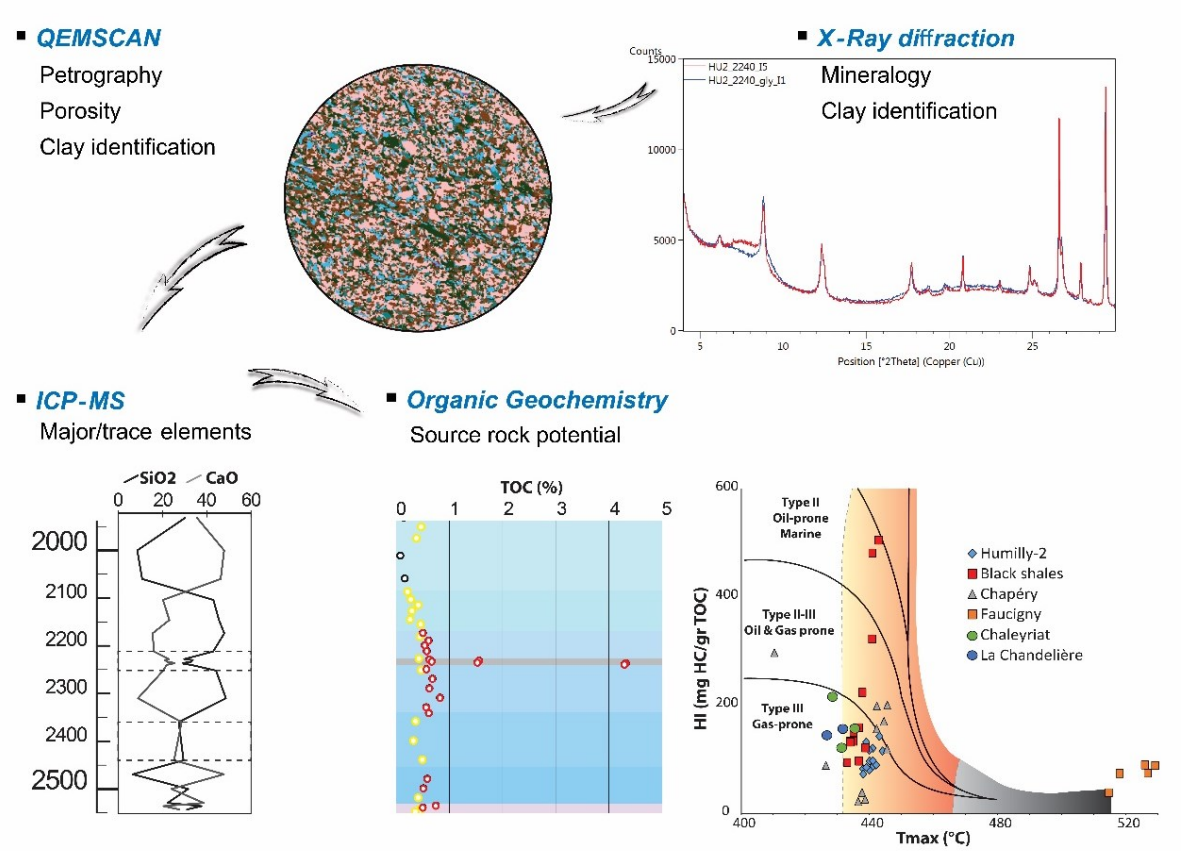

Figure 67: Summary of proposed analytical workflow to estimate the source-rock potential of the Swiss Plateau.

2) Seismic Interpretation

The second part of the workflow focuses on the seismic interpretation (stratigraphic horizon mapping and structural analysis) of data that have not yet been interpreted. It will include seismic facies analysis of the stratigraphic levels containing the source rocks as well as well-log correlations as shown in chapter 2. This part if the workflow is crucial for:

- defining the spatial distribution and thickness of the potential source rocks and reservoirs
- extrapolating the seismic facies throughout the basin (specifically the ones containing source-rock layers) and correlate these with petrographic studies of the analytical part of the workflow (Figure 67)

The determination of unconventional petroleum systems involves the identification of tight to very tight reservoirs (Figure 68a). Porosity and permeability values from the Greater Geneva Basin indicate that tight to very tight reservoirs are distributed throughout the entire stratigraphic column, from the Lower Trias (Buntsandstein) to the Oligo-Miocene Freshwater Molasse (Figure 68b). In central Switzerland, the Upper Muschelkalk dolomites have been identified in past studies as a target for deep geothermal energy production and CO_2 storage (Chevalier et al., 2010). The permeability and porosity of these dolomites tend to decrease with depth, probably as a result of compaction and diagenesis, and signify that reservoirs are tight to very tight in the deepest portion of the basin towards the south (Figure 68c). We also plan to sample potential reservoirs, in order to characterize petrophysical properties (e.g. permeability and porosity) that will serve as input in the subsequent basin modelling simulation.

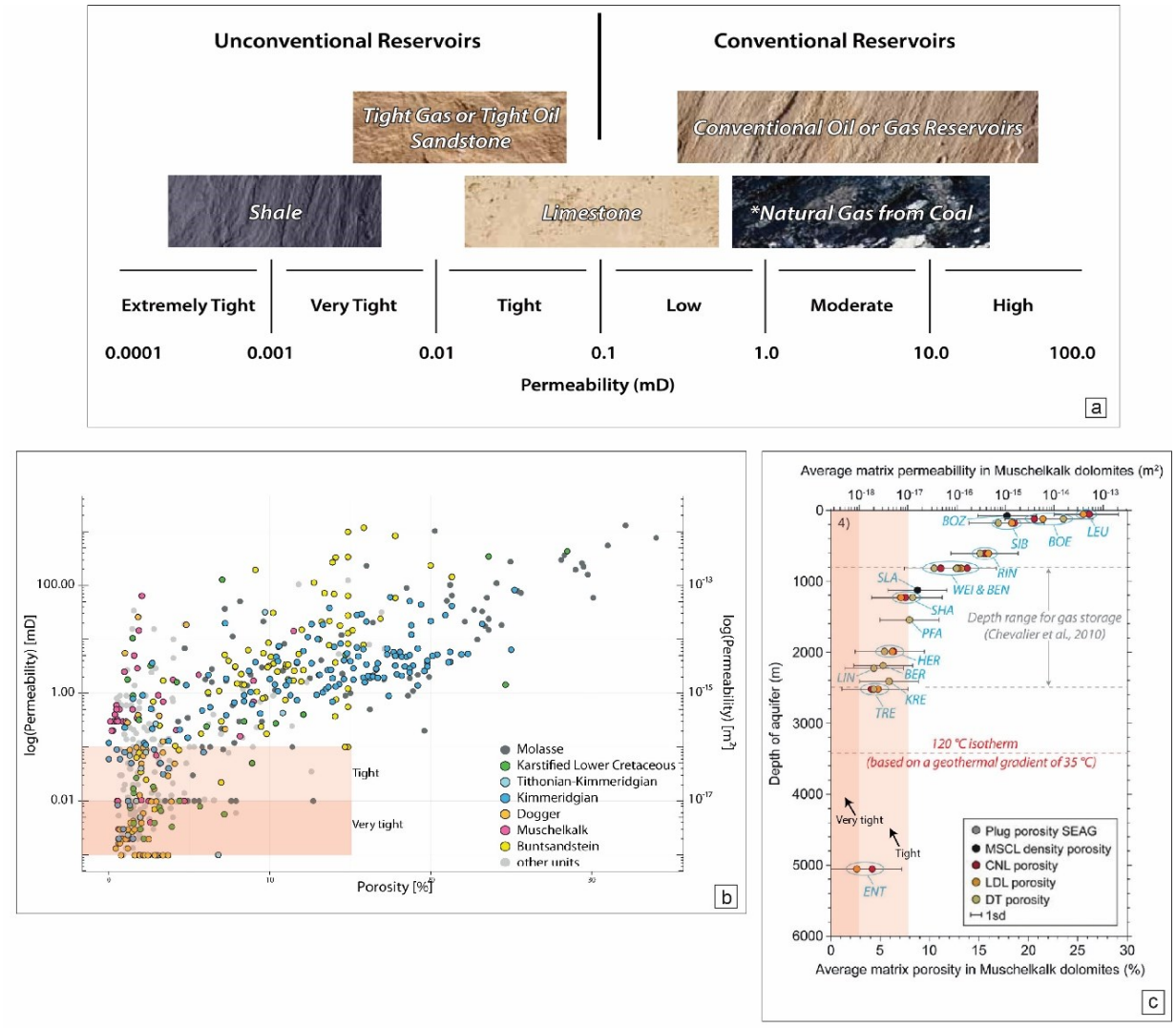

Figure 68: (a) Type and permeability ranges of conventional and unconventional hydrocarbon reservoirs (modified from CSUR, 2012). (b) Porosity (%) and permeability (milli darcy, mD) of potential reservoirs in the Greater Geneva Basin (RUSILLON 2018) Ranges of permeability indicating tight and very tight unconventional reservoirs are highlighted by coloured bars. (c) Average porosity and permeability –depth trend of the Muschelkalk muddy dolomites in central Switzerland, according to different method (see legend). Ranges of permeability indicating tight and very tight unconventional reservoirs are highlighted by the coloured bars (modified from ASCHWANDEN et al. 2019).

3) Basin and petroleum system modelling (BPSM)

The third part of the workflow involves the BPSM approach. According to the concept of BPSM, geological models at small scale and at the whole basin scale are created, and then a simulation of the basin evolution is performed by calibrating the paleo-heatflow and paleo-bathymetry (Figure 69). The paleo-heatflow is calibrated by using a simple McKenzie crustal model based on the tectonic history of the modelled basin. The idea is to develop two scales of basin modelling:

- Small-scale basin modelling in key selected areas from 1D to 3D;
- Large-scale basin modelling of the entire Swiss Plateau based on the GeoMol model.

The two types of models can be run parallel and improved incrementally each time new data are acquired for refining the resolution of the model.

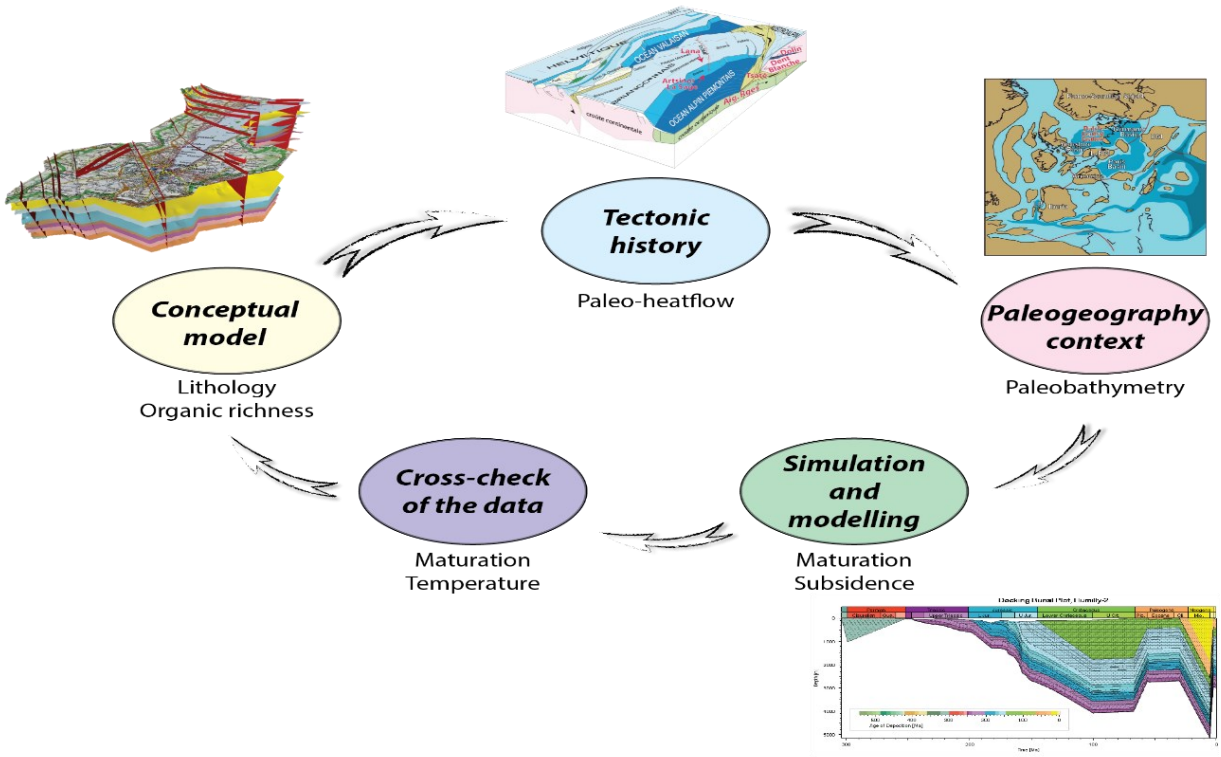

Figure 69: Summary of proposed modelling workflows to estimate the unconventional potential of the Swiss Plateau.

The purpose of the basin modelling in 3D is to predict the hydrocarbon generation and migration in a potential reservoir. 3D basin modelling of the GGB is currently underway in order to improve the knowledge about the source-rock maturation at depth, especially in the Toarcian Posidonia shale and the Permo-Carboniferous unit, and to correlate the migration of hydrocarbons towards the surface with hydrocarbon seepages.

Thermal modelling is a complementary method for determining whether hydrocarbons (1) have been completely expulsed by the source rock since their generation, (2) have migrated and accumulated in reservoirs or (3) have been lost through the ground surface (as indicated by the abundant seeps in Switzerland). This modeling integrates the 3D geological model, which determines the formation of traps, seals and fault migration paths, and the geochemical parameters of the source rock, which in turn determine the timing of generation and expulsion of the hydrocarbons from the kerogen.

4) Common risk segment map of the Swiss Plateau (CRS)

CRS mapping and risking uses all available geological and exploration history data to create a view of the play-scale risks and dependencies (Figure 70). This work is based on the play element mapping and uses the boundaries (segments) that have been created.

The play is subdivided into segments having similar probability characteristics, and the boundaries indicate changes in either geology or confidence (data quality and/or density). Probability values are assigned to each segment.

The number of maps or chance factors that go into the CRS mapping may vary, but experience has shown that play-level and prospect-level maps for reservoir, charge and entrapment are usually sufficient to describe the risks:

- **In play definition** observations from basin focus are taken to determine the logical number of discrete plays as well as the areal distribution of each play.
- **A play test database** is assembled to understanding what we know and where we know it, The goal is to identify which wildcats had technical success or failure after testing the play and why key wells failed. Geological boundaries of the petroleum system elements are shown by creating play element maps of reservoir, charge and entrapment (lithologic and structural elements of the seal) and building a summary play map. In the absence of sufficient calibration data, appropriate analogues for building a model for the play are identified.
- **In CRS mapping and risking** play element maps and well data are used to define dependent and independent risk factors within the proper confidence level. These maps are convolved to define the play "sweet spots" and then "reality-checked" with the existing prospect portfolio.
-

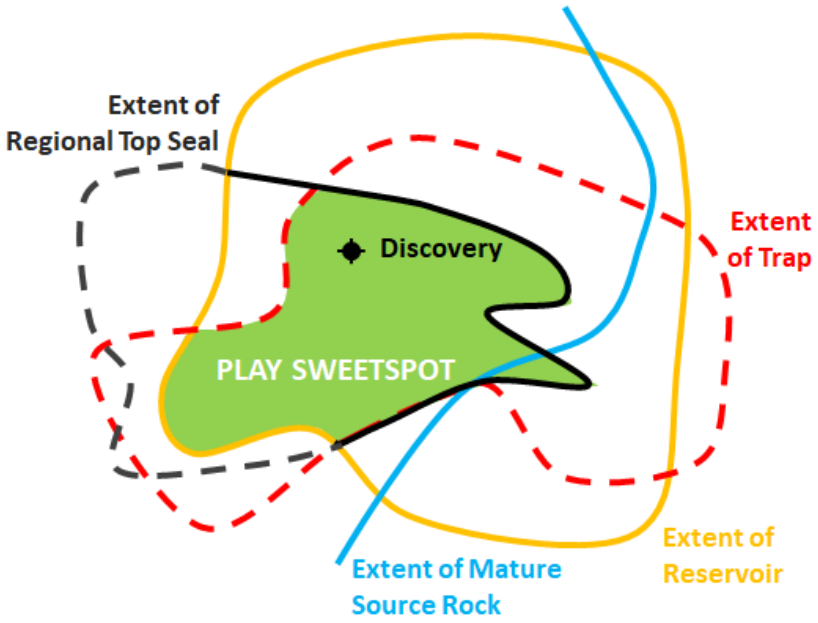

Figure 70: Example of Common Segment Risk map (not on scale). This tool shows the spatial distribution of each petroleum play elements also known as segments (e.g. reservoir, mature source rock, regional top seal and trap) and the results of their superposition which helps in identifying the play sweetspots, i.e. where the likelihood of finding hydrocarbon accumulations is higher. The occurrence of discoveries or hydrocarbon field in the sweetspot area corroborates the indications resulting from the CSR mapping exercise.

7. Acknowledgments

This work was funded by the Federal Office of Energy (OFEN) and the Federal Office of Topography swisstopo. We thank Gunter Siddiqi (OFEN) and Roland Baumberger (swisstopo), who initiated and encouraged the project. We also thank Lance Reynolds (swisstopo) and Robin Allenbach (swisstopo) for their help in providing the data and for the fruitful discussions. Further words of thanks go to the reviewers of this report, Christian Minning and Milan Beres (swisstopo).

We are also grateful to NAGRA and SEAG, who kindly give access to their data and thus contribute to the successful progress of the UNCONGAS project. We particularly thank Michael Schnellmann (NAGRA), Patrick Lahusen (SEAG) and Werner Leu (Geoform) for their help.

8. References

AJUABA, S., SACHSENHOFER, R.F., MEIER, V., GROSS, D., SCHNYDER, J., OMODEO-SALÉ, S., MOSCARIELLO, A. & MISCH, D. (2023): Coaly and lacustrine hydrocarbon source rocks in Permo-Carboniferous graben deposits (Weiach well, Northern Switzerland). – Marine Petrol. Geol. *150*, 106–147

ALTINDAG, R. (2003): Correlation of specific energy with rock brittleness concepts on rock cutting. – J. South. afric. Inst. Min. and Metall. 2003/3, 163–172.

ASCHWANDEN, L., DIAMOND, L. W. & ADAMS, A. (2019): Effects of progressive burial on matrix porosity and permeability of dolostones in the foreland basin of the Alpine Orogen, Switzerland. – Marine and Petrol. Geol. *100*, 148–164.

BELLAHSEN, N., MOUTHEREAU, F., BOUTOUX, A., BELLANGER, M., LACOMBE, O., JOLIVET, L. & ROLLAND, Y. (2014): Collision kinematics in the western external Alps. – Tectonics *33*/6, 1055–1088.

BERNER, U. & FABER, E. (1996): Empirical carbon isotope/maturity relationships for gases from algal kerogens and terrigenous organic matter, based on dry, open-system pyrolysis. – Org, Geochem. *24*/10–11, 947–955.

CAPUZZO N. & WETZEL A. (2004): Facies and basin architecture of the Late Carboniferous Salvan-Dorenaz continental basin (Western Alps, Switzerland/France). – Sedimentology *51*, 675–697.

CHAROLLAIS J., WEIDMANN, M., BERGER, J.-P., ENGESSER, B., HOTELLIER, J.-F., GORIN, E. G., REICHENBACHER, B. & SCHAFER, P. (2007): The Molasse in the Greater Geneva area and its substratum. – J. Arch. Sci. *60*/2, 59–173.

CHEVALIER, G., DIAMOND, L. W. & LEU, W. (2010): Potential for deep geological sequestration of CO_2 in Switzerland: a first appraisal. – Swiss J. of Geosci. *103*/3, 427–455.

CONNAN, J. & CASSOU, A. M. (1980): Properties of gases and petroleum liquids derived from terrestrial kerogen at various maturation levels. – Geochim. cosmochim. Acta *44*/1, 1–23.

Canadian Society for Unconventional Resources (2012): Understanding tight oil. Information about Canada's emerging energy resources. – Canadian Society for unconventional Resources, Calgary.

DEMBICKI, H. (2009): Three common source rock evaluation errors made by geologists during prospect or play appraisals. – Bull. Amer. Assoc. Petroleum Geol. 93/3, 341–356.

DEVILLE, É. & SASSI, W. (2006): Contrasting thermal evolution of thrust systems: An analytical and modelling approach in the front of the western Alps. – Bull. Amer. Assoc. Petroleum Geol. *90*/6, 887-907.

DO COUTO, D., GAREL, S., MOSCARIELLO, A., BOU DAHER, S., LITTKE, R. & WENIGER, P. (2021): Origins of hydrocarbons in the Geneva Basin: insights from oil, gas and source rock organic geochemistry. – Swiss J. Geosci *114*/11, 10–28.

DOLSON, J. (2016): Understanding Oil and Gas Shows and Seals in the Search for Hydrocarbons. – Springer International Publishing.

DOORNENBAL, H. & STEVENSON, A. (2010): Petroleum Geological Atlas of the Southern Permian Basin Area. – EAGE, Utrecht.

ELIE, M. & MAZUREK, M. (2008): Biomarker transformations as constraints for the depositional environment and for maximum temperatures during burial of Opalinus Clay and Posidonia Shale in northern Switzerland. – Appl. Geochem. *23*/12, 3337–3354.

ESPITALIE, J., DEROO, G. & MARQUIS, F. (1985a): La pyrolyse Rock-Eval et ses applications: Première Partie. – Rev. Inst. français du Pétrole *40*/5, 563–580.

— (1985b): La pyrolisis Rock-Eval et ses applications: Deuxième partie. – Rev. Inst. français du Pétrole *40*/6, 755–784.

— (1986): La pyrolyse Rock-Eval et ses applications: Troisième partie. – Rev. Inst. français du Pétrole 41/1, 73–89.

Esso Recherches et Exploitation Pétrolières (1970a): Rapport de fin de sondage du forage d'exploration de Chapéry. – ESSO REP, Bordeaux.

— (1970b): Rapport de fin de sondage du forage d'exploration de Faucigny. – ESSO REP, Bordeaux.

— (1989): Rapport de fin de sondage du forage d'exploration de Chaleyriat. – ESSO REP, Bordeaux.

— (1990): Rapport de fin de sondage du forage d'exploration de La Chandelière. – ESSO REP, Bordeaux.

— (1992a): Rapport de fin de sondage du forage d'exploration de Charmont. – ESSO REP, Bordeaux.

— (1992b): Rapport de fin de sondage du forage d'exploration de Chatillon 1D. – ESSO REP, Bordeaux.

ETIOPE, G., ZWAHLEN, C., ANSELMETTI, F. S., KIPFER, R. & SCHUBERT, C. J. (2010): Origin and flux of a gas seep in the Northern Alps (Giswil, Switzerland). – Geofluids *10*/4, 476–485.

FABER, E., SCHMIDT, M. & FEYZULLAYEV, A. A. (2015): Geochemical Hydrocarbon Exploration - Insights from Stable Isotope Models. – Oil Gas europ. Mag. *41*/2, 93–98.

GORIN, G., SIGNER, C. & AMBERGER, G. (1993): Structural configuration of the western Swiss Molasse Basin as defined by reflection seismic data. – Eclogae geol. Helv. *86*/3, 693–716.

GOTTLIEB, P., WILKIE, G., SUTHERLAND, D., HO-TUN, E., SUTHERS, S., PERERA, K., JENKINS, B., SPENCER, S., BUTCHER, A. & RAYNER, J. (2000): Using quantitative electron microscopy for process mineralogy applications. – J. Min. Metall. Mater. Soc. *52*, 24–25.

GREBER, E., LEU, W. & WYSS, R. (1995): Erdgasindikationen in der Schweiz: Grundlagen zur Charakterisierung des Gasgefahrenpotentials im Untergrund. – Schweiz. Ing. Archit. *113*/24, 567–572.

HEFNY, M., ZAPPONE, A., MAKHLOUFI, Y. DE HALLER, A. & MOSCARIELLO, A. (2020): A laboratory approach for the calibration of seismic data in the western part of the Swiss Molasse Basin: the case history of well Humilly-2 (France) in the Geneva area. – Swiss J. Geosci. *113*/11, 227–256.

JARVIS, G.T. & MCKENZIE, D.P. (1980): Sedimentary basin information with finite extension rates. – Earth and Planet. Sci. Lett. *48*/1, 42–52.

JIANFA, C., YONGCHANG, X. & DIFAN, H. (2000): Geochemical Characteristics and Origin of Natural Gas in Tarim Basin, China. – Bull. Amer. Assoc. Petroleum Geol. *84*/5, *591*–606.

LAFARGUE, E., MARQUIS, F. & PILLOT, D. (1998): Rock-Eval 6 Applications in Hydrocarbon Exploration, Production, and Soil Contamination Studies. – Oil & Gas Sci. Technol. *53*/4, 421–437.

Landesgeologie (2017): GeoMol: Geologisches 3D-Modell des Schweizer Molassebeckens – Schlussbericht. – Ber. Landesgeol. *10*.

LANDIS, C. R. & CASTAÑO, J. R. (1995): Maturation and bulk chemical properties of a suite of solid hydrocarbons. – Org. Geochem. *22*/1, 137–149.

LANGFORD, F. F. & BLANC-VALLERON, M. M. (1990): Interpreting Rock-Eval pyrolysis data using graphs of pyrolyzable hydrocarbons vs. total organic carbon. – Bull. Amer. Assoc. Petroleum Geol. *74*/6, 799–804.

LEU, W. (2012): Swiss oil/gas exploration and lessons learnt. – Bull. angew. Geol. *17*/1, 49–59.

— (2014): Potenzial der Kohlenwasserstoff-Ressourcen in der Nordschweiz. – Nagra Arb. Ber. NAB *14*-70.

LEU, W. & GAUTSCHI, A. (2014): The shale gas potential of the Opalinus Clay and Posidonia Shale in Switzerland – A first assessment. – Schweiz. Bull. angew. Geol. *19*/2, 95–107.

LEWAN, M. D., HENRY, M. E., HIGLEY, D. K. & PITMAN, J. K. (2002) Material-balance assessment of the New Albany-Chesterian petroleum system of the Illinois basin. – American Association of Petroleum Geologists. – Bulletin, 86, 745–77.

LIU, Q., DAI, J., LI, J. & ZHOU, Q. (2008): Hydrogen isotope composition of natural gases from the Tarim Basin and its indication of depositional environments of the source rocks. – Sci. China Ser. D: Earth Sci. *51*, 300–311.

MCCAIN, W. D. (1990): The Properties of Petroleum Fluids – second edition. – PennWell Books, Tulsa.

MAGOON, L. B. & DOW, W. G. (1994): The petroleum system – From source to trap. – Mem. Amer. Assoc. Petroleum Geol. *60*, 3–24.

MAKHLOUFI Y., RUSILLON E., BRENTINI M., MOSCARIELLO A., MEYER M. & SAMANKASSOU E. (2018): Dolomitization of the Upper Jurassic carbonate rocks in the Geneva Basin, Switzerland and France. – Swiss J. Geosci. *111*, 475–50.

MARTI, J. (1969): Rapport de fin de sondage d'Humilly 2. – Société nationale des pétroles d'Aquitaine. Direction exploration et production, Pau. – *13*.

MAZUREK, M., HURFORD, A. J. & LEU, W. (2006): Unravelling the multi-stage burial history of the Swiss Molasse Basin: integration of apatite fission track, vitrinite reflectance and biomarker isomerisation analysis. – Basin Res. *18*/1, 27–50.

MONTERO-SERRANO, J.-C., FÖLLMI, K. B., ADATTE, T., SPANGENBERG, J. E., TRIBOVILLARD, N., FANTASIA, A. & SUAN, G. (2015): Continental weathering and redox conditions during the early Toarcian Oceanic Anoxic Event in the northwestern Tethys: Insight from the Posidonia Shale section in the Swiss Jura Mountains. – Palaeogeogr. Palaeoclimatol. Palaeoecol. *429*, 83–99.

MOSCARIELLO A. (2016): Geothermal exploration in SW Switzerland. – Europ. Geothermal Congr. Strasbourg, 19.–24. September 2016.

MOSCARIELLO A. (2019): Exploring for geo-energy resources in the Geneva Basin (Western Switzerland): opportunities and challenges. – Swiss Bull. angew. Geol. *24*/2, 105–124.

MOSCARIELLO, A., GORIN, G., CHAROLLAIS, J. & RUSSILLON, E. (2014): Geology of Western Switzerland and nearby France in a Geo-Energy perspective. –19th Int. Sedimentol. Congr. Geneva, 18.–22. August 2014.

MOSCARIELLO, A., GUGLIELMETTI, L., OMODEO SALÉ, S., DE HALLER, A., ERUTEYA, O. E., LO, H. Y., CLERC, N., MAKLOUFHI, Y., DO COUTO, D., FERREIRA DE OLIVEIRA, G., PEROZZI, L., DE OLIVEIRA FILHO, F., HOLLMULLER, P., QUIQUEREZ, L., NAWRATIL DE BONO, C. F., MARTIN, F. & MEYER M. (2020): Heat production and storage in Western Switzerland: advances and challenges of intense multidisciplinary geothermal exploration activities, an 8 years progress report. – Proc. World Geothermal Congr. Reykjavik, Iceland, April 26th – May 2nd 2020.

NAGRA (1986): Sondierbohrungen Weiach, Riniken, Schafisheim, Kaisten, Leuggern: Geophysikalische Daten. – Nagra tech. Ber., NTB *85*–50.

OMODEO SALÉ, S., ERUTEYA, O.E., CASSOLA T., A. BANIASAD, A. & MOSCARIELLO, A. (2020): A basin thermal modelling approach to mitigate geothermal energy exploration risks: The St. Gallen case study (eastern Switzerland). – Geotherm. 87.

OMODEO SALÉ, S., HAMIDI,Y., VILLAGOMEZ, D. & MOSCARIELLO, A. (2021): Quantifying Multiple Erosion Events in the Distal Sector of the Northern Alpine Foreland Basin (North-Eastern Switzerland), by Combining Basin Thermal Modelling with Vitrinite Reflectance and Apatite Fission Track Data. – Geosci. *11*, 2.

OSTERA, H. A., GARCIA, R., MALIZIA, D., KOKOT, P., WAINSTEIN, L. & RICCIUTTI, M. (2016): Shale gas plays, Neuquén Basin, Argentina: chemostratigraphy and mud gas carbon isotopes insights. – Braz. J. of Geol. *46* (supply 1), 181–196.

PAOLACCI, S. (2013): Seismic facies and structural configuration of the Western Alpine Molasse Basin and its substratum (France and Switzerland). – Thesis Univ. Geneva (unpubl.).

PATERSON, M. S. & TENG-FONG, W. (2005): Experimental rock deformation - the brittle field. – Springer-Verlag, Berlin Heidelberg.

PEREZ R. & MARFURT K. (2013) Calibration of Brittleness to Elastic Rock Properties via Mineralogy Logs in Unconventional Reservoirs. Search and Discovery. – November 11, 2013 AAPG International Conference and Exhibition, Cartagena, Colombia, September 8–11.

PETERS, K. E., & CASSA, M. R. (1994): Applied Source-Rock Geochemistry. In: MAGOON L. B. & DOW W. G. (Eds.): The Petroleum System – From Source to Trap. – Mem. Amer. Assoc. Petrol. Geol. *60*.

PETERS, K. E., WALTERS, C. C. & MOLDOWAN, J. M. (2005a): The biomarker guide. – Volume 1: Biomarkers and Isotopes in the environment and Human History. – Cambridge University Press, Cambridge.

— (2005b): The biomarker guide. – Volume 2: Biomarkers and Isotopes in Petroleum Exploration and Earth History. Cambridge University Press, Cambridge.

PIRRIE, D., BUTCHER, A. R., POWER, M. R., GOTTLIEB, P. & MILLER, G. L. (2004): Rapid quantitative mineral and phase analysis using automated scanning electron microscopy (QemSCAN); potential applications in forensic geoscience. In: PYE, K. & CROFT, D. J. (Eds.): Forensic Geosciences – Principles, Techniques and Applications (p. 123–136). – Geol. Soc., London, Spec. Publ. *232*.

RUSSILON, E. (2018): Characterisation and rock typing of deep geothermal reservoirs in the Greater Geneva Basin (Switzerland & France). – Terre & Env. *141*.

RYBACH, L. (1992): Geothermal potential of the Swiss Molasse Basin. – Eclogae geol. Helv. *85*/3, 733–744.

SCHEGG, R. & LEU, W. (1996): Clay mineral diagenesis and thermal history of the Thonex well, western Swiss Molasse basin. – Clays and Clay Miner. *44*, 693–705.

SCHEGG, R., CORNFORD, C. & LEU, W. (1999): Migration and accumulation of hydrocarbons in the Swiss Molasse Basin: implications of a 2D basin modeling study. – Marine and Petrol. Geol. *16*/6, 511–531.

SCHEGG, R., LEU, W., CORNFORD, C. & ALLEN, P.A. (1997): New coalification profiles in the Molasse Basin of Western Switzerland: Implications for the thermal and geodynamic evolution of the Alpine Foreland. – Eclogae geol. Helv. *90*/1, 79–96.

SCHOENHERR, J., LITTKE, R., URAI, J. L., KUKLA, P. A. & RAWAHI, Z. (2007): Polyphase thermal evolution in the Infra-Cambrian Ara Group (South Oman salt basin) as deduced by maturity of solid reservoir bitumen. – Org. Geochem. *38*/8, 1293–1318.

SIGNER, C. & GORIN, G. (1995): New geological observations between the Jura and the Alps in the Geneva area, as derived from reflection seismic data. – Eclogae geol. Helv. *88*, 235–265.

SCHMOKER, J. W. (1994): Volumetric calculation of hydrocarbons generated. In: L. B. Magoon & W. G. Dow (Eds.): The Petroleum System – From Source to Trap (p. 232–329). –Mem. Amer. Assoc. Petrol. Geol. *60*.

SOMMARUGA, A., EICHENBERGER, U. & MARILLIER, F. (2012): Seismic Atlas of the Swiss Molasse Basin. Edited by the Swiss Geophysical Commission. – Matér. Géol. Suisse, Géophys., *44*.

SOMMARUGA, A., GRUBER, M. & MOSAR, J. (2016): Synthèse des données géologiques utiles pour la construction d'un modèle du sous-sol du Canton de Fribourg. – Geofocus, *39*.

SONG, J., LITTKE, R., WENIGER, P., OSTERTAG-HENNING, C. & NELSKAMP, S. (2015): Shale oil potential and thermal maturity of the Lower Toarcian Posidonia Shale in NW Europe. – Intern. J. of Coal Geol. *150–151*, 127-153.

SUVA (2002): Verhütung von Unfällen durch Brände und Explosionen bei der Erstellung von Untertagbauten in Erdgas führenden Gesteinsschichten. – Techn. Merkbl. 66102.d.

SWEENEY, J. J. & BURNHAM, A. K. (1990): Evaluation of a simple model of vitrinite reflectance based on chemical kinetics. – Bull. Amer. Assoc. Petrol. Geol. *74*/10, 1559–1570.

TISSOT, B. P. & WELTE, D. H. (1984): Petroleum Formation and Occurrence, Second ed. –Springer, New York.

TODOROV, I., SCHEGG, R. & WILDI, W. (1993): Thermal maturity and modelling of Mesozoic and Cenozoic sediments in the south of the Rhine Graben and the Eastern Jura (Switzerland). – Eclogae geol. Helv. *86*/3, 667–692.

TRABUCHO-ALEXANDRE, J., DIRKX, R., VELD, H., KLAVER, G. & DE BOER, P. L. (2012): Toarcian black shales in the Dutch central graben: record of energetic, variable depositional conditions during an oceanic anoxic event. – J. sediment. Res. *82*/2, 104–120.

TRIBOVILLARD, N., ALGEO, T. J., LYONS, T. & RIBOULLEAU, A. (2006): Trace metals as paleoredox and paleoproductivity proxies: An update. – Chem. Geol. *232*/1–2, 12–32.

WANG, F. P. & GALE, J. F. W. (2009): Screening criteria for shale-gas systems. – Gulf Coast Assoc. of geol. Soc. – Transactions 59th Annual Convention Sept. 27.–29. 2009 Shreveport Louisiana, 779–793.

WHITICAR, M. J. (1999): Carbon and hydrogen isotope systematics of bacterial formation and oxidation of methane. – Chem. Geol. *161*/1–3, 291–314.

WHITICAR, M.J., FABER, E., SCHOELL, M. (1986): Biogenic methane formation in marine and freshwater environments: CO_2 reduction vs. acetate fermentation – Isotope evidence. – Geochim. Cosmochim. Acta *50*/5, 693–709.

WYGRALA, B.P. (1989): Integrated study of an oil field in the southern Po Basin, Northern Italy. – Ber. der Kernforschungsanlage Jülich 2313.

WYSS, R., GREBER, E., FREIMOSER, M. & SCHENKER, F. (2002): Grundlagen zur Charakterisierung der Erdgasgefährdung bei Untertagbauten. – Bull. angew. Geol. 7/1, 45–65.

Wyss, R. (2001): Der Gasausbruch aus einer Erdsondenbohrung in Wilen (OW). – Bull. angew. Geol. 6/1, 25–40.

ZHU, G., WANG, Z., DAI, J., SU, J. (2014): Natural gas constituent and carbon isotopic composition in petroliferous basins, China. – J. asian Earth Sci. 80, 1–17.

ZOU C. (2017): Unconventional petroleum geology. – Elsevier, Amsterdam.

Annex 1

Wells	Depth	Strati-graphic age	TOC (%)	S1 (mg HC/g)	S2 (mg HC/g)	S3 (mg CO_2/g)	HI (mg /g TOC)	OI (mg CO_2/g TOC)	Tmax (°C)	PI
Humilly-2	2174		0.50	0.06	0.67	0.28	133	56	435	0.08
Humilly-2	2182		0.45	0.08	0.60	0.18	133	40	434	0.12
Humilly-2	2190		0.61	0.14	0.80	0.26	132	43	434	0.15
Humilly-2	2200		0.54	0.08	0.51	0.26	94	49	433	0.14
Humilly-2	2212		0.58	0.07	0.56	0.25	97	43	437	0.11
Humilly-2	2228	Toarcian	0.43	0.06	0.64	0.23	149	54	435	0.09
Humilly-2	2230		0.62	0.07	0.76	0.23	121	36	439	0.08
Humilly-2	2232		1.56	0.38	3.49	0.29	224	19	438	0.10
Humilly-2	2234		0.67	0.14	1.06	0.25	158	37	437	0.12
Humilly-2	2236		1.53	0.37	4.93	0.27	322	18	441	0.07
Humilly-2	2238		4.32	1.41	21.80	0.63	505	15	443	0.06
Humilly-2	2240		4.29	1.18	20.65	0.65	481	15	441	0.05
Humilly-2	2250		0.57	0.08	0.69	0.19	120	34	441	0.10
Humilly-2	2252		0.47	0.10	0.62	0.50	132	107	439	0.14
Humilly-2	2270	Pliensbachian	0.68	0.06	0.56	0.19	82	28	438	0.10
Humilly-2	2290		0.63	0.07	0.89	0.25	142	40	443	0.07
Humilly-2	2310		0.83	0.08	0.95	0.41	115	49	444	0.08
Humilly-2	2330		0.57	0.07	0.66	0.26	117	47	440	0.10
Humilly-2	2342		0.62	0.05	0.53	0.25	86	41	441	0.09
Humilly-2	2360		0.37	0.04	0.27	0.21	73	58	438	0.13
Humilly-2	2400		0.33	0.05	0.26	0.20	80	61	440	0.16
Humilly-2	2440	Sinemurian	0.49	0.05	0.48	0.26	97	53	440	0.09
Humilly-2	2480		0.59	0.12	0.57	0.29	97	50	441	0.17
Humilly-2	2500		0.51	0.06	0.46	0.23	89	44	442	0.12
Humilly-2	2520		0.42	0.04	0.35	0.24	85	57	439	0.10
Faucigny-1	4001.0		0.93	0.11	0.82	0.20	88	21	529	0.12
Faucigny-1	4007.0		1.02	0.13	0.75	0.26	74	26	518	0.15
Faucigny-1	4015.0	Upper Lias	0.93	0.10	0.84	0.12	90	13	526	0.11
Faucigny-1	4020.0		1.03	0.10	0.76	0.19	74	19	527	0.12
Faucigny-1	4026.0		1.59	0.21	1.07	1.00	68	63	527	0.16
Faucigny-1	4027.0		1.56	0.19	0.59	0.22	38	14	515	0.24
Faucigny-1	4035.0		0.94	0.06	0.39	0.15	42	16	560	0.13
Chapeiry-1	3624.0		0.35	0.02	0.14	0.20	39	55	438	0.13
Chapeiry-1	3642.0		0.32	0.01	0.08	0.21	26	64	439	0.11
Chapeiry-1	3669.0	Upper Lias	3.52	1.23	7.04	0.52	200	15	446	0.15
Chapeiry-1	3670.0		2.21	1.01	3.75	0.68	170	31	445	0.21
Chapeiry-1	3677.0		0.63	0.02	0.14	0.66	22	106	436	0.13
Chapeiry-1	3719.4	Lower Lias	1.46	0.30	1.74	0.40	119	28	445	0.15
Chapeiry-1	3719.8		0.33	0.33	0.30	0.25	89	76	426	0.52

Wells	Depth	Strati-graphic age	TOC (%)	S1 (mg HC/g)	S2 (mg HC/g)	S3 (mg CO_2/g)	HI (mg /g TOC)	OI (mg CO_2/g TOC)	Tmax (°C)	PI
Chapeiry-1	3720.9		1.39	2.21	4.12	0.57	297	41	410	0.35
Chapeiry-1	3722.7		3.29	3.34	6.52	0.36	198	11	442	0.34
Chapeiry-1	3728.8		4.15	3.05	6.48	0.53	156	13	442	0.32
Chaleyriat-1	480	Toarcian	0.97	0.22	2.08	0.33	215	34	428	0.10
Chaleyriat-1	510		0.79	0.04	1.23	0.31	157	39	435	0.03
Chaleyriat-1	560		0.76	0.04	0.93	0.48	121	63	431	0.04
La Chandelière	1130.0	Toarcian	0.21	0.05	0.30	0.64	144	310	427	0.14
La Chandelière	1150.0		0.30	0.05	0.47	0.54	156	180	432	0.10

Rock-Eval pyrolysis results of samples from Liassic sections in the studied wells. Samples between brackets contain less than 0.5 % of TOC and are not plotted in the graphs.

Annex 2

Wells	Depth	Stratigraphic age	TOC (%)	S1 (mg HC/g)	S2a (mg HC/g)	S3 (mg CO_2/g)	HI (mg HC/g TOC)	OI (mg CO_2/g TOC)	Tmax (°C)	PI
Humilly-2	3039.8		1.12	0.10	0.85	0.15	76	13	449	0.11
Humilly-2	3040.7	Carboniferous	1.11	0.09	0.61	0.16	55	15	465	0.13
Humilly-2	3049		0.23	0.11	0.37	1.08	161	470	461	0.23
La Chandelière	1562.1	Carboniferous	0.11	0.04	0.53	0.38	467	337	545	0.07
Chaleyriat-1	1365.0	Carboniferous	0.88	0.03	0.45	1.21	51	137	514	0.06
Charmont-1	1798.0		5.10	0.30	4.69	0.51	92	10	430	0.06
Charmont-1	1825.0		22.57	1.50	44.25	5.63	196	25	435	0.03
Charmont-1	1892.0		31.81	2.28	69.39	8.50	218	27	433	0.03
Charmont-1	1894.0	Carboniferous	54.85	3.88	126.84	5.91	231	11	435	0.03
Charmont-1	1920.0		16.09	0.71	21.59	3.67	134	23	437	0.03
Charmont-1	2023.0		7.19	0.33	6.43	1.28	89	18	460	0.05
Charmont-1	2108.5		57.33	6.36	125.66	6.19	219	11	450	0.05
Chatillon-1D	1578.5	Carboniferous	8.24	0.52	7.78	0.64	94	8	444	0.06

Rock-Eval pyrolysis results of Carboniferous sections in the studied wells

Annex 3

Well	Sample	Age	U(ppm)	TOC [%]
Humilly-2	HU2 2174	Toarcian	1.7000	0.5035
	HU2 2212		2.0000	0.5772
	HU2 2228		3.0000	0.4278
	HU2 2230		2.2000	0.6248
	HU2 2234		2.6000	0.6694
	HU2 2236		4.4000	1.5300
	HU2 2238		5.0000	4.3183
	HU2 2240		4.6000	4.2918
	HU2 2252	Pliensbachian	2.5000	0.4693
	HU2 2310		2.4000	0.8271
	HU2 2360	Sinemurian	2.2000	0.3674
	HU2 2440		2.3000	0.4938
	HU2 2500		2.0000	0.5137
Chapéry-1	CHY 3624	Upper Lias	1.5	0.3538
	CHY 3642		1.3	0.3201
	CHY 3669		5.1	3.5189
	CHY 3670		3.3	2.2063
	CHY 3677		2.2	0.6256
	CHY 3719.4		4.7	1.4592
	CHY 3720.8	Lower Lias	0.4	0.3328
	CHY 3720.9		2.2	1.3856
	CHY 3722.7		4.1	3.2874
	CHY 3728.8		4.4	4.1451
Faucigny-1	FAY 4001	Aalenian Toarcian	2.7	0.9322
	FAY 4007		2.2	1.0191
	FAY 4015		2.3	0.9344
	FAY 4020		2.5	1.0262
	FAY 4026		2.4	1.5858
	FAY 4027		2.7	1.5554
	FAY 4035		2.8	0.9427
Chaleyriat-1	CYT 480	Lias	2	0.9675
	CYT 510		2.3	0.7869
	CYT 560		2.4	0.7644
La Chandelière-1D	LCD 1130	Lias	1.1	0.2059
	LCD 1150		1.1	0.2991

Uranium content (in ppm) of the Lower Jurassic samples and their respective TOC (in %).

Annex 4

Well	Depth (m)	Calcite	Chamosite	Chlorite	Clay minerals	Clinochlore	Dolomite	Illite	Illite-Smectite	Kaolinite	Quartz	TOC	Brittleness index	GR
Humilly-2	2104	45.15	0.34	0.03	0.01	0.03	1.28	20.98	0	0.25	27.35	0.28	0.299170493	62.8976
	2146	31.68	0.05	0.01	0.01	0.01	0.51	6.66	0.01	0.19	57.29	0.26	0.597818875	19.651
	2174	70.58	0.09	0.01	0	0.01	1.29	9.34	0.01	0.01	15.16	0.50	0.169581544	44.1516
	2212	4.42	0.39	0.04	0.02	0.05	0.3	59.18	0.03	0.94	28.04	0.58	0.30153031	69.2326
	2228	41.42	0.17	0.05	0.08	0.03	2	23.94	0.34	4.78	9.17	0.43	0.135545413	64.6313
	2230	43.26	0.21	0.05	0.1	0.03	1.96	29.84	0.33	5.87	9.83	0.62	0.128006289	55.7876
	2234	25.29	0.27	0.07	0.17	0.05	1.91	40.78	0.67	7.94	12.73	0.67	0.16167964	74.6834
	2236	44.23	0.09	0.03	0.09	0.02	1.07	27.4	0.62	1.63	12.82	1.53	0.15514354	68.0084
	2238	37.22	0.13	0.06	0.12	0.05	1.3	29.28	1.8	0.72	12.61	4.32	0.158774881	33.9174
	2240	29.83	0.14	0.06	0.12	0.05	1.13	35.37	2.47	1.1	14.74	4.29	0.177712017	55.7458
	2252	19.93	0.17	0.02	0.04	0.07	4.09	10.42	0.12	2.17	57.24	0.47	0.647355102	68.6056
	2310	7.87	1.7	0.08	0.19	0.31	0.54	27.29	0.46	13.27	31.63	0.83	0.382215881	68.0314
	2360	27.43	0.68	0.05	0.09	0.08	0.62	30.8	0.02	7.51	25.59	0.37	0.281110428	46.0125
	2440	46.8	0.55	0.1	0.11	0.08	2.53	19.78	0.07	8.07	13.88	0.49	0.177474879	60.1827
La Chandelière-1D	1130	34.68	0.01	0	0	0.02	1.51	0.52	0.02	0.16	53.59	0.21	0.607390577	21.2125
	1150	27	0.02	0	0.01	0.01	2.12	0.27	0.04	0.56	62.82	0.30	0.697161869	37.2152
Faucigny-1	4007	17.09	0.83	0.09	0.05	0.1	1.65	35.57	0.3	2.66	32.42	1.02	0.371217592	51.4688
	4027	16.88	0.28	0.06	0.05	0.06	2.03	41.32	0.52	1.09	26.3	1.56	0.314269904	48.7051
	4035	11.41	0.58	0.04	0.03	0.09	1.48	41.93	0.05	1.36	34.5	0.94	0.38934029	56.0931
Chapéry-1	3642	0	0.02	0	0	0	0.06	83.5	0	0.04	1.95	0.32	0.023401993	58.4242
	3670	33.41	0.18	0.07	0.08	0.06	1.11	34.69	0	1.01	14.58	2.21	0.179526952	63.6252
	3719.4	1.21	0.13	0.09	0.03	0.01	13.37	69.85	0	0.13	5	1.46	0.201250689	37.9018
	3719.8	96.37	0.04	0.05	0	0	0.31	0.06	0.02	0.01	1.6	0.33	0.0193334	31.4691
	3722.7	68.6	0.06	0.02	0.01	0.02	0.3	13.99	0	0.02	13.98	3.29	0.142390784	41.3262

Mineral composition of Toarcian shales samples and brittleness index, obtained applying the WANG & GALE's formula (2009). GR (gamma ray) is extracted from the electric logs curves at the exact depth of samples.

Annex 5

Well	Depth	Stratigraphic age	TOC (%)	Pr/Ph	Pr/nC17	Ph/nC18	TAR	CPI	C29 norHop/ C30 Hop	C31 Hop 22S/ (22R+22S)	St C27	St C28	St C29
Humilly-2	2232	Toarcian	1.56	1.94	0.38	0.33	-	-	-	-	-	-	-
Humilly-2	2236		1.53	2.06	0.83	0.63	-	-	0.34	0.58	34.69	23.79	41.52
Humilly-2	2238		4.32	1.51	0.76	0.75	0.04	1.38*	0.37	0.57	31.37	27.59	41.03
Humilly-2	2240		4.29	1.42	0.69	0.65	0.03	-	0.30	0.66	34.96	24.65	40.39
Humilly-2	3038.8	Carb.	1.12	1.53	0.61	0.48	0.93	1.06	-	-	35.66	33.25	31.09
Humilly-2	3040.7		1.11	0.88	0.63	0.66	2.5	1.05	-	-	35.15	33.5	31.35
Chatillon-1D	1578.5	Carb.	8.24	1.06	0.97	1.09	0.15	1.27	0.38	0.57	29.13	20.27	50.61
Charmont-1	1892	Carb.	31.81	6.88	4.04	0.58	0.15	1.48*	0.87	0.58	21.46	16.35	62.19
Charmont-1	1894		54.85	6.75	2.08	0.32	0.28	1.74*	0.83	0.58	23.39	20.70	55.91
Charmont-1	2108.5		57.33	6.23	2.30	0.41	0.03	-	1.09	0.58	21.81	24.66	53.53
Chapeiry-1	3669	Toarcian	3.52	1.76	0.51	0.42	0.01	-	-	-	-	-	-
Chapeiry-1	3720.9		1.39	1.26	1.59	1.18	0.24	1.48	0.74	0.60	42.22	28.29	29.49
Chapeiry-1	3722.7		3.29	0.87	0.60	0.62	0.44	1.13	0.73	0.58	48.94	19.43	31.63
Chapeiry-1	3728.8		4.15	1.23	0.44	0.41	0.13	1.11	0.35	0.61	36.66	25.15	38.19
Roulave bitumen	Surface	-	-	0.62	3.05	40.45	0.15	-	0.31	0.57	36.04	24.38	39.58
Satigny bitumen	Surface	-	-	-	-	-	-	-	0.39	0.42	-	-	-
Satigny bitumen	Surface	-	-	-	-	-	-	-	0.31	0.5	-	-	-

Overview of biomarker ratios determined in this study. (Abbreviations: Pr = pristane; Ph = phytane; TAR = Terrigenous Aquatic Ratio; CPI = Carbon Preference Index; Hop = hopane; Str = sterane). * CPI25-29 value

Annex 6

Components	Units	SAT1	SAT2	SAT1	SAT2
		[100 µl]	[200 µl]		
Hydrogen	[Vol%]	nd	nd		
CO	[Vol%]	0	0		
CO2	[Vol%]	0	0		
O2+Ar	[Vol%]	3.16	4.09		
Nitrogen	[Vol%]	11.55	14.86		
				vol. % in 100 µL	vol. % in 200 µL
Methane	[ppm]	2660	6114	53.2	61.14
Ethane	[ppm]	14.8	34.5	0.3	0.35
Ethene	[ppm]	0	0	0	0
Propane	[ppm]	6.5	14.7	0.13	0.15
Propene	[ppm]	0	0	0	0
i-Butane	[ppm]	4.9	11.2	0.1	0.11
n-Butane	[ppm]	1.6	3.7	0.03	0.04
i-Pentane	[ppm]	1.1	2.6	0.02	0.03
n-Pentane	[ppm]	0	0.6	0	0.01
i-Hexane	[ppm]	1.5	1.6	0.03	0.02
n-Hexane	[ppm]	0.4	0.5	0.01	0.01
C1/(C2+C3)		124.9	124.3		
δ13C-CH4	[‰ VPDB]	-52.5			
δ13C-C2H6	[‰ VPDB]		-23.5		
δ13C-C3H8	[‰ VPDB]		-21.4		
δ2H-CH4	[‰ SMOW]		-231		

Chemical components and isotopic composition of the gas retrieved from Satigny. Sample SAT1 and SAT2 comes from the same gas accumulation, retrieved at few minutes interval. C1/C2+C3 is a usual term to count the amount of carbon atoms in CnHn+2 molecules, obtained by dividing the amount of CH4 above the sum of C2H6 and C3H8.

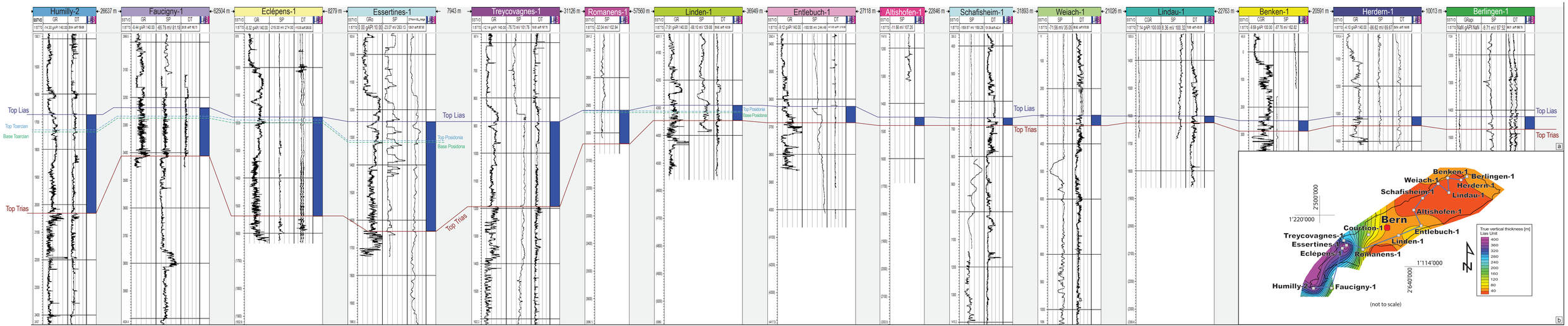

Well logs used to calibrate the seismic data interpolation, where the Lias unit boundaries were defined. Where possible, the Toarcian black-shale unit (Posidonia) was identified (thin blue lines).
On the lower right corner: interpolated depth map of the Lias unit (meters) and location of the wells shown in the figure.